University of Algarve

Faculty of Sciences and Technology

Professional Activity Report
(To obtain the Master degree in Biological Engineering)

Tânia Cristina da Luz Palma

Supervisor: Prof. Dr. Anabela Romano
Supervisor: Prof. Dr. Maria Clara Costa
FCT/UALG

Faro

2013

University of Algarve

Faculty of Sciences and Technology

Professional Activity Report
(To obtain the Master degree in Biological Engineering)

Tânia Cristina da Luz Palma

Supervisor: Prof. Dr. Anabela Romano
Supervisor: Prof. Dr. Maria Clara Costa
FCT/UALG

Faro

2013

Professional Activity Report
(To obtain the Master degree in Biological Engineering)

"Declaração de autoria de trabalho"

"Declaro ser a autora deste trabalho, que é original e inédito. Autores e trabalhos consultados estão devidamente citados no texto e constam da listagem de referências incluídas."

"The content of this report is of the exclusive responsibility of the author"

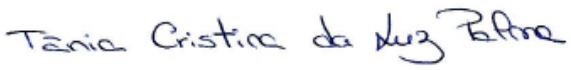

Acknowledgements

I am deeply grateful to Professor Dr. Maria Clara Costa to give me the opportunity to work in her research group in Environmental Technology Laboratory and also I would like to express my sincere gratitude to Professor Dr. Anabela Romano that gave me the chance to integrate her research team.
I would like to address my special thanks to Dr. Robert Renaville that accepted me in his team in Progenus S.A.
I am also grateful to Dr. Olinda Monteiro for her guidance and support.
I am thankful to all them for their guidance along my professional activity and for their support.
I am grateful to all members of team from where I had the lucky to pass for all the joy and very good moments that I spent with them.
I am especially thankful to Sandra Gonçalves and Ana Assunção for their unconditional support and to Tiago for his help.

In a personal level, I am deeply thankful to my family, especially to my grandparents, to my cousin Palminha and to my godmother Bárbara and Manuel, to Smail and to all my friends old and new.
I will be forever grateful to my parents that always give me strength and all the support that I need to go ahead and fulfill my dreams.

I. Summary of professional activity

After completing my degree in Biotechnological Engineering, I did a professional training of 6 months in the enterprise Progenus S.A. (Gembloux – Belgium) financed under the Leonardo da Vinci Program and during two years and two and half months I was research fellow in the research project FCT: PTDC/AGR-AAM/102664/2008 with the title "Is *Plantago almogravensis* an aluminium hyperaccumulator? Elucidation of the tolerance mechanism using micropropagated plants" under the supervision of Prof. Dr. Anabela Romano. Currently, I am working in environmental remediation for metal removal and/or recovery using chemical and biological approaches, under the coordination of Prof. Dr. Maria Clara Costa – Centro de Ciências do Mar do Algarve.

In Progenus S.A. my work consisted at genotyping and in the identification of SNPs (Single Nucleotide Polymorphisms) of interest and of major genes affecting the regulation, composition and percentage of fatty acids (FA) and of mono-unsaturated fatty acids (MUFAs) in the milk cows. The results presented are part of my traineeship report. As research fellow, in the project FCT: PTDC/AGR-AAM/102664/2008, my work was based in the use of micropropagation techniques as well as subsequent assays to assess aluminium (Al) tolerance of *Plantago almogravensis* and *P. algarbiensis* that are two critically endangered plantain species. From this professional activity resulted three publications of papers in international journals with referees index (ISI) and the exposure of a poster at an international conference.

Actually, I am working in the Environmental Technologies laboratory in bioremediation studies. This work includes enrichment of anaerobic bacteria communities from environmental samples and screening of their resistance and ability to recover palladium(II) from aqueous media. Simultaneously, other study is in course, which consists on the synthesis of metal sulphide nanoparticles using sulphide generated by sulphate-reducing bacteria (SRB). The obtained nanoparticles are being applied in the degradation of emerging pollutants.

Keywords: Polymerase chain reaction (PCR); Single nucleotide polymorphisms (SNPs); Plant *in vitro* propagation; Aluminium tolerance; Bio-recovery; Synthesis of metal sulphide nanoparticles

II. Resumo da atividade profissional

Após concluir a licenciatura em Engenharia Biotecnológica fiz um estágio profissional de 6 meses na Empresa Progenus S.A. (Gembloux-Bélgica) financiado pelo Programa Leonardo Da Vinci. Durante dois anos e dois meses e meio foi Bolseira de Investigação no Projeto de Investigação FCT: PTDC/AGR-AAM/102664/2008 com o título "Será a espécie *Plantago almogravensis* hiperacumuladora de alumínio? Elucidação dos mecanismos de tolerância usando plantas micropropagadas" sob a orientação da Prof. Dr. Anabela Romano. Atualmente, estou a fazer um estudo de Remediação Ambiental para remoção e/ou recuperação de metais usando estratégias químicas e biológicas, sob a direção da Prof. Dr. Maria Clara Costa – Centro de Ciências do Mar do Algarve.

Na empresa Progenus S.A. o meu trabalho consistiu na genotipagem e na identificação de Polimorfismos de Nucleótidos Simples (SNPs) de interesse e na identificação dos principais genes que afetam a regulação, composição e percentagem de ácidos gordos (FA) e de ácidos gordos monoinsaturados (MUFAs) em bovinos leiteiros. Estudos anteriores demonstraram que as enzimas Esterase-coenzima A desaturase (SCD), a Proteína de Ligação ao Elemento Regulador de Esterol-1 (SRBP-1) e a Síntase de ácidos gordos (FASN) apresentavam interessantes correlações entre a sua atividade enzimática e a composição de ácidos gordos (FA) e na percentagem de ácidos gordos mono-insaturados (MUFAs). Para a genotipagem dos genes SCD, SREBP-1 e FASN procedeu-se à otimização de métodos baseados em reação em cadeia da polimerase (PCR).

Os genes de 5 raças de gado bovino, Holstein, Simmental, Blanc Blue, Pie Rouge, Pie Noir, foram genotipados no exão 5 de SCD, no intrão 5 de SREBP-1. Procedeu-se a um ensaio SNapShot para uma rápida deteção de polimorfismos de nucleótidos simples (SNPs) existentes no domínio da Tioesterase (TE) e dos exões 1 e 34.

Na Bélgica, a raça Holstein é a mais importante em termos de produção de leite. No exão 5 do gene SCD, três importantes SNP foram encontrados, no entanto só um na posição 10329 codifica para um codão diferente AA: alanina (alelo C) ou valina (alelo T). Uma inserção longa nos 84 pares de bases (tipo longo: L) e uma deleção (tipo curto: S) foram encontradas no intrão 5 no SREBP-1 do gado estudado. Todas as Holstein estudadas para o genótipo SREBP-1 apresentaram o tipo LL sendo assim homozigóticas para o tipo L. A nível do gene FASN foi verificada a existência do tipo homozigótico

g.17924GG para o qual se verifica uma maior quantidade de ácidos gordos monoinsaturados no leite.

Os resultados apresentados nesta Tese pertencem ao meu relatório de estágio profissional entregue ao Dr. Renaville e ao Gabinete de Mobilidade da UALG.

Como Bolseira de Investigação no projeto FCT: PTDC/AGR-AAM/102664/2008 o meu trabalho baseou-se na utilização de técnicas de micropropagação e nos subsequentes ensaios para avaliar a tolerância ao alumínio de duas espécies em perigo de extinção, *Plantago almogravensis* e *P. algarbiensis*. Alguns estudos sugeriram que estas espécies têm a capacidade de tolerar elevadas concentrações de elementos tóxicos como o Alumínio, podendo ser a bioacumulação uma estratégia de sobrevivência. Protocolos de propagação *in vitro* destas espécies permitem a sua produção em larga escala possibilitando assim o seu estudo em condições laboratoriais controladas. Então foram utilizadas técnicas que permitiram avaliar a forma como o pH afeta o crescimento *in vitro* e estudar os efeitos do alumínio no crescimento de rebentos e plântulas e nos parâmetros bioquímicos e fisiológicos de ambas as espécies de Plantago.

Observou-se que o pH do meio não afetou a proliferação e o enraizamento *in vitro*. Os resultados obtidos permitiram concluir que as espécies de Plantago estão aptas para crescer *in vitro* num meio com um valor de pH mais baixo que o normalmente utilizado em culturas de tecidos vegetais, o que está de acordo com o fato que ambas as espécies colonizam solos ácidos. Ambas as espécies acumulam quantidades semelhantes e consideráveis de Al nos seus tecidos, principalmente nas raízes. A espécie *P. algarbiensis* quando submetida a pH baixo e à exposição de Al sofreu um decréscimo no conteúdo dos pigmentos fotossintéticos dos rebentos.

Contudo, demonstrou-se que ambas as espécies são tolerantes ao Al^{3+} e ao H^{+} e que *P. almogravensis* parece ter uma maior capacidade de adaptação permitindo manter a sua fisiologia celular e crescimento nestas condições de stress. Algumas elucidações acerca de como os ácidos orgânicos e compostos fenólicos tomam parte no mecanismo de tolerância ao alumínio de *P. algarbiensis* and *P. almogravensis*.

Foram estudados os requisitos de temperatura/luz na germinação e os efeitos do Al na germinação das sementes. Os melhores resultados de germinação foram obtidos aos 15ºC para a luz e escuro, juntamente com o menor tempo de germinação média. Estes resultados são essenciais para o desenvolvimento de estratégias de conservação para estas espécies de Plantago.

Desta atividade profissional resultaram três artigos publicados em revistas internacionais com índex (ISI) e a exposição de um Poster numa Conferência internacional.

Neste momento, estou a trabalhar no Laboratório de Tecnologias Ambientais. Este trabalho inclui o enriquecimento de comunidades bacterianas provenientes de amostras ambientais e o screening da sua resistência e capacidade de recuperar Metais do Grupo da Platina (PGMs), nomeadamente o Paládio (II). Entre as várias amostras testadas provenientes da recolha de lamas de uma Planta de Tratamento de Águas Residuais de Lagos (Sul de Portugal) isolou-se um consórcio bacteriano resistente ao metal com a capacidade de recuperar Pd (II). Esta comunidade bacteriana foi mantida em condições anaeróbias em meio com e sem sulfato. O consórcio teve a capacidade de recuperar 50 mg/L de Pd (II) de uma solução aquosa. E removeu 98% de Pd (II) de uma solução aquosa contendo 70 mg/L de Pd (II) na presença de sulfato e 82.7% de 70 mg/L de Pd (II) na ausência de sulfato. Desta forma, este consórcio demonstrou uma excelente resistência ao paládio (II), consequentemente pode ser um potencial candidato à remoção de Pd (II) de um meio aquoso. Uma vez que é difícil manter uma ótima performance da cultura, está a decorrer um estudo de quais as melhores condições de armazenamento e a estabilidade da comunidade bacteriana.

Simultaneamente, outro estudo está a decorrer. Este consiste na síntese de nanopartículas de sulfuretos metálicos usando o sulfureto produzido pelas bactérias sulfato-redutoras.

Os precipitados de ZnS e PbS e os seus nanocómpositos de TiO_2 são obtidos através da síntese na qual se utiliza sulfureto gerado pelas bactérias sulfato redutoras, os quais são analisados por difração de Raio-X (DRX). Os precipitados dos nanocómpositos de ZnS-TiO_2 e PbS- TiO_2 obtidos, analisados por DRX revelou a existência de rutilo e anatase, duas das formas cristalinas de TiO_2, o tamanho das partículas dos nanocómpositos foi estimado na ordem dos 20 nm. As nanopartículas obtidas estão a ser aplicadas em estudos de degradação de poluentes emergentes.

Palavras-chave: Reação em cadeia da Polimerase (PCR); Polimorfismos de nucleotídeos simples (SNPs); Propagação *in vitro* de plantas; Tolerância ao alumínio; Bio-recuperação; Síntese de nanopartículas de sulfuretos metálicos

III. Table of contents

IV. Image list

V. Table list

VI. Abbreviations

aa – Aminoacid
ACP – Acyl carrier protein
AOIs – Areas of interest
BA – 6-benzyladenine
bp – base pairs
CAP – Chloramphenicol
CAT – Catalase
Chl – Chlorophyll
Dp – diameter of the particles
DW – Dry weight
EDTA – Ethylenediaminetetraacetic acid
EDX – Energy-Dispersive X-ray Spectroscopy
ETR – Electron transport rate
F Primer – Forward primer
FA – Fatty acids
FASN – Fatty acid synthase
FW – Fresh weight
GPX – Guaiacol peroxidase
IAA – Indole-3-acetic acid
KM – Kubelka-Munk
LM – Longissimus muscle
MDA – Malondialdehyde
MDH – Malate dehydrogenase
MGT – Mean Germination Time
MPM – modified Postgate medium
MS – Murashige and Skoog
MUFA – Mono-unsaturated fatty acids
N – Absolute frequency
NADP-ICDH – Nicotinamide Adenine Dinucleotide Phosphate – dependent Isocitrate Dehydrogenase
NPs – Nanoparticles
NTB – Nitroblue tetrazolium
ORF - Open reading frame
Pb – Lead
PbS – Lead Sulphide
PCR – Polymerase chain reaction
Pd – Palladium
PEPCase – Phosphoenolpyruvate carboxylase
PGMs - Platinum Group Metals
PL – Phospholipids
PPFD – Photosynthetically-active photon flux density
Pt – Platinum
PUFAs – Polyunsaturated fatty acids
QTL – Quantitative trait loci
R - Reflectance
R Primer – reverse primer
RB – Pie Rouge
RFLP – Restriction Fragment Length Polymorphism

Rh – Rhodium
ROS – Reactive oxygen species
RWC – Relative water content
SCD – Stearoyl coenzyme A desaturase
SEM – Scanning Electron Microscopy
SFA – saturated fatty acids
SNP – Single nucleotide polymorphisms
SOD – Superoxide dismutase
SRB – Sulphate-reducing bacteria
SRE – sterol regulatory element
SREBP-1 – Sterol regulatory element binding protein-1
TAG – Triacylglycerols
TE – Thioesterase
TEM - Transmission electron microscopy
TBA – Thiobarbituric acid
TCA – Trichloroacetic acid
TW – Turgid weight
UTR – Untranslated region
UV – Ultraviolet
WR – Blanc Bleu
XRD – X-ray powder diffraction
ZB – Pie Noir
Zn – Zinc
ZnS – Zinc sulphide

VII. Technical and Scientific description

Chapter 1 - Improvement of the dietetic and nutricional qualities of milk and milk's by-products by selection of the genetic potential of cattle.

1.1. Summary

The professional training in Progenus was under the direction of Dr. Robert Renaville. This work was a part of an important agro-food project, in order to obtain an improvement of dietetic and nutritional qualities of milk by selection of the genetic potential of bovine cattle, especially of the Walloon region - Belgium. This study consisted at genotyping and identification of SNPs (Single Nucleotide Polymorphisms) of interest and of major genes affecting the regulation, composition and percentage of fatty acids (FA) and of mono-unsaturated fatty acids (MUFAs) in the milk cows. Previous studies have shown that stearoyl-CoA desaturase (SCD), sterol regulatory element-binding protein 1 (SREBP-1), and fatty acid synthase (FASN) genes presented interesting correlations between their enzymatic activity and fatty acid (FA) composition and MUFAs percentages. Thus, it was performed the optimization of a method for genotyping SCD, SREBP-1 and FASN genes based on PCR.

In this study, cows of 5 breeds, Holstein, Simmental, Blanc Blue, Pie Rouge, Pie Noir, were genotyped at exon 5 of SCD, at intron 5 of SREBP-1. A SNapShot assay was performed for fast and simple detection of SNPs in the FASN gene (exons 1, 34 and exons 39, 42 in the thiosterase (TE) domain).

In Belgium, Holstein is the most important breed in terms of milk production. In this breed's exon 5 of SCD gene, three SNP were found, however only one (position 10329) codes for a different AA codon: alanine (allele C) or valine (allele T).

Large 84 bp insertion (long type: L) and deletion (short type: S) were found in intron 5 of bovine SREBP-1 in the studied cattle. All the Holstein studied for the genotype of bovine SREBP-1 gene presented type LL thereby being homozygous L type. Holstein breed also presented g.17924GG homozygous type of FASN gene, reponsible for higher MUFA milk content.

Keywords: Polymerase chain reaction (PCR); Restriction Fragment Length Polymorphism (RFLP); Stearoyl-coenzyme A desaturase (SCD); Sterol regulatory element binding protein-1 (SRBP-1); Fatty acid synthase (FASN); Single nucleotide polymorphisms (SNPs)

1.2. Introduction

The milk fatty acid (FA) profile is far from the optimal fat composition in regards to human health [1]. Dietary fatty acids are known to have a major influence on human health, particularly in countries whose populations are well-nourished, such as in developed countries where milk and meat are major components of dietary intake. It is generally accepted that saturated fats containing fatty acids with a chain length of 14 or 16 carbons, commonly found in beef meat and cow's milk, are risk factors in coronary heart disease. For example, myristic acid (C14:0) is hypercholesterolemic and raises concentrations of both low-density lipoprotein and high-density lipoprotein cholesterol compared with oleic acid (C18:1). In contrast, those fatty acids with a carbon chain length of at least 18, especially unsaturated fatty acids, are considered to be beneficial to human health [2]. The FA fraction of ruminant's milk contains several compounds of great interest for human health, such as monounsaturated FA (mainly oleic acid) and conjugated linoleic acids (CLA) [3]. The natural sources of variation, such as feeding or genetics, could be used to increase the concentrations of unsaturated fatty acids. The impact of feeding is well described. However, genetic effects on the milk FA composition begin to be extensively studied [1].

Studies aimed at finding efficient strategies to improve the nutritional quality of milk concluded that feeding supplementation is the most efficient way to modify milk FA, but a recent study suggested that the genetic improvement of the nutritional quality of milk based on FA profile may be possible [1].

For few years, some Belgian and Dutch breeders used specific feeding to increase the concentrations of unsaturated FAs in their milk, especially of omega-3 (ω-3) and CLA. Although this method is efficient, the effects are not durable. If the feeding supplementation stops, the improvement of FA composition disappears. So, animal selection using genetic variability of FAs should transmit from generation to generation this nutritional improvement. For this propose, a selection index needs to be developed [2].

The search for loci affecting FA profiles and their use in marker assisted selection programs offer an alternative to modify nutritional qualities of milk through genetic selection [3].

1.2.1. Stearoyl-CoA desaturase (SCD) gene

The SCD gene level expression is pointed out as one of the possible origins of FA variation in milk. This gene is expressed in several tissues and organs, principally in mammary gland and adipose tissue but also in liver, muscle, lung, brain, heart [4] and SCD mRNA expression is affected by environmental factors including diet and age.

The SCD plays a key role because is the rate-limiting enzyme in the cellular biosynthesis of mono-unsaturated fatty acids (MUFAs). It is located in the endoplasmic reticulum and catalyzes the insertion of a cis double bond between carbons 9 and 10 (Δ^9-position) in a large spectrum of medium- and long-chain saturated fatty acids, with preferences for C16:0 (palmitic acid) and C18:0 (linoleic acid) [4, 5].

The SCD gene was also indicated as a primary candidate gene to change the proportion of saturated vs. unsaturated FA in milk, also increasing the conjugated linoleic FA content, which is purported to possess anticarcinogenic properties [6].

The SCD gene has been mapped in cattle on the bovine chromosome BTA26 (26q21). The complete bovine SCD mRNA, which spans 5.1 kb and codes for a protein of 355 aa, has been cloned and sequenced (GenBank accession No. AY241932). Few authors identified eight single nucleotide polymorphisms (SNPs) in various bovine breeds (Holstein, Jersey and Brown-Swiss): three SNP's were detected on the 5^{th} exon (A702G, C762T, and T878C) and 5 were found in the 3' untranslated region (UTR) of the SCD gene [3, 4].

Taniguchi and colleagues [7] identified two types of SCD gene with SNPs in the ORF of SCD cDNA, in which an amino acid replacement at 878 bp (T to C) was predicted to cause substitution from valine (type V) to alanine (type A) in the SCD protein and also found the nucleotide substitutions at 702 bp (G to A), 762 bp (C to T) in open reading frame (ORF), and 1905 bp (T to C), 3143 bp (C to T), 3351 bp (A to G), 3537 bp (A to G), and 4736 bp (A to G) in 3' untranslated region (UTR).

Some authors have classified the SCD gene into three genotypes, VV, VA, and AA genotyping the SCD gene by PCR-RFLP (Fig. 1.1) and compared fatty acid composition among them [7, 8].

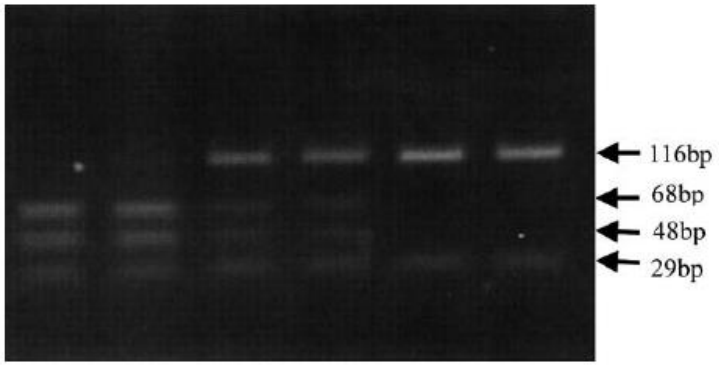

Figure 1.1 – Genotyping of SCD at the 878 bp polymorphic position. Digestion of an amplified fragment, including 878 bp polymorphic position by restriction enzyme Fnu4HI, shows genotypes AA (mutant C), VA (heterogygotic C/T), and VV (mutant T). The arrowheads show the size of the DNA fragment (bp). The DNA fragments were size fractioned by using 1% agarose gel. [7].

The three SNP of exon 5 are in linkage disequilibrium that result in 2 haplotypes; one of these SNP (position 10329) is the site of an amino acid replacement, substitution of valine (V) (allele T) for alanine (A) (allele C) [6, 7]. The Val (valine) variant was identified as the ancestral allele. Some authors found that the Val residue may change the enzyme catalytic activity compared with Ala (alanine) [7, 8].

They showed that, in Japanese Black cattle, allele C (type A) was more frequently associated with a higher content of MUFA in carcasses, and suggested that genotyping for this region would be a useful tool for selection of favorable beef carcasses [7] and consequently also for milk selection.

Comparison of MUFA content and melting point in fat tissue among three SCD genotypes and sire groups (Table 1.1).

Table 1.1 – Effects on MUFA (%) content and melting point (ºC) in fat tissue among three SCD genotypes and sire groups [7].

Effect	*n*	*MUFA (%)*	*Melting point (°C)*
Genotype			
AA	278	58.8 ± 0.1^{a}	25.4 ± 0.2^{a}
VA	635	58.2 ± 0.1^{b}	26.1 ± 0.1^{b}
VV	90	57.1 ± 0.3^{c}	27.6 ± 0.3^{c}

Mean values with different superscripts in the same column differ significantly ($P<0.001$).

MUFA indicates the percentage of mono-unsaturated fatty acids including C14:1, C16:1, and C18:1; n – Absolute frequency

These genetic studies have demonstrated associations of SNPs in bovine SCD gene with higher MUFA content and lower melting point in *longissimus muscle* (LM) adipose

tissues and with enhanced content of oleic acid and total MUFAs in milk cows. It was verified that SCD type A gene contributed to higher MUFA percentage and lower melting point in intramuscular fat (Table 1.1) [7].

Some authors [7, 8] found that heterozygous Val/Ala (alleles C/T) animals had higher C16:1/C16:0 in intramuscular fat than did homozygous Val (alleles TT) animals. Whereas, milk of homozygous AA cows had greater content of cis-9 C18:1 and total monounsaturated fatty acids and higher C14:1/C14 ratio than did milk of VV cows [4].

1.2.2. Sterol regulatory element binding protein (SREBP-1) gene

The sterol regulatory element binding proteins (SREBPs) have three SREBP isoforms, SREBP-1a, SREBP-1c, SREBP-2, each one have different roles in lipid synthesis. *In vivo* studies using transgenic and knockout mice suggested that SREBP-1c is involved in FA synthesis and insulin induced glucose metabolism (particularly in lipogenesis), whereas SREBP-2 is relatively specific to cholesterol synthesis. The SREBP-1a isoform seems to be implicated in both pathways [9].

Thus, SREBPs belong to the original basic helix-loop-helix-leucine zipper family of transcription factors that are considered as master regulators of cholesterogenesis and lipogenesis, regulating lipid homeostasis by controlling the gene expression of a range of enzymes which are relevant to lipid and fatty acid metabolism in tissue, therefore are required for endogenous cholesterol, FA (such as SCD enzyme gene expression), triacylglycerol and phospholipid synthesis [9, 10].

The bovine SREBP-1 gene detected revealed the most similarity with human SREBP-1a sequence [10], which binds a sterol regulatory element (SRE) sequence at the upstream of SCD gene and has a transcriptional regulatory activity [9]. Hoashi and colleagues found that bovine SREBP-1 includes 3441 bp corresponding to 1146 of the deduced amino acids [10].

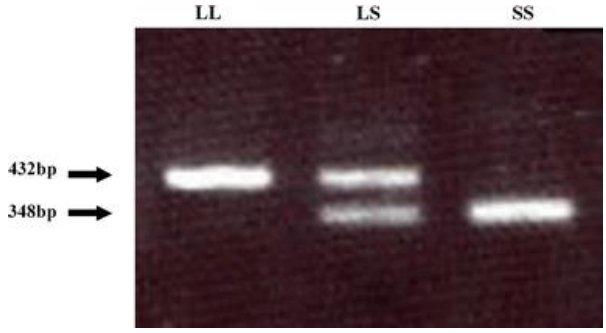

Figure 1.2 – Genotyping of *SREBP-1* indel polymorphism in intron 5. The arrowheads show the size of DNA fragment (bp). These DNA fragments were size fractionated using 1% agarose gel [10].

The PCR products of bovine SREBP-1 revealed the existence of a large 84 bp insertion (long type of 432 bp: L) and deletion (short type of 348 bp: S) in the intron 5 (Fig. 1.2), although there was no notable mutation in exon regions [10].

SREBP genotypes might affect MUFA content through regulation of SCD expression [10]. The comparison between SREBP-1 and SCD genotypes in terms of the unsaturated fatty acid content, and melting point is shown in Table 1.2.

Table 1.2 – Comparison of MUFA content and melting point of intramuscular fat among SREBP-1 and SCD genotypes [10].

Genotype	*N*	*MUFA (%)*	*Melting point (ºC)*
SREBP-1			
LL	98	57.7 ± 0.3a	26.7 ± 0.4a
LS	437	58.1 ± 0.2a	26.3 ± 0.2a
SS	71	59.0 ± 0.3b	25.1 ± 0.4b
SCD			
AA	143	59.3 ± 0.2a	24.8 ± 0.3a
AV	418	58.4 ± 0.2b	25.9 ± 0.2b
VV	45	57.1 ± 0.4c	27.4 ± 0.5c

Mean values with different alphabets in the same column differ significantly ($P<0.05$).
MUFA indicates the percentage of monounsaturated fatty acids including C14:1, C16:1, and C18:1.

In terms of a genetic polymorphism the ANOVA revealed that the effects of both SCD and SREBP-1 genotypes were significant for the physiologic characteristics of cattle fat. In SCD mutation (Val293Ala), the genotype AA showed 2.1% higher MUFA percentage than the genotype VV. The genotype AA showed at 2.5ºC lower melting point than the genotype VV. In the SREBP-1, the genotype SS showed 1.3% higher MUFA percentage than the genotype LL. In addition, the genotype SS showed a 1.6ºC lower melting point than the genotype LL (Table 1.2) [10]. And when the genotype of bovine SREBP-1 gene was (L/S) having heterozygous L and S type, the percentage of MUFAs was higher than that in the case of genotype (L/L) having homozygous L type (Table 1.2).

The results shown in Table 1.3 represent the relation among the combination of these both genotypes, the unsaturated fatty acid content, and melting point.

Table 1.3 – Comparison of MUFA content and melting point of intramuscular fat in the relation among the combination of the SREBP-1 and SCD genotypes [11].

Genotype	*N*	*MUFA (%)*	*Melting point (ºC)*
SREBP-1/ SCD			
LL/AA	24	58.5 ± 0.48	26.0 ± 0.66
LL/AV	67	58.0 ± 0.29	26.4 ± 0.39
LL/VV	7	56.3 ± 0.89	28.4 ± 1.22
LS/AA	99	59.3 ± 0.89	24.9 ± 0.32
LS/AV	309	58.2 ± 0.13	26.3 ± 0.18
LS/VV	29	57.3 ± 0.44	27.3 ± 0.60
SS/AA	20	59.2 ± 0.53	24.3 ± 0.72
SS/AV	42	59.6 ± 0.36	24.7 ± 0.50
SS/VV	9	57.2 ± 0.78	27.3 ± 1.10

Mean values with different alphabets in the same column differ significantly ($P<0.05$).

Based on these results, it can be evaluated that, if a cattle has a combination of "S type" as SREBP-1 genotype and "A type" as SCD genotype, then the cattle will produce better quality of beef. Especially, if a cattle has three or more alleles, as a total number of a number of "S type" alleles of SREBP-1 genotype and a number of "A type" alleles of SCD genotype, then the cattle can be evaluated to produce better quality of beef, with higher unsaturated fatty acid content and lower melting point [11]. Thus, the relation among the combination of the SREBP-1 and SCD genotypes that presented higher MUFA percentage and lower melting point were LS/AA, SS/AA, and SS/AV revealing that these combinations are also the best in terms of milk quality, however the combinations did not differ significantly among them (Table 1.3).

1.2.3 – Fatty acid synthase (FASN) gene

Fatty acid synthase (FASN) is a complex homodimeric enzyme that regulates *de novo* biosynthesis of long-chain fatty acids in mammals. With seven active sites, FASN is a cytosolic enzyme which catalyzes all the reaction steps in the synthesis of palmitate from acetyl-Coenzyme A and malonyl-Coenzyme A in the presence of NADPH. In animals the synthesis of FASN is a regulated process which depends on diet and hormones at all stages of life, even during neonatal development and differentiation. Because FASN enzyme plays a central role in *de novo* lipogenesis in mammals, it is a candidate gene for fat content in milk animals [2].

Roy and colleagues [12] reported the localization of the bovine FASN gene on bovine (BTA) chromosome 19q22 where several quantitative trait loci (QTL) affecting milk-fat content and related traits have been described by fluorescence in situ hybridization and somatic cell hybrid analysis [12].

Zhang and colleagues [13] hypothesized that variation in the thioesterase (TE) domain of FASN gene among the individuals would be a candidate for heritable differences in fatty acid composition and might be used to improve the healthfulness of the fatty acid composition of beef while maintaining other positive physical and chemical attributes of the product [13]. The TE domain within the FASN complex is responsible for the termination of fatty acid synthesis and release of newly synthesized saturated fatty acids (SFA), mainly C16:0, by hydrolyzing the acyl-S-phosphopantetheine thioester, which is bound to the proceding acyl carrier protein (ACP) domain. Both C14acyl-ACP and C16acyl-ACP are substrates for TE. The TE domain of FASN, therefore, plays an essential role in the determination of the product chain length of FASN [13].

The TE domain is located at 3'-end of FASN and is encoded within four exons (exons 39-42).

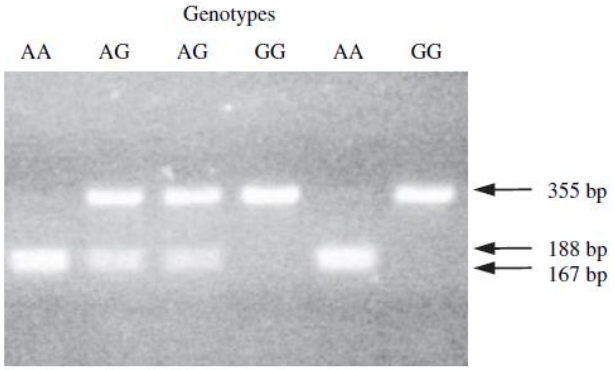

Figure 1.3 – Genotyping the g.17924A>G polymorphism. The DNA digested with the restriction enzyme MscI revealed the genotypes g.17924AA, 17924AG, 17924GG. Arrows indicate the size of DNA fragments (bp). These DNA fragments were size fractionated on 2% agarose gels [13].

Three nucleotide substitutions were identified in this domain, which were AF285607: g.17924A>G, g.18663C>T and g.18727C>T. Polymorphism g.17924A>G was predicted to result in an amino acid replacement from threonine (ACC) to alanine (GCC) in FASN protein (Fig. 1.3) The other two SNPs, g.18663C>T and g.18727C>T, are silent mutations [13]. Among the three SNPs identified, the g.17924A>G and g.18663C>T SNPs were significantly associated with the concentrations of several fatty acids in phospholipids (PL), triacylglycerols (TAG) and total lipids. The percentages of

oleic acid (C18:1), docosapentaenoic acid (C20:5) and total MUFA were greater in Angus cattle with the g.17924GG genotype than those with the g.17924AA genotype [13]. The mutations g.15603G>A and g.15531C>A are directly associated with the fatty acid composition of milk and the g.16021G allele in exon 34 (resulting in an alanine) is associated with increased milk-fat content [12]. The G>C substitution identified in the bovine FASN gene (g.841 G>C) changes the putative Sp1 transcription factor-binding site in the untranslated exon 1; that is because, whereas allele G contains a Sp1-binding site, allele C does not. RNA secondary structure prediction within the 5'-UTR predicts two different structures for these alleles [12].

It was evidenced that SNPs in the bovine FASN gene are associated with variation in the fatty acid composition of adipose fat and milk fat [2].

Thus, the authors concluded that functionally advantageous SNPs of the FASN gene may be used as DNA markers to select breeding stock with healthier fatty acid content of *Longissimus muscle* (LM) [13] and milk.

1.3. Objectives

The main objective of this work was the identification of genetic mutations (polymorphisms) in the most important genes that affect fatty acid production and composition of bovine milk, in order to do a selection of cattle using the genetic variability of fatty acids that should be transmitted from generation to generation, thus leading to a nutritional improvement. Therefore, the search for loci affecting FA profiles and their use in marker selection programs offer an alternative to modify nutritional qualities of milk through genetic selection. To achieve this aim it was performed the genotyping of SCD, SREBP-1, and FASN genes in order to establish a comparison of the genetic analysis of cattle with the fatty acid composition of milk.

1.4. Material and methods

1.4.1. Solutions and buffers

- Extraction Solutions:

NE: 10 mM NaCl, 10 mM EDTA, pH 7.0 (0.29 g NaCl, 1.86 g EDTA, H_2O in 500 ml, pH 7.0) was used to lyse red blood cells and to remove hemoglobin.

Solution A: 200 mM NaOH was used to lyse white cells

Solution B: 200 mM HCl + 100 mM Tris-HCl, pH 8.5 (10 ml 1M Tris-HCl, pH 8.5; 1.67 ml HCl; H_2O in 100 ml)

- Electrophoresis buffer:

TAE 0.5x: (Tris-Acetate-EDTA): Tris base 20mM, Acetic Acid 20mM and EDTA 0.5mM

a) 1.5% agarose gel

- 1.5 g agarose (Eurogentec "Molecular Biology Grade")
- 100 mL of TAE 0.5X buffer
- 8 µl of ethidium bromide (GeneChoice)

b) 3% agarose gel

- 3 g agarose (Eurogentec "Molecular Biology Grade")
- 100 mL of TAE 0.5X buffer
- 8 µl of ethidium bromide (GeneChoice)

1.4.2. Methods

1.4.2.1. Fast DNA extraction from whole bovine blood

Protocol, used in case of need, to extract genomic DNA from blood samples instead of the already given genomic DNA by l'Unité de Zootechnie of the Walloon Region.
It was added 200 µl of blood in an eppendorf, in order to wash the blood three times with NE solution. The solution was centrifuged 10 seconds at 14000 *g*, the supernatant was discarded. After, the NE was added to the pellet and the previous steps were repeated twice. After the wash step it was added 50 µl of solution A to the pellet, the

solution was mixed and placed at 97 °C for 15 min. Finally, 50 µl de solution B was added. The solution was mixed and then it was ready used for PCR.

1.4.2.2. PCR-RFLP – SCD gene

A polimerase chain reaction - restriction fragment length polymorphism (PCR-RFLP) was realized in order to detect nucleotide substitutions in the exon 5 of the bovine SCD gene. A PCR-RFLP was performed at 878 bp mutation site counted from the translation initiation site, using the following primer set (GenBank accession, nº AY241932): (Forward - F, sense primer); (Reverse - R, antisense primer)

F - 5'- ATGTATGGATACCGCCCTTATGAC - 3';

R - 5'- TGCTGCTTAGGGTATTAGGTTACGTGCCAGAAA - 3'

The PCR amplification was performed with 1 µl of genomic DNA (the genomic DNA was provided by l'Unité de Zootechnie of the Walloon Region), 2.5 µl of 10X PCR buffer (GE Healthcare, Illustra), 200 µM final concentration of each nucleotide (dNTPs from GE Healthcare), 10 pmol of each primer (Sigma), 1 unit of Taq polymerase (GE Healthcare, Illustra,), and double-distilled water to a final volume of 25 µl.

Amplifications were performed with thermal cycler, PTC-200 DNA Engine (MJ Research, Inc.), with the following thermo-cycling protocol: initial denaturation at 94ºC for 2 min, followed by 30 cycles of 94ºC for 30 s, 60ºC for 30 s, and 72ºC for 1 min, with final extension step, 72ºC for 7 min.

The 1.5 % agarose gel was charged with 5 µl of PCR products mixed with 2 µl of 6X Orange DNA Loading Dye (Fermentas). O'GeneRuler 50 bp DNA Ladder (Fermentas) was used to size and estimate the approximate quantification of the DNA fragments on agarose gel. The migration was performed at 100 V for 25 min. The obtained bands of DNA were visualised using the program QuantityOne (BioRad).

The obtained fragment was digestible with Fnu4H1 enzyme.

The digestion with the restriction enzyme was performed with 20 µl of PCR product mixed with 1U of Fnu4H1 (LabLife) and incubated at 37ºC for 2 h, the inactivation of enzyme was at 65ºC for 20 min.

The 3 % agarose gel was charged with 5 µl of PCR products mixed with 2 µl of 6X Orange DNA Loading Dye (Fermentas). O'GeneRuler 50 bp DNA Ladder (Fermentas) was used to size and estimate the approximate quantification of the DNA fragments on agarose gel. The migration was performed at 100 V for 45 min. The obtained bands of DNA were visualised using the program QuantityOne (BioRad).

1.4.2.3. PCR – SREBP-1 gene

The primers set used for PCR amplification were as follows: (F, sense primer); (R, antisense primer) – (GenBank accession nº AB355703)

F-5'-CCACAACGCCATCGCCATCGAGAAACGCTAC-3';

R-5'-GGCCTTCCCTGACCTCCCAACTTAG-3'.

The PCR amplification was performed with 1 µl of genomic DNA (provided by l'Unité de Zootechnie of the Walloon Region), 2.5 µl of 10X PCR buffer (GE Healthcare), 200 µM final concentration of each nucleotide (dNTPs from GE Healthcare), 10 pmol of each primer (Sigma), 1 unit of Taq polymerase (GE Healthcare, Illustra), and double-distilled water to a final volume of 25 µl.

Amplifications were performed with thermal cycler, PTC-200 DNA Engine (MJ Research, Inc.), with the following thermo-cycling protocol: initial denaturation at 94ºC for 2 min, followed by 30 cycles of 94ºC for 30 s, 60ºC for 30 s, and 72ºC for 1 min, with final extension step, 72ºC for 7 min.

The 1.5 % agarose gel was charged with 5 µl of PCR products mixed with 2 µl of 6X Orange DNA Loading Dye (Fermentas). O'GeneRuler 50 bp DNA Ladder (Fermentas) was used to size and estimate the approximate quantification of the DNA fragments on agarose gel. The migration was performed at 100 V for 30 min. The bands of DNA were visualized using QuantityOne (BioRad) software.

1.4.2.4. PCR and SNapShot assay – FASN gene

Genetic analyses of the FASN polymorphisms were made by PCR method. On the basis of the FASN gene sequence (GenBank acession Nº AF285607) the following primers were designed:

Mutant 1 (SNAP 1 - g.841G→C - exon 1) - F-5'-CAGAGTGACCCAAGTACGC-3';

R-5'-CGGAAGTTGCGAGTCGGGAA-3'.

Mutant 2 (SNAP 2 - g.15531C→A); (SNAP 3 - g.15603G→A); (SNAP 4 - g.16021A→G - exon 34);

F-5'-GCTGAAGGCGGGCATCCGGA-3';

R-5'-GGCCGAGGCAGGTGCTAA-3'.

Mutant 3 (SNAP 5 - g.17924A→G - exon 39); (SNAP 6 - g.18663C→T - exon 42);

F-5'-AGAGCTGACGGACTCCACA-3';

R-5'-CTACCTACCACGGCAACGTG-3'.

PCR amplifications were performed in 25 µl volume of reaction mixture containing: 1 µl of genomic DNA, 10 picomoles of each primer (Sigma), 1 unit of Taq DNA Polymerase (GE Healthcare), 2.5 µl of 10X PCR buffer (GE Healthcare), 200 µM final concentration of each nucleotide (GE Healthcare). Amplifications were performed with thermal cycler, PTC-200 DNA Engine (MJ Research, Inc.) with the following protocol: 94ºC for 2 min; followed by 35 cycles of 94 ºC for 30 s, 60 ºC for 45 s and 72ºC for 60 s; with a final extension step at 72ºC for 7 min.

The PCR product was purified by SNaPshot (High Pure PCR Product Purification kit, 1732668, Roche) to remove dNTPs and primers.

The primers used for SNapshot PCR amplification were as follows (GenBank accession Nº AF285607):

Mutant 1 SNAP 1 - 5'-CCTCAGCCGTTCGCACAGCC-3'

Mutant 2 SNAP 2 - 5'-AAACACATCGGCAAAGTGGT-3'

Mutant 2 SNAP 3 - 5'-GCAGCAGTGCGTGAACAGGG-3'

Mutant 2 SNAP 4 - 5'-CCAGCGACGTCAGC-3'

Mutant 3 SNAP 5 - 5'-CCGTGTTCCACAGCCTGGCC-3'

Mutant 3 SNAP 6 - 5'-TTTGCTGCGCGTTCCTTCTA-3'

The SNapShot reaction mix it was performed, using a SNaPshot® Multiplex Kit (Applied Biosystems), thus for each mutant a reaction mixture consisted of 4 µl of double-distilled water, 16 µl of SNP ready and 4 µl of primer mixture, SNAP 1 primer for mutant 1, SNAP 2, 3, 4 primers mix for mutant 2 and SNAP 5, 6 primers mix for mutant 3 and after 6 µl of this reaction mix was joined together with 4 µl of purified PCR product of the three mutants samples.

The amplification was performed using a thermo-cycling protocol with an initial denaturation at 94ºC for 2 min, followed by 35 cycles of 94ºC for 30 s, 60ºC for 45 s, and 72ºC for 1 min, with final extension step, 72ºC for 7 min (SNAP program), to stop the reaction was added 1 µl of alkaline phosphatase and CIP program. The sequence was verified by GeneMapper 4.0 (Applied Biosystems).

1.5. Results

1.5.1. PCR-RFLP – SCD gene

In this work bovine SCD gene of Holstein, Simmental, Blanc Bleu (WR), Pie Rouge (RB) and Pie Noir (ZB) breeds was genotyped at exon 5 by PCR-RFLP (Fig. 1.4 and 1.5).

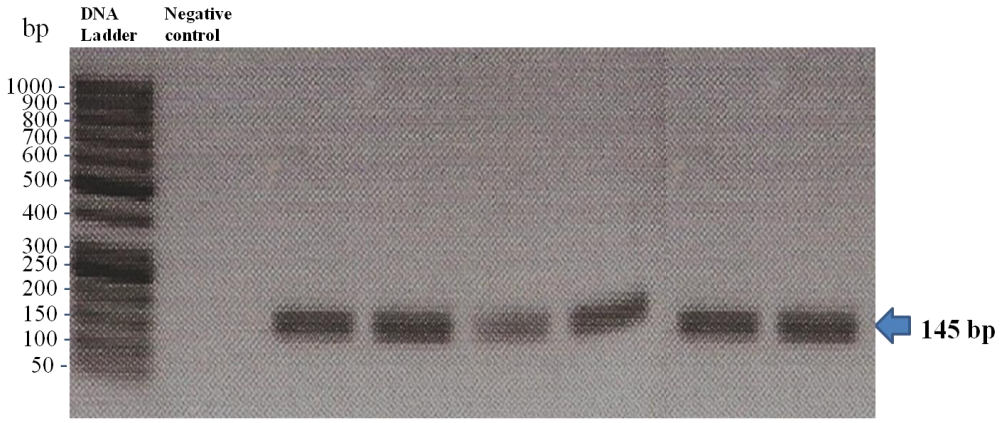

Figure 1.4 – Genotyping of SCD in the exon 5 at the g.10329 mutation site (878 bp polymorphic position). Representative result of all the samples analyzed. The arrowheads show the size of the SCD gene DNA fragment (bp). The DNA fragments were size fractioned by using 1.5% agarose gel.

The PCR revealed the expected 145 bp fragment comprising exon 5 of bovine SCD gene which was amplified at the g.10329 mutation site (Fig. 1.4).

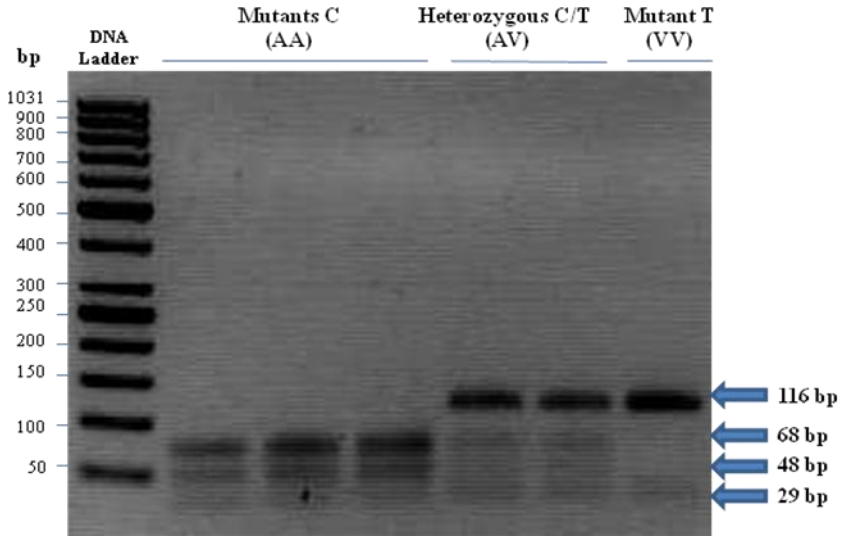

Figure 1.5 – Genotyping of SCD at the 878 bp polymorphic position. Representative result of all the samples analyzed. Digestion of an amplified fragment, including 878 bp polymorphic position by restriction enzyme Fnu4HI, shows genotypes AA (mutant C), AV (heterogygote C/T), and VV (mutant T). The arrowheads show the size of the SCD gene DNA fragment (bp). The DNA fragments were size fractioned by using 3% agarose gel.

The studied breeds were classified into three genotypes, VV, VA, and AA (Fig 1.5 and Table 1.3), in order to compare milk's fatty acids composition among the several breeds according to the bibliography.

According to some authors [10, 11] the SCD type A gene contributed to higher MUFA percentage and lower melting point in intramuscular fat.

Table 1.4 – Distribution of SCD genotypes (Mutant C (AA); heterozygote C/T (AV); mutant T (VV)) in the 96 Holstein, 114 Simmental, 35 Blanc Bleu, 49 Pie Rouge and 36 Pie Noir cattle breeds samples considered.

Cattle breeds	Genotype	Absolute frequency (n)	Relative frequencies (%)
Holstein	**AA**	41	42.71
	AV	52	54.17
	VV	3	3.125
	Total	**96**	**100**
Simmental	**AA**	25	21.93
	AV	60	52.63
	VV	29	25.44
	Total	**114**	**100**
Blanc Blue (WR)	**AA**	18	51.43
	AV	15	42.86
	VV	2	5.71
	Total	**35**	**100**
Pie Rouge (RB)	**AA**	31	63.27
	AV	14	28.57
	VV	4	8.16
	Total	**49**	**100**
Pie Noir (ZB)	**AA**	22	61.11
	AV	13	36.11
	VV	1	2.78
	Total	**36**	**100**

The SCD polymorphisms have been found in Holstein, Simmental, Blanc Blue, Pie Rouge and Pie Noir cattle breeds (Fig. 1.5 and Table 1.4).

1.5.2. PCR – SREBP-1 gene

To survey polymorphisms it was performed a PCR to amplify the 5 intron of bovine SREBP-1. As Taniguchi and colleagues [7], in this work it was observed a length polymorphism in the amplified products of intron 5. To estimate the gene frequencies of the 84-bp deletion (short type: S) and insertion (long type: L), the genotyping of 76 Holstein, 47 Simmental, 33 Blanc Bleu (WR), 48 Pie Rouge (RB), and 36 Pie Noir (ZB) breeds was performed (Fig. 1.6 and Table 1.5).

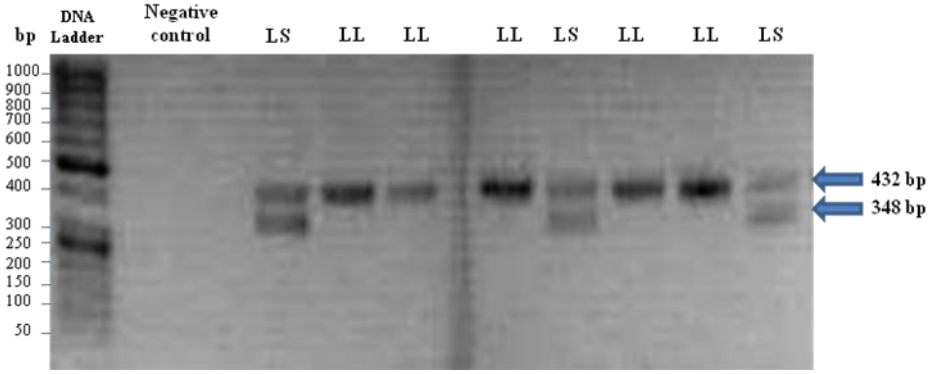

Figure 1.6 – Genotyping of SREBP-1 indel polymorphism in intron 5. Representative result of all the samples analyzed. The arrowheads show the size of the DNA fragment (bp). The DNA fragments were size fractioned by using 1.5% agarose gel.

The different lengths of PCR products were detected as S (348 bp) or L (432 bp) types (Figure 1.6).

The distribution of SREBP-1 genotypes in the 76 Holstein, 47 Simmental, 33 Blanc Blue, 48 Pie Rouge and 36 Pie Noir cattle breeds samples was analyzed (Table 1.5).

Table 1.5 – Distribution of SREBP-1 genotypes in the 76 Holstein, 47 Simmental, 33 Blanc Blue, 48 Pie Rouge and 36 Pie Noir cattle breeds samples considered.

Cattle breeds	Genotype	Absolute frequencies (n)	Relative frequencies (%)
Holstein	LL	76	100
	LS	-	-
	SS	-	-
	Total	76	100
Simmental	LL	41	87.2
	LS	6	12.8
	SS	-	-
	Total	47	100
Blanc Blue (WR)	LL	33	100
	LS	-	-
	SS	-	-
	Total	33	100
Pie Rouge (RB)	LL	45	93.75
	LS	3	6.25
	SS	-	-
	Total	48	100
Pie Noir (ZB)	LL	35	97.22
	LS	1	2.78
	SS	-	-
	Total	36	100

The genotyping frequency of Holstein was 100% in LL type, whereas genotyping frequencies of Simmental were 41% LL type and 6 % LS type. Although the genotype SS type was not found in the studied bovine breeds (Table 1.5).

1.5.3. PCR and SNapShot assay – FASN gene

The SNaPshot® Multiplex System primer extension-based method enables multiplexing up to 10 single nucleotide polymorphisms (SNPs). This system is used to screen and

confirm SNPs and to detect minor sequence variations. This system is of great utility for genotyping, mutation, detection and mapping.

Fatty acid synthase (FASN) is a multifunctional protein that carries out the fatty acids synthesis, playing a central role in *de novo* lipogenesis in mammals.

A SNapShot assay was performed for several quantitative trait loci (QTL) and in TE domain affecting milk-fat content in order to identify single nucleotide polymorphisms (SNPs) in bovine FASN gene (Figure 1.7, 1.8 and 1.9).

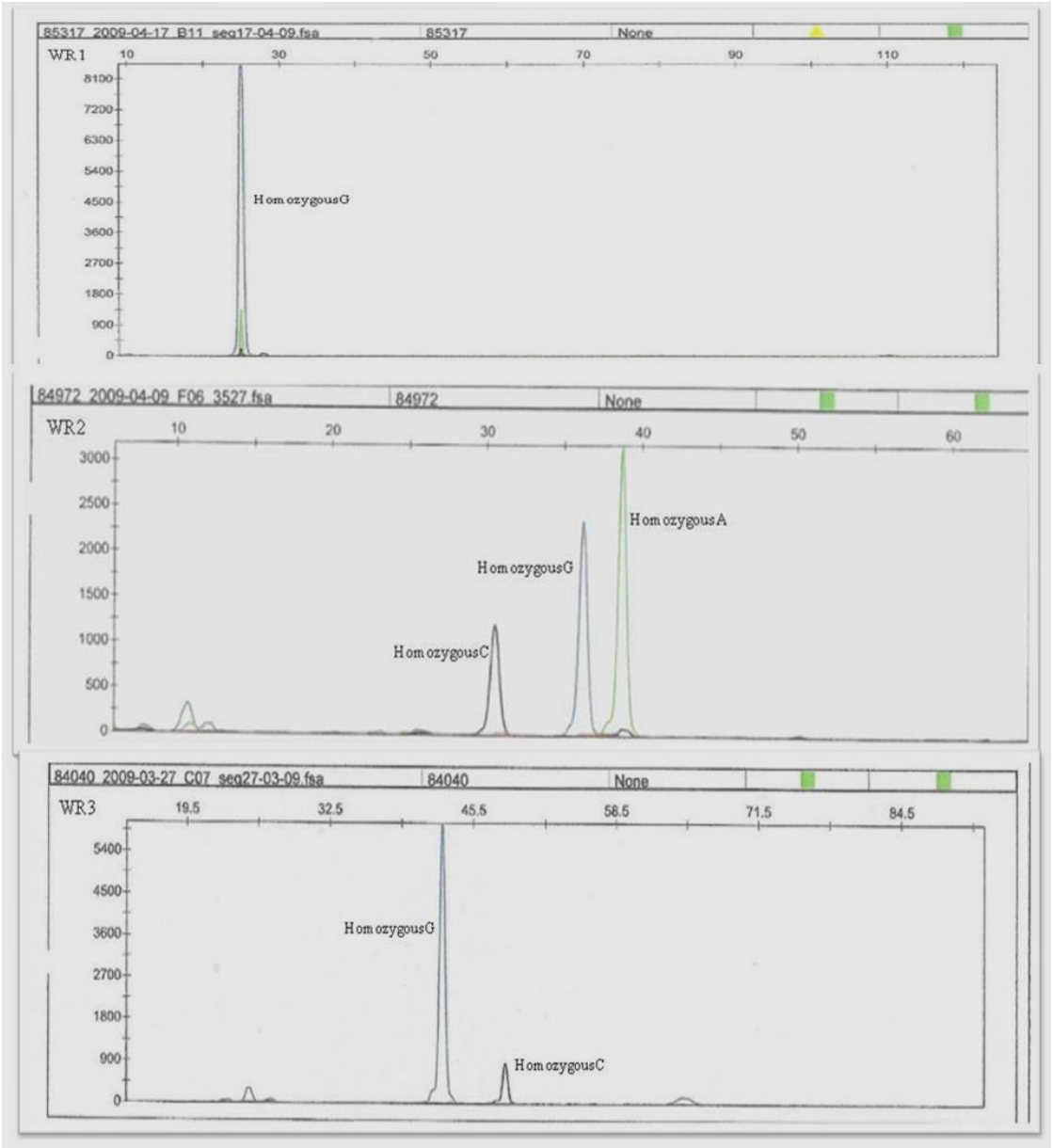

Figure 1.7 – SNapShot DNA sequencing identified several single base pair changes of FASN gene. The mutante 1 sample represented a homozygous G at g.841 position, the mutante 2 samples presented homozygous C (g.15531C), G (g.15603G) and homozygous A (g.16021A) genotypes, and the mutant 3 presented homozygous G (g.17924G) and homozygous C (g.18663C). Sample 1 of Blanc Bleu breed: WR1

(mutant 1), WR2 (mutant 2), WR3 (mutant 3). The nucleobases are represented by different colours: Adenine – Green; Cytosine – Black; Guanine – Blue; Thymine – Red

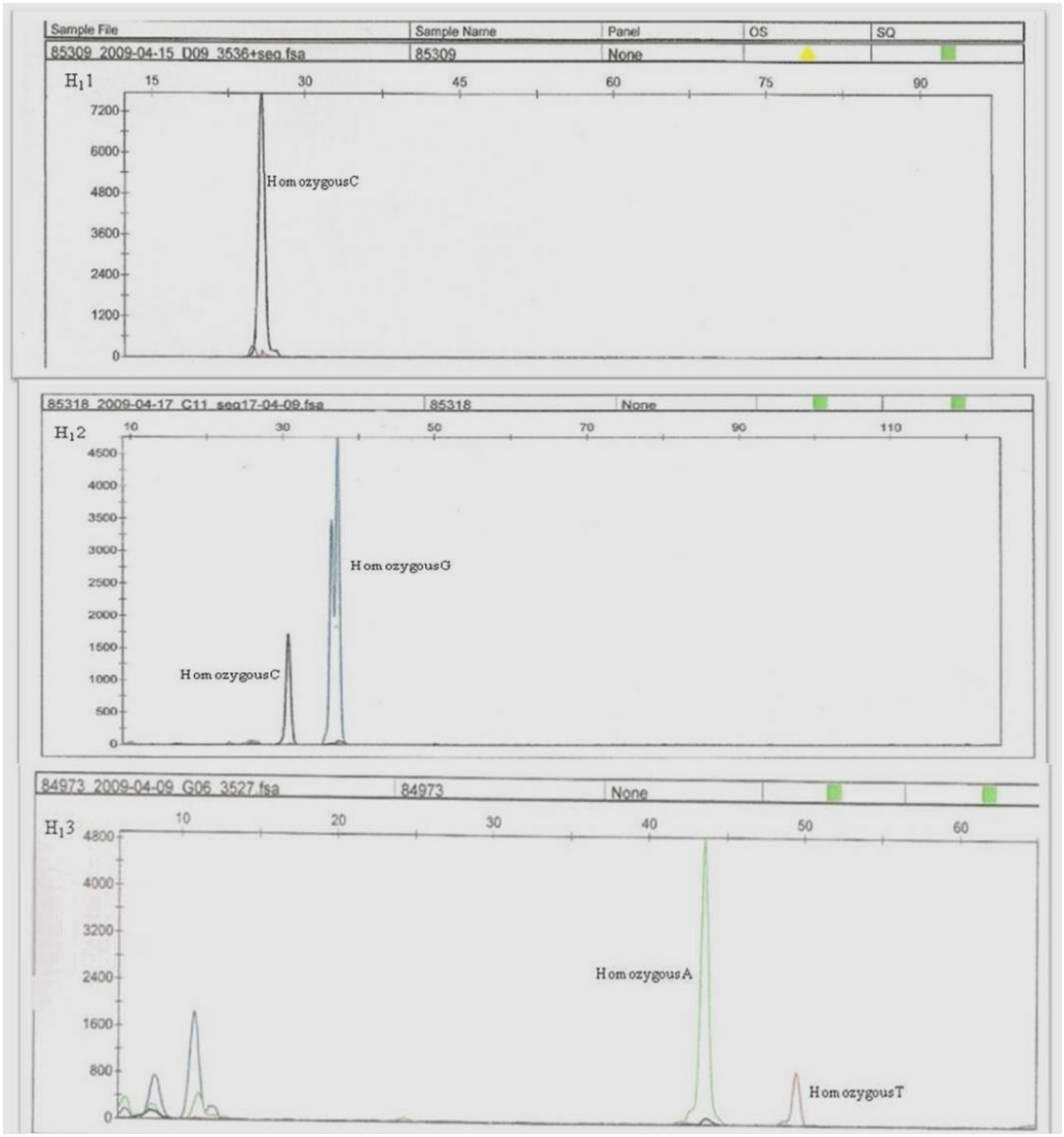

Figure 1.8 – SNapShot DNA sequencing identified several single base pair changes of FASN gene. The mutante 1 sample represented a homozygous C genotype at g.841 position, the mutante 2 samples presented homozygous C (g.15531C), G (g.15603G) and the mutant 3 presented homozygous A (g.17924) and homozygous T (g.18663). Sample 1 of Holstein breed: $H_1$1 (mutant 1), $H_1$2 (mutant 2), $H_2$3 (mutant 3). The nucleobases are represented by different colours: Adenine – Green; Cytosine – Black; Guanine – Blue; Thymine – Red

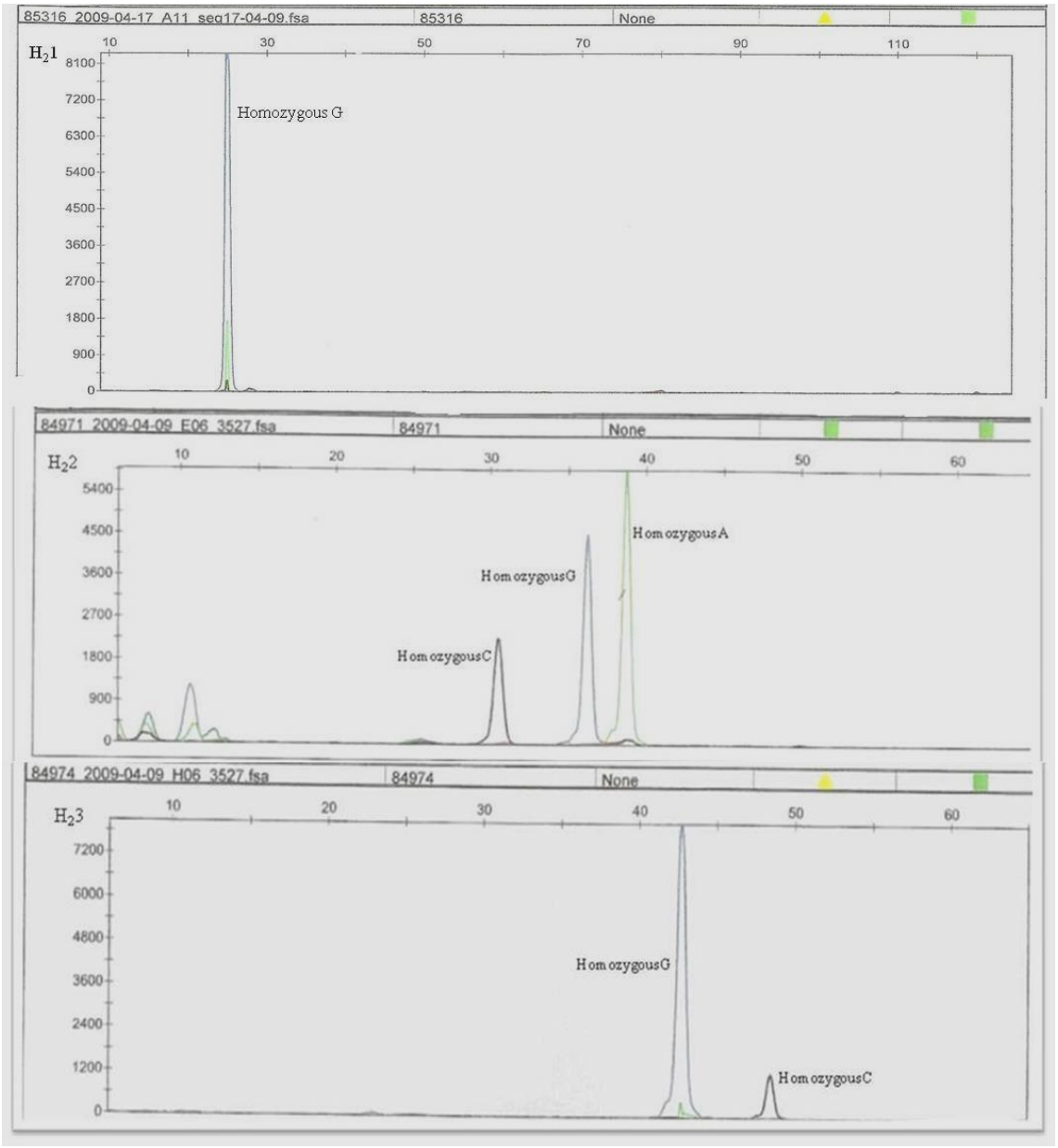

Figure 1.9 – SNapShot DNA sequencing identified several single base pair changes of FASN gene. The mutante 1 sample represented a homozygous G genotype at g.841 position, the mutante 2 samples presented a homozygous C (g.15531) and G (g.15603) and homozygous A (g.16021) genotypes, and the mutant 3 presented homozygous G (g.17924) and homozygous C (g.18663) genotypes. Sample 2 of Holstein breed: $H_2$1 (mutant 1), $H_2$2 (mutant 2), $H_2$3 (mutant 3). The nucleobases are represented by different colours: Adenine – Green; Cytosine – Black; Guanine – Blue; Thymine – Red

By SNapShot DNA sequencing of FASN gene several single base pair changes were identified in samples of Blanc Blue and Holstein breeds (Fig. 1.7, 1.8 and 1.9).

1.6. Discussion

In Belgium, the Holsteins are the most important cattle breed and they are preferred over the other cattle breeds for the higher content of milk production.

Taniguchi and colleagues [7] found that in the three SCD genotypes differences were significant in MUFA percentage (high in type AA, middle in type AV, low in type VV) and the melting points were also significantly different between SCD genotypes (high in type VV, middle in type VA, and low in type AA).

Moioli and colleagues [6] calculated the allele frequency of the Val/Ala variant in 4 Italian breeds and found that frequency of the Val allele was the highest in Simmental (47.62%) and minimal in Chianina (22.73%). As well in this work it was found the higher VV percentage in Simmental (25.44%). Holstein presented only 3% of VV genotype and 42.71 % of AA type (Table 1.4).

In this study Holstein and Blanc Bleu breeds presented 100% LL type, whereas Simmental, Pie Rouge and Pie Noir also presented LS type for SREBP-1 genotype (Fig.1.6 and Table 1.5).

Therefore, if the genotype of bovine SREBP-1 gene is (S/S), such cattle with (S/S) can be estimated to produce better quality of milk or of beef (better taste and texture), compared with cattle with (L/L). Such polymorphism on SREBP-1 gene may be associated with the unsaturated fatty acid percentage in beef or milk fat, because the SREBP-1 gene expression level was correlated and may affect SCD gene expression level, leading to differences in fatty acid composition in the fat tissue of cattle.

Based on the bibliography, it can be evaluated that, if a cattle has a combination of “S type” as SREBP-1 genotype and “A type” as SCD genotype, then its cattle will produce better quality of milk, with higher unsaturated fatty acid content and lower melting point.

According to Table 1.3 and the obtained results it was possible to verify the followed combinations: LL/AA; LL/AV; LL/VV; LS/AA; LS/AV and LS/VV. The combination LS/AA presented the higher MUFA percentage and lower melting point, followed by LL/AA, LS/AV, LL/AV, LS/VV and finally the lower MUFA percentage and higher melting point was obtained for LS/VV combination.

The Simmental breed presented the best combination (LS/AA) from all of the breeds tested in this study, although the Simmental breed is not the best in terms of milk

production (quantitatively), whereas in the studied Holsteins only was found the combination LL/AA.

The FASN gene was identified as a positional candidate gene for some quantitative trait loci (QTL) because the location of FASN on bovine Chromosome 19q22 coincided with the estimate location of the observed QTL, and because variation in FASN activity might explain animal-to-animal variation in fatty acid composition [2, 14].

Genetic variants of FASN have been reported recently to be associated with the percentage in bovine milk [2].

In the obtained results Blanc Bleu (WR) and Holstein breeds presented the g.841CC genotype, responsible for high milk fat content, however Holstein also had g.841GG genotype the best combination in terms of MUFA content, thus less milk fat. Both breeds had g.15531CC, g.15603GG, g.16021AA, g.17924GG and g.18663CC genotypes (Fig. 1.7, 1.8 and 1.9) all of them responsible for high MUFA content in milk, while the Holstein breed sample 1 presented g.17924AA and g.18663TT genotypes (Fig. 1.8) associated with the highest content of milk fat.

Some authors [12, 13, 14] found the G to C substitution in the untranslated exon1 (g.841G>C), the allele C is significantly associated with high milk-fat content and they also found an A>G substitution in exon 34 (g.16021A>G), which determine a non-conservative substitution of threonine by alanine. The G allele in exon 34 (resulting in an alanine) is associated with increased milk-fat content. Roy and colleagues found homozygous animals for the threonine variant only in the low fat content group, although the allele was low frequency (0.03) [12, 14]. Consequently, an allelic substitution at g.15531 (A instead of C) or g.15603 (A instead of G) led to an increase in the C14:0 percentages in milk fat and a corresponding reduction in the C18:1 percentage in milk [2]. Cattle with g.18663CC genotypes had greater C18:1 and MUFA contents than did the cattle with 18663TT genotype [13]. The cattle with g.17924GG genotype presented higher percentages of C18:1 and lower percentage of C16:0 compared with the cattle with g.17924AG genotype this can be explained by GG genotype being in a linkage disequilibrium with SNPs of fatty acid elongase, resulting in the phenotype with higher rates of C16:0 elongation. The cows with GG genotype also had lower percentage of C14:0 than did the cattle with AA genotype [15]. Therefore, the g.17924GG genotypes had significantly greater health index, C18:1 and total MUFA compared to the AA genotypes, whereas the g.17924AA genotypes were more favorable in C20:3 and polyunsaturated fatty acids (PUFAs) [16].

1.7. Conclusion

In this study, cows of 5 breeds, Holstein, Simmental, Blanc Blue, Pie Rouge, Pie Noir, were genotyped at exon 5 of SCD, at intron 5 of SREBP-1 and at exons 1, 34 and exons 39-42 (thiosterase domain) of FASN gene.

In Belgium, Holstein is the most important breed in terms of milk production. In this breed's exon 5 of SCD gene, three SNP were found, however only one (position 10329) codes for a different AA codon: alanine (allele C) or valine (allele T).

A large 84 bp insertion (long type: L) and deletion (short type: S) were found in intron 5 of bovine SREBP-1 in the studied cattle. All the Holstein studied for the genotype of bovine SREBP-1 gene presented type LL thereby being homozygous L type.

For Holstein breed was verified the existence of Homozygous g.17924GG and for both Blanc Bleu (WR) and Holstein breeds were detected the g.18663CC, corresponding to genotypes associated with the highest MUFA content and consequently a decrease in milk fat.

The animal characteristics in fat composition are dependent on genetic variability of individual FAs and their groups. The application of these characteristcs to change in fat composition are of particular interest and are the focused on genetic and phenotypic correlations related to milk production and proportion/production of FAs, as well as relations between individual FAs.

1.8. Bibliographic references

[1] – Arnould, V. M.- R., Soyeurt, H. (2009) Genetic variability of milk fatty acids. J Appl Genet 50 (1), 29–39.
[2] – Morris, C. A., Cullen, N. G., Glass, B. C., Hyndman, D. L., Manley, T. R., Hickey, S. M., McEwan, J. C., Pitchford, W. S., Bottema, C. D. K., Lee, M. A. H. (2007) Fatty acid synthase effects on bovine adipose fat and milk fat. Mamm. Genome 18, 64-74.
[3] – Mele, M., Conte, G., Castiglioni, B., Chessa, S., Macciotta, N. P. P., Serra, A., Buccioni, A., Pagnacco, G., Secchiari, P. (2007) Stearoyl-Coenzyme A Desaturase Gene Polymorphism and Milk Fatty Acid Composition in Italian Holsteins. J.Dairy Sci. 90:4458-4465.
[4] – Soyeurt, H., Dehareng, F., Mayeres, P., Bertozzi, C. and Gengler, N. (2008) Variation of Δ^9- desaturase activity in dairy cattle. J. Dairy Sci. 91:3211–3224.
[5] – Garcia-Fernández, M., Gutiérrez-Gil, B., García-Gámez, E., Arranz, J.-J. (2009) Genetic variability of the Stearoyl-CoA desaturase gene in sheep. Mol. and Cellular probes 23, 107-111.
[6] – Moioli, B., Contarini, G., Avalli, A., Catillo, G., Orru, L., De Matteis, G., Masoero, G., Napolitano, F. (2007) *Short Communication:* Effect of Stearoyl-Coenzyme A Desaturase Polymorphism on Fatty Acid Composition of Milk J. Dairy Sci. 90:3553–3558.
[7] – Taniguchi, M., Utsugi, T., Oyama, K., Mannen, H., Kobayashi, M., Tanabe, Y., Ogino, A., Tsuji, S. (2004) Genotype of stearoyl-CoA desaturase is associated with fatty acid composition in Japanese Black cattle. Mamm. Genome 14, 142-148.
[8] – Zhang, S. (2005). Association of genetic variation to healthful of beef. Iowa State University Animal Industry Report. [cited 2013; Available from: www.ans.iastate.edu/report/air/2005.pdf].
[9] – Eberlé, D., Hegarty, B., Bossard, P., Ferré, P., Foufelle, F. (2004) SREBP transcription factors: master regulators of lipid homeostasis. Biochimie 86, 839-848.
[10] – Hoashi, S., Ashida, N., Ohsaki, H., Utsugi, T., Sasazaki, S.,Taniguchi, M., Oyama, K., Mukai, F., Mannen, H. (2007) Genotype of bovine sterol regulatory element binding protein-1 (SREBP-1) is associated with fatty acid composition in Japanese Black cattle. Mamm. Genome 18:880-886.
[11] – Tsuzi, S., Mannen, H. (2007) Method of Determining Gene Relating to Favorable Beef Taste and Texture. PCT/JP2006/301841 [cited 2013; Available from: https://data.epo.org/publication-server/rest/v1.0/publication-dates/20071017/patents/EP1845159NWA1/document.pdf].
[12] – Roy, R., Ordovas, L., Zaragoza, P., Romero, A., Moreno, C., Altarriba, J. and Rodellar, C., (2006) Association of polymorphisms in the bovine FASN gene with milk-fat content Anim. Genetics 37, 215-218.
[13] – Zhang, S., Knight, T. J., Reecy, J. M., and Beitz, D. C. (2008) DNA polymorphisms in bovine fatty acid synthase are associated with beef fatty acid composition. Animal Genetics, 39, 62-70.
[14] – Roy, R., Gautier, M., Hayes, H., Laurent, P., Eggen, A., Osta, R., Zaragoza, P., and Rodellar, C., (2001) Assignment of fatty acid synthase (FASN) gene to bovine chromosome 19 (19q22) by in situ hybridization and confirmation by hybrid somatic cell mapping. Cytogenetics and Cell Genetics 93, 141-2.
[15] Nafikov, R., Schoonmaker, J., Reecy, J. M., Spurlock, D. M., Beitz, D. C., Koehler, K. J. and Minick-Bormann, J. (2009) "Effects of A17924G Genotypes Associated with Thioesterase Domain of Fatty Acid Synthase and K232A Genotypes of

Diacylglycerol Acyltransferase-1 on Milk Fatty Acid Composition in Holstein Dairy Cows ,"Animal Industry Report: AS655, ASL R2433. [Cited 2013: Available at: http://lib.dr.iastate.edu/ans_air/vol655/iss1/56].
[16] Maharani, D., Jo, C., Jeon, J.-T. and Lee, J. H. (2011) Quantitative Trait Loci and Candidate Genes Affecting Fatty Acid Composition in Cattle and Pig Korean J. Food Sci. Ani. Resour. Vol. 31, No. 3, pp. 325-338.

Chapter 2 - Study of aluminum tolerance in *Plantago almogravensis* and *P. algarbiensis* species.

2.1. Summary

As research fellow in the project FCT: PTDC/AGR-AAM/102664/2008, my work was based in the use of micropropagation techniques to assess aluminium (Al) tolerance in two critically endangered plantain species *Plantago almogravensis* Franco and *Plantago Algarbiensis* Samp. Some studies suggested that these species are able to tolerate very high concentrations of toxic elements as Al, so bioaccumulation could be a strategy of survival. *In vitro* propagation protocols of these species allowed their production in large scale enabling their use in studies under laboratorial controlled conditions. Thus, I used micropropagation techniques in order to evaluate how low pH and Al affect *in vitro* growth and to study the effects of Al on shoots and plantlets growth, biochemical and physiological parameters of both *Plantago* species.

It was observed that medium pH did not affect *in vitro* proliferation and rooting. Based on the results obtained it was concluded that *Plantago* species are apt to grow *in vitro* in medium with pH values much lower than the usually used in tissue culture, which is in agreement with the fact that both species colonize acid soils. Both species accumulated considerable and similar amounts of Al in their tissues, mainly in the roots. Although our data showed that both species are tolerant to Al^{3+} and H^{+}, *P. almogravensis* appeared to be more adapted to maintain cellular physiology and growth under those conditions. Some insights concerning to aluminum tolerance mechanism were also studied, namely the activities of enzymes involved in organic acids metabolism.

A study of temperature/light germination requirements and effects of Al on seed germination and seedling growth was also performed. The best germination results were obtained at 15°C under either light or darkness, along with the shortest mean germination time. The results are crucial to study the effect of Al during germination phase and to develop conservation strategies for these *Plantago* species.

Keywords: *Plantago almogravensis*; *P. algarviensis*; Plant *in vitro* propagation; Plant growth; Aluminium tolerance; Antioxidant enzymes

2.2. Introduction

Acid soils are predominant on the earth's surface and have been estimated to occur on about 40% of the world's arable soils and 12% of the land in crop production have a pH below 5.5 [1]. Moreover, soil acidification is increasing in world-wide. With the decrease of soil pH, active aluminum (Al) in soil shows a great increase, resulting in toxicity to plants [2]. Whereas low pH can restrict plant growth by itself, in most cases it is the dissolution of toxic metals, particularly Al, which can negatively affect plant growth and development. Dissolution of just a small amount of Al compounds in soils can result in serious Al toxicity to susceptible plant species. Disturbance of the metabolism by excessive Al or heavy metal appears to happen in multiple ways, causing a reduction of chlorophyll content, inhibiting plant growth and respiration, changing the ultra-structure of the cell organelles, and altering the activity and quantity of the key enzyme of various metabolic pathways [3, 4].

High concentrations of heavy metals in plant tissues can induce the disorder in nutrient metabolism, as a consequence leading to abnormal growth. While, reactive oxygen species (ROS) can cause oxidative damage to the bio-molecules such as lipid, protein and nucleic acids, leading to cell membrane peroxidation, loss of ions, protein hydrolysis, and even DNA strand breakage [2]. However, some plant species have evolved sophisticated mechanisms to handle with Al stress.

Plantago almogravensis Franco and *Plantago algarbiensis* Samp. are endemic species from Portuguese Southwest coast and Western-centre of Algarve region (Portugal), respectively, that are in risk of global extinction. Both are included in the Red List of Threatened Species [5] legally protected under European Habitats Directive 92/43/CEE and by the Portuguese law. The *P. almogravensis* dominance, in areas where no other kind of vegetation exists (vegetation gaps), suggest that this species is able to tolerate very high concentrations of toxic elements as Al, so bioaccumulation could be a strategy of survival. *P. algarbiensis* occurs in clay-rich soils and prefers areas that are located downstream from small spring or clearings of low acidophilic brushes [6]. Recently there have been doubts if these two species of *Plantago* are in reality a single species. Thus, in this project we decide to include also *P. algarbiensis* in our studies.

Since *P. almogravensis* and *P. algarbiensis* are protected, the first difficulty of conducting studies relies on the availability of plants. To obviate this difficulty an *in vitro* propagation protocol was developed for these species by team members [7]. Using

these protocols clonal plants can be produced in large scale, thus reducing the pressure on wild stocks, and used in further studies under laboratorial controlled conditions to evaluate Al physiological and biochemical effects and to elucidate the Al tolerance mechanism.

There is great evidence that organic acids play an important role in the Al tolerance mechanisms of a range of plant species. Some organic acids are able to complex Al^{3+} into forms that are not toxic to plants. Al tolerance mechanisms that involve organic acids can be divided into external and internal detoxification, with some plant species apparently using both types of mechanism [8].

Some plants can tolerate Al because they exclude it from the root apices. Thus, many plant species that are Al tolerant exude organic acids, such as citric, oxalic and malic, in response to Al and these organic acids chelate the Al protecting the roots from Al toxicity [9].

Some plants have the remarkable ability of accumulating Al in shoots and roots, this species have evolved mechanisms that allow Al move through the plant and across of membranes. Studies revealed the role of organic acids in complexing internal Al, researchers have identified Al complexed with oxalate and to citrate, both are strong chelators of Al, thus protecting cellular components from the phytotoxic effects of Al [10].

As *P. almogravensis* and *P. algarbiensis* species are endangered and in risk of global extinction practical measures to ensure the conservation of the maximum genetic diversity of these species, are urgently required. Seed cryopreservation is an important tool to store germplasm for long periods and has been successfully applied to the preservation of seeds of several wild and endangered species [11]. To implement seed cryopreservation and to determine the effect of Al during the germination and to evaluate the Al tolerance of these species, first it is necessary to know the seed germination requirements. Since germination may be the first decisive step for survival of plants under Al stress at low pH [12], it is important to determine the effect of Al during this stage to establish the Al tolerance. For that, the prior study of the germination requirements is necessary. No information is available on the germination of *P. algarbiensis* or *P. almogravensis* seeds. Thus, having in mind the application of conservation strategies and the evaluation of Al tolerance, it is important to study the germination requirements of these species.

2.3. Objectives

The main objective of this work was to study the tolerance of *P. almogravensis* and *P. algarbiensis* to low pH and Al using micropropagated plants. The specific aims of this study were:

i) to study the effect of medium pH on *in vitro* growth and biochemical parameters;

ii) to investigate the effect of low pH and Al treatment for 7 days on plant growth, nutrient contents and several physiological parameters;

iii) to evaluate the activities of enzymes involved in organic acids metabolism, as an attempt to understand the Al detoxification mechanism;

iv) to study the seed germination requirements of these *Plantago* species.

2.4. Materials and Methods

2.4.1. Plant material and growth conditions

In vitro cultures and micropropagated plantlets of *P. almogravensis* and *P. algarbiensis* were produced starting from *in vitro* germinated seeds.

Several genotypes of *P. almogravensis* (shoots of ~6 cm in length) and *P. algarbiensis* (shoots of ~3 cm length) were maintained *in vitro* for 6 weeks in MS medium (Murashige and Skoog) [13] supplemented with 0.2 mg/L 6-benzyladenine (BA) as described by Gonçalves *et al.* [7]. Plantlets (root inducing) were obtained by cultivating the shoots for 3 weeks in ½MS medium (half-strength macronutrients) supplemented with 0.5 mg/L indole-3-acetic acid (IAA) (pH 5.75). The shoots and plantlets were maintained at 25 ± 2ºC with a 16-h photoperiod (cool white fluorescent lamps, 69 µmol $m^{-2} s^{-1}$).

2.4.2. How medium pH affects *in vitro* growth and biochemical parameters

To study the effect of medium pH on proliferation, *P. almogravensis* and *P. algarbiensis* shoots (about 5 and 3 cm of size, respectively) were inoculated in MS medium supplemented with 0.2 mg/L BA. For root induction, shoots of *P. almogravensis* and *P. algarbiensis* with equal size were inoculated in ½ MS medium (half strength macronutrients) supplemented with 0.5 mg/L IAA. Every medium were supplemented with 2% (w/v) sucrose and solidified with 0.5% (w/v) gelrite. The pH was adjusted to 4.50, 5.00 or 5.75 before autoclaving, at 121ºC and 1.1 kg/cm^2 for 20 min. The post-autoclave pH values were measured after medium cooling until 40ºC. After 6 weeks, the shoot proliferation was measured by the proliferation frequency, the number of shoots, the length of the longest shoot and the rooting was evaluated in terms of root frequency, root number and the longest root length. The pH of the culture media was measured at the end proliferation or rooting phases after harvesting cultures. Media were liquefied and cooled until 40ºC before pH measurements. As control, the pH values in the culture media maintained during 6 weeks in the same incubation conditions but without cultures were also measured.

To evaluate the influence of medium pH on *in vitro* proliferation and rooting three repetitions with 10 shoots each were performed.

The effect of medium pH in the level of lipid peroxidation, protein content and antioxidant enzyme activities were evaluated in plantlets at the end of rooting stage. The samples of shoots and roots analyzed were randomly collected from different Erlenmeyers.

2.4.2.1. Determination of lipid peroxidation

The lipid peroxidation was estimated by determining the malondialdehyde (MDA) content according to the thiobarbituric acid-reactive-substances method [20]. Fresh tissue was ground in 0.1% (w/v) trichloroacetic acid (TCA) using mortar and pestle and then centrifuged at 10,000 *g* for 5 min. After centrifugation, the supernatant was mixed to either 20% (w/v) TCA (-TBA solution) or 0.5% (w/v) thiobarbituric acid (TBA) prepared in 20% (w/v) TCA (-TBA solution). The mixture was heated at 95ºC for 30 min and then quickly cooled on ice. After centrifugation at 3,000 *g* for 10 min, the concentration of MDA was calculated from the absorbance at 532, 600 and 440 nm using the extinction coefficient of 157 $mM^{-1}.cm^{-1}$ and expressed as nmol MDA g^{-1} fresh weight (FW).

2.4.2.2. Enzyme assays and soluble protein

The activities of the superoxide dismutase (SOD; EC 1.15.1.1), catalase (CAT; EC 1.11.1.6), ascorbate peroxidase (APX; EC 1.11.1.11) and guaiacol peroxidase (GPX; EC 1.11.1.7) were measured in extracts from shoots and roots after 6 weeks of culture. Fresh tissue (100 mg) was ground in a pre-chilled mortar and was homogenized in solution consisting of 50 mM sodium phosphate (pH 7.0), 0.1 mM ethylenediaminetetraacetic acid (EDTA), 1% (w/v) polyvinylpolypyrrolidone and 2.5 mM dithiothreitol.

For APX the homogenizing solution contained 5 mM ascorbate. The homogenate was centrifuged at 20,000 *g* for 10 min at 4ºC. The supernatant was used for enzyme activities and protein content assays. The SOD activity was assayed using the method of Beauchamp and Fridovich (1971) [14] by monitoring the inhibition of the photochemical reduction of nitroblue tetrazolium chloride (NBT). The reaction mixture contained 50 mM sodium phosphate buffer (pH 7.8), 10 mM methionine, 0.075 mM NBT, 0.2 mM riboflavin and 20 µl enzyme extract. One unit of SOD was defined as the amount of enzyme required to result in a 50% inhibition of the rate of NBT reduction measured at 560 nm in the presence of riboflavin in the light during 6 min. The CAT

activity was determined by the method described by Aebi (1983) [15]. The reaction mixture consisted of 50 mM sodium phosphate buffer (pH 7.0), 40 mM H_2O_2 and 20 µl enzyme extract. The CAT activity was measured by following the decrease in absorbance at 240 nm (ε= 39.4 $mM^{-1}.cm^{-1}$) due H_2O_2 decomposition. One unit of CAT was defined as the amount of enzyme which breaks down 1 µmol H_2O_2 per min. The activity of APX was determined as described previously by Nakano and Asada (1981) [16]. The reaction mixture contained 50 mM sodium phosphate buffer (pH 7.0), 0.5 mM ascorbic acid, 0.2 mM EDTA, 0.5 mM H_2O_2 and 20 µl enzyme extract. The oxidation of ascorbic acid in the reaction mixture was measured using the rate of decrease in absorbance at 290 nm (ε = 2.8 $mM^{-1}.cm^{-1}$). One unit of APX was defined as the amount of enzyme which breaks down 1 µmol of ascorbate per min. The GPX activity was measured as outlined by Egley *et al.* (1983) [17] through monitoring the increase in absorbance at 470 nm due to tetraguaiacol formation (ε = 26.6 $mM^{-1}.cm^{-1}$). The reaction mixture consisted of 50 mM sodium phosphate buffer (pH 7.0), 8 mM guaiacol, 8 mM H_2O_2 and 20 µl enzyme extract. One unit of GPX was defined as the amount of enzyme to produce 1 µmol tetraguaiacol per min. These assays were performed with a total volume of 1 ml at 25 ± 2ºC. The specific enzyme activity for all enzymes was expressed as unit mg^{-1} protein. Detection of total soluble protein was determined by the Bradford method (Bradford 1976) [18], using bovine serum albumin as standard.

2.4.3. Effect of low pH and Al on growth, biochemical and physiological parameters of *P. almogravensis* and *P. algarbiensis*

2.4.3.1. Stress treatments

Low pH stress was applied by transferring shoots and plantlets to ¼ MS liquid medium with the pH adjusted to 4.00 (stress) or 5.75 (control). Al stress was applied by transferring shoots and plantlets to ¼ MS liquid medium with the pH adjusted to 4.00 containing 10 mg/L Al^{3+} that are approximately 400 µM $AlCl_3$, that correspond to 140 µM Al^{3+} activity, as estimated by Geochem-EZ. Shoots and plantlets were inoculated individually in 32 × 200 mm test tubes containing 20 ml liquid medium on filter paper bridges, and incubated for 7 days under the conditions described above.

2.4.3.2. Plant growth and relative water content

The length of shoots and plantlets (leaves and roots) were measured before and after treatments. Shoots and plantlets were then collected and were dried at 63ºC until reached a constant weight and the dry weight (DW) determined. Plant water status was assessed by measuring relative water content (RWC) in five fresh leaves and calculated as 100X(FW - DW)/(TW - DW), where FW is the fresh weight, TW is turgid weight (determined after submersing the petioles for 24 h in distilled water) and DW is the dry weight (determined after drying at 63ºC until constant weight).

2.4.3.3. Determination of Al and nutrients contents

The Al, calcium (Ca), phosphorus (P), potassium (K) and magnesium (Mg) contents in plant tissues were determined by atomic absorption spectrophotometry (GBC, Avanta-Sigma, USA) following standard methods [19]. Samples were ground, dry-ashed at 500ºC and digested in an acidic solution.

The level of antioxidant enzyme activities were analyzed in samples of shoots and roots randomly collected.

2.4.3.4. Enzyme assays and soluble protein

The activities of antioxidant enzymes and the amounts of soluble protein were measured in shoots and plantlets of all the treatments studied, using the methods as described above in the section 2.4.2.1.

2.4.3.5. Photosynthetic pigments analysis

Photosynthetic pigments were extracted with 100 % acetone from fresh plant material (25 mg) and the absorbance of the extract solutions was measured in a spectrophotometer at 661.6, 644.8 and 470 nm. Pigment contents were estimated as described by Lichtenthaler (1987) [21].

2.4.4. Insights on Al tolerance mechanism:

Effects of Al in the activity of the enzymes related to the organic acids metabolism

The activity of enzymes related to the organic acids metabolism was investigated in response to Al treatment. Shoots and plantlets produced were cultured in ¼MS liquid medium containing 0 or 10 mg/L Al (~400µM $AlCl_3$), with the pH adjusted to 4.00.

After 7 days of incubation in medium with and without Al, 100 mg of fresh plant tissue was macerated and resuspended in extraction buffer (100 mM Tris-HCl pH 8.0, 5 mM $MgCl_2$, 1 mM EDTA, 5 mM DTT (1,4-dithio-DL-treitol), 10% v/v glycerol and 1% Triton-X 100). Extracts were centrifuged at 20,000 *g* for 5 min at 4ºC and the pellets discarded. Citrate synthase activity was measured spectrophotometrically according to Srere *et al.* [22] by monitoring the reduction of Acetyl-CoA in the presence of DTNB at 412 nm, NADP-ICDH and fumarase activity was measured following the procedure of Bergmeyer *et al.* [23] MDH and PEPCase activity was measured using the procedure of Miller *et al.* [24] and Blanke *et al.* [25], respectively.

2.4.5. Study of seed germination requirements

Mature seeds of *P. algarbiensis* were collected in July 2009 and June 2010 from wild plants growing in a natural population in Algoz (Algarve region, Portugal). *P. almogravensis* seeds were collected from wild plants growing in Vila Nova de Milfontes (Portugal). Since just one population of this species is known and the over-harvesting of seeds may represent a threat, seeds were only collected in June 2010. Seeds were collected from 20 individuals of each species randomly selected within the population area. After their collection the seeds were stored in hermetic sealed glass jars inside paper bags and kept in the dark under laboratory conditions at 25 ± 2°C for two months.

The seed water content was determined in three replicates of 25 randomly selected seeds using the low temperature oven method (103°C for 17 h; ISTA, 2003). For each species, 75 randomly selected seeds were observed using a stereomicroscope, the image was captured with a digital Motic camera and seed length and width measured using the software Motic Images 2000. The length-to-width ratio was also calculated. Three replicates of 100 seeds were used to quantify seed weight.

The seeds were sown in 9 cm diameter glass Petri dishes on 0.5% (w/v) bactoagar without nutrients. Germination tests were done at constant 15 or 25°C and alternating 25/15°C under 16 h light / 8 h dark photoperiod (light) or continuous darkness. The light was provided by cool-white fluorescent lamps at a photon flux density of 69 μmol $m^{-2}.s^{-1}$. Germination was recorded every 2 days over a total 40 days incubation period and the criterion for germination was visible radical protrusion. At the end of the germination period, results were expressed as final germination percentage (mean value ± standard error) and mean germination time (MGT, mean value in days ± standard

error). The MGT was determined according to the formula described by Ellis and Roberts [26].

2.4.6. Statistical analysis

The data were subjected to analysis of variance (ANOVA) using SPSS for Windows (release 19.0, SPSS Inc., California). For additional pairwise comparisons, Duncan's New Multiple Range Test was used. Differences were considered significant at $P<0.05$. Final germination percentages were transformed prior to statistical analysis.

2.5. Results and Discussion

2.5.1. How medium pH affects *in vitro* growth and biochemical parameters of *P. algarbiensis* and *P. almogravensis*

The pH of the culture medium is a relevant factor for the *in vitro* shoot and root formation and healthy culture growth. Some plants have the capacity to tolerate a wide range of pH, whereas in others pH tolerance is limited.

The cultures were grown in the conditions described in the subsection 2.4.1 of material and methods.

Variations in the pH of proliferation and rooting media, after autoclaving and after 6 weeks, with and without being cultured with *P. algarbiensis* and *P. almogravensis* plantlets were measured (Table 2.1).

Table 2.1 – Changes in the pH of proliferation and rooting media after autoclaving and after 6 weeks, with or without *P. algarbiensis* and *P. almogravensis* plantlets [27].

Medium	Initial PH	Post-autoclave	pH after 6 weeks		
			Without plantlets	*P. algarbiensis*	*P. almogravensis*
Proliferation	4.50	4.20 ± 0.01 b	4.11 ± 0.02 b	3.65 ± 0.10* c	4.60 ± 0.07* a
	5.00	4.52 ± 0.01 ab	4.39 ± 0.04 b	3.72 ± 0.13* c	4.68 ± 0.07* a
	5.75	4.97 ± 0.02 a	4.74 ± 0.01 a	3.50 ± 0.03* b	4.72 ± 0.18* a
Rooting	4.50	4.26 ± 0.02 a	4.08 ± 0.01 b	3.15 ± 0.05 d	3.46 ± 0.09 c
	5.00	4.74 ± 0.02 a	4.35 ± 0.06 b	2.92 ± 0.08 d	3.62 ± 0.09 c
	5.75	5.09 ± 0.01 a	4.85 ± 0.02 b	3.15 ± 0.10 a	3.72 ± 0.10 c

Values are expressed as the mean ± SE (n = 3). In each row, mean values followed by different letters are significantly different at $P<0.05$, according to Duncan's test

*Significant different between proliferation and rooting media for each original pH ($P<0.05$)

Variations in medium pH can occur during culture, depending on the medium composition, initial pH, and plant species [28]. Thus, in this work the pH was monitored after autoclaving and at the end of the subculture period. Post-autoclave pH values were lower (0.20 to 0.75 units) than the pre-autoclave in all the media tested (Table 2.1). Moreover, the pH decreased becoming more acid over the 6 week period in medium without plantlets. This acidification was previously observed by some research teams, they found that it can be caused by dehydration of media and/or by the precipitation of medium components such as mineral nutrients [29, 30].

Independently of the initial pH, after 6 weeks of multiplication or rooting period, there were not differences with respect to the final medium pH, for both species (Table 2.1).

When cultures of both species were inoculated, a clear decrease was observed in the pH of all media after 6 weeks, excepting for *P. almogravensis* multiplication media (Table 2.1). Furthermore, the lowest pH values were observed in the rooting media of both species (Table 2.1). These results make sense once that soil acidification by roots has been demonstrated for many plant species [31].

The effect of medium pH (4.50, 5.00 and 5.75) on proliferation and rooting of *P. algarbiensis* and *P. almogravensis* shoots was studied (Fig. 2.1).

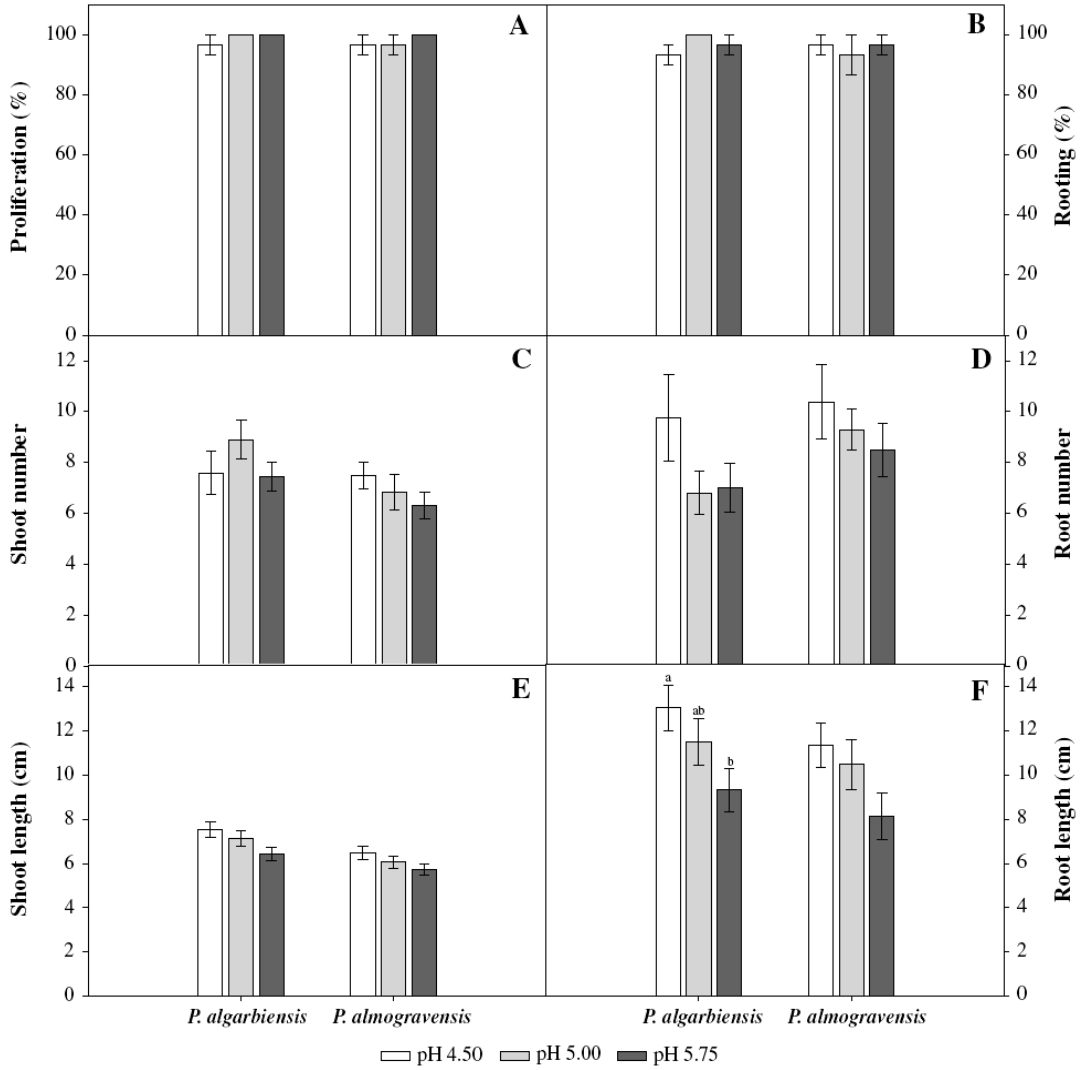

Figure 2.1 – Effect of medium pH (4.50, 5.00 and 5.75) on proliferation (A) and rooting (B), shoot and root number (C and D, respectively), shoot and root length (E and F, respectively) of *P. algarbiensis* and *P. almogravensis* species [27]. Values are expressed as the mean ± SE (n = 3). For each species, mean values followed by different letters are significantly different at $P<0.05$ and the absence of letters reveals that no differences were observed, according to Duncan's test.

According to Fig. 2.1A multiplication frequencies of both species were very high, near 100%, in all the medium pH tested, and no significant differences were observed in the mean number of shoots (Fig 2.1C) and in the shoot length (Fig 2.1E). The plantlets had a normal development under all the medium pH tested, without visually observed damages caused by low pH. Also high rooting frequencies (Fig 2.1B) were achieved for both *Plantago* species. It was observed that root number (Fig 2.1D) and length (Fig 2.1F) were not affected by pH levels for *P. almogravensis*, whereas *P. algarbiensis* roots were longer at pH 4.50 than at pH 5.75 (Fig 2.1F) what can be explained by the

fact that nutrient bioavailability often decreases at low pH then the strategy to enhance nutrient acquisition could be the increase of root surface area [32].

The lipid peroxidation was estimated by determining the malondialdehyde (MDA) content, a decomposition product of polyunsaturated fatty acids [33].The damaged membranes release MDA which is therefore considered a good stress indicator [34]. Thus, the effect of medium pH in MDA content was measured in *P. algarbiensis* and *P.almogravensis* plantlets (shoot and root) (Table 2.2).

Table 2.2. Contents of MDA in *P. algarbiensis* and *P.almogravensis* plantlets (shoot and root) cultured in media with different pH [27].

Species	pH	MDA (nmol/g FW)	
		Shoot	Root
P. algarbiensis	4.50	70.52 ± 8.11 a	40.60 ± 3.50 a
	5.00	26.97 ± 4.01 b	29.12 ± 4.12 b
	5.75	26.05 ± 5.68 b	30.90 ± 2.08 b
P. almogravensis	4.50	59.51 ± 8.96 a	47.10 ± 4.11 a
	5.00	48.32 ± 9.06 a	31.21 ± 2.99 b
	5.75	42.12 ± 4.22 a	29.76 ± 3.02 b

Values are expressed as the mean ± SE (n = 5). For each species and in each column, mean values followed by different letters are significantly different at $P<0.05$, according to Duncan's test

It was observed that MDA content was higher in shoots of *P. algarbiensis* cultured at pH 4.50 whereas shoots of *P. almogravensis* presented no differences for all pH tested. The level of lipid peroxidation increased in roots of both species cultured at pH 4.50 (Table 2.2).

The increase in the content of lipid peroxidation in shoots of *P. algarbiensis* and in roots of both species grown in medium with low pH indicates membrane damage stress and was analytically detectable before growth differences appeared.

Soluble protein content is a significant indicator of metabolic changes, and it is known to respond to a vast variety of stresses [35]. The effect of medium pH (4.50, 5.00 and 5.75) on soluble protein content in shoots and roots of *P. algarbiensis* and *P. almogravensis* is represented in the Fig. 2.2 (A) and (B), respectively.

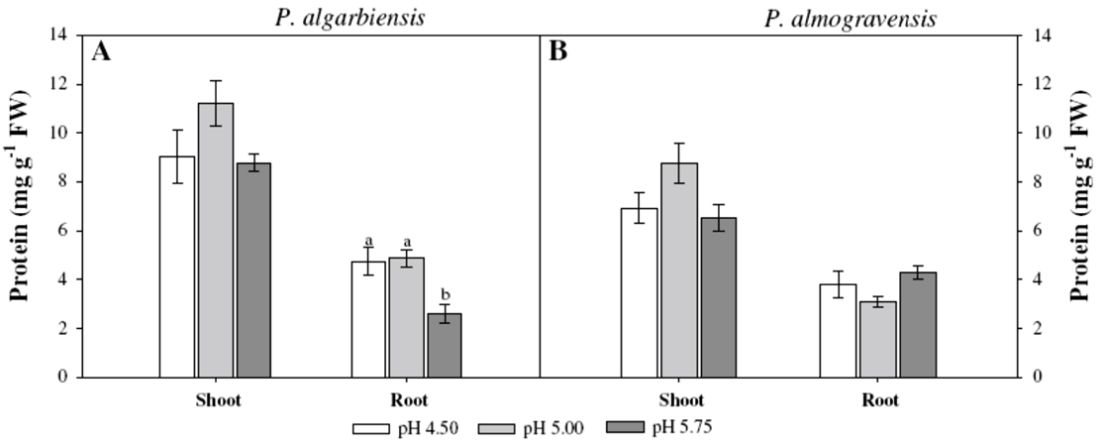

Figure 2.2 – The effect of medium pH (4.50, 5.00 and 5.75) on soluble protein content in shoots and roots of *P. algarbiensis* (A) and *P. almogravensis* (B) [27]. Values are expressed as the mean mean ± SE (n = 5). For each species, mean values followed by different letters are significantly different at P<0.05 and the absence of letters indicates that no significant differences were observed.

In *P. algarbiensis* the content of soluble protein was significantly high in roots developed at pH 4.50 and 5.00 (Fig. 2.2A), whereas in *P. almogravensis* no significant differences were observed between all the pH values tested (Fig. 2.2B).

A higher quantity of soluble protein has been reported in several plant species under unfavorable growth conditions [36]. Thus, *P. algarbiensis* was having a stronger response to Al stress than *P. almogravensis*.

One of the plant responses to environmental stress is the generation of ROS (reactive oxygen species).

Thus, to investigate the antioxidant response of *P. algarbiensis* and *P. almogravensis* shoots and roots to medium pH, the activities of SOD, CAT, APX and GPX were measured (Fig. 2.3).

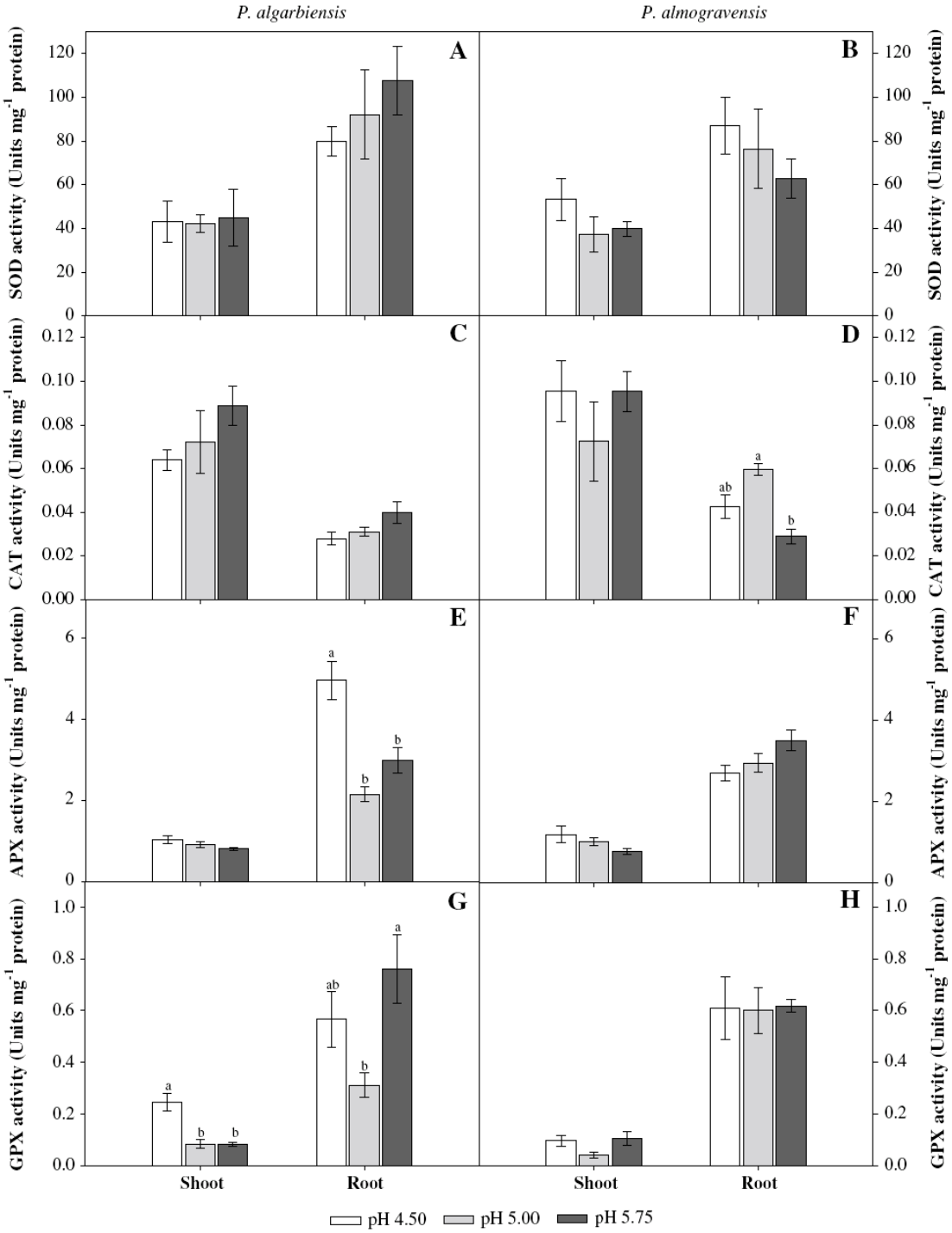

Figure 2.3 – Effect of medium pH (4.50, 5.00 and 5.75) on SOD (A, B), CAT (C, D), APX (E, F) and GPX (G, H) activities in shoots and roots of *P. algarbiensis* and *P. almogravensis* [27]. Values are expressed as the mean ± SE (n = 5). For each species, mean values followed by different letters are significantly different at $P<0.05$ and the absence of letters indicates that no significant differences were observed.

No significant changes in SOD activity were observed in shoots and roots of both *Plantago* species cultured in medium with different pH values (Fig. 2.3A, B). The CAT activity was not affected by the pH of the medium in *P. algarbiensis*, whereas at pH

5.00 a significant activation of this enzyme was observed in roots of *P. almogravensis* as in comparison with pH 5.75 (Fig. 2.3C, D). In *P. algarbiensis* there was a significant increase in APX and GPX activity in roots and shoots, respectively, grown at pH 4.50. The APX and GPX activity of *P. almogravensis* shoots and roots was not affected by medium pH (Fig. 2.3E, F) and G, H, respectively). The obtained results revealed that after 6 weeks of culture SOD activity was unaffected by the pH of the culture medium in both *Plantago* species, but small changes were detected in the activity of the other enzymes. This is admissible because superoxide anions could also be reduced through non-enzymatic pathways [37].

2.5.2. Effect of low pH and Al on *P. algarbiensis* and *P. almogravensis* plantlet growth and biochemical parameters

2.5.2.1. Effect of low pH and Al on *P. algarbiensis* and *P. almogravensis* plantlet growth

The evaluation of low pH effects is important for a better understanding and correct interpretation of Al toxicity. Since, low pH increases the concentration of soluble ions leading to high H^+ activity, and promotes the release of Al, which easily results in Al toxicity in plants. On the other hand, low pH (high H^+ activity) in root medium may directly inhibit plant growth [38]

Al is reported to inhibit the plant growth, mainly that of root. Symptoms of Al toxicity are also manifested in shoot which are regarded as the consequence of injuries to root system. Besides this, Al also interferes with the water relations (relative water content) and membrane permeability, decreases photosynthetic activity and causes chlorosis and necrosis of leaves resulting in a decrease in the growth of plants [1,3,4].

However, there is increasing evidence suggesting that these two stresses differ in their inhibition of plant growth [39] and that resistance to Al and to protons is controlled by separate mechanisms [38]. Therefore, it is necessary to evaluate the effects of low pH separately from the combination of low pH and Al to better understand H^+ toxicity.

To evaluate the effect of low pH and Al on *P. almogravensis* and *P. algarbiensis* growth plantlets of both species were cultured for 7 days in $^1/_4$MS liquid medium supplemented with 0 or 400 µM $AlCl_3$ (approximately 10 mg/L Al^{3+}), with the pH adjusted to 4.00 with and without Al. Medium at pH 5.75 without Al was used as control. Roots and shoots were separated to measure their length and fresh weight. Then

roots and shoots were dried in oven and weighed to determine their dry mass (Table 2.3).

Table 2.3 – Effect of low pH and Al on the elongation and DW of *P. algarbiensis* and *P. almogravensis* shoots and plantlets [40].

pH	Al (µM)	Elongation (mm)			DW (mg)		
		Shoot	Plantlet		Shoot	Plantlet	
			Leaves	Roots		Leaves	Roots
P. algarbiensis							
5.75	0	2.13 ± 0.38 a	11.33 ± 2.30 a	36.27 ± 2.75 a	60.81 ± 5.55 a	85.11 ± 8.88 a	11.51 ± 0.90 a
4.00	0	2.60 ± 0.65 a	8.13 ± 1.11 a	39.93 ± 1.91 a	65.17 ± 7.64 a	81.38 ± 9.50 a	13.28 ± 1.13 a
4.00	400	1.87 ± 0.29 a	9.27 ± 1.83 a	26.93 ± 1.60 b	51.24 ± 4.87 a	86.89 ± 5.97 a	10.94 ± 0.99 a
P. almogravensis							
5.75	0	2.07 ± 0.48 a	6.93 ± 0.77 a	24.67 ± 3.07 a	84.67 ± 7.35 a	131.37 ± 10.14 a	17.75 ± 2.08 a
4.00	0	2.67 ± 0.46 a	5.13 ± 0.72 a	26.60 ± 4.52 a	74.21 ± 8.65 a	118.59 ± 10.37 a	16.37 ± 1.08 a
4.00	400	1.73 ± 0.49 a	4.20 ± 0.88 a	21.27 ± 4.23 a	80.45 ± 5.94 a	125.44 ± 9.12 a	14.15 ± 1.38 a

Values are expressed as the mean ± SE (n = 15). For each species and in each column, mean values followed by different letters are significantly different at $P < 0.05$, according to Duncan's test

The presence of Al in the nutrient medium did not cause reduction in growth (length, fresh and dry mass of root and shoot) of *P. almogravensis* plantlets. On the other hand, the root growth was affected by Al in *P. algarbiensis* plantlets (Table 2.3).

2.5.2.2. Determination of Al accumulation and nutrient contents in *P. algarbiensis* and *P. almogravensis*

The Al accumulation in *P. algarbiensis* and *P. almogravensis* shoots and plantlets (leaves and roots) were measured after 7 days of culture in medium containing 400 µM Al (Fig. 2.4).

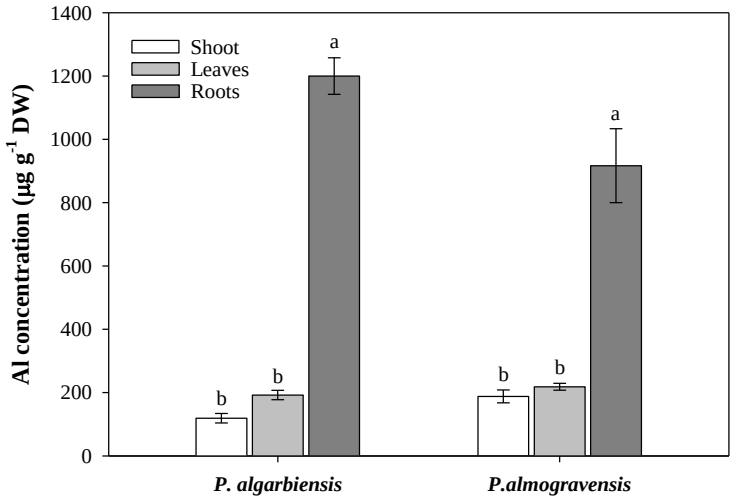

Figure 2.4 – Aluminum accumulation in *P. algarbiensis* and *P. almogravensis* shoots and plantlets (leaves and roots) after 7 days of culture in medium containing 400 µM Al [40]. Values are expressed as the mean ± SE (n = 3). For each species, mean values followed by different letters are significantly different at $P<0.05$, according to Duncan's test. No significant differences ($P<0.05$) were observed between species in the same organ.

The results demonstrated that shoots and plantlets of both *P. algarbiensis* and *P. almogravensis* accumulated considerable amounts of Al (120-1200 µg/g DW) when cultivated in medium supplemented with Al (Fig. 2.4). For each type of plant material (shoots, leaves and roots) analyzed these species accumulated similar Al contents. Shoots and plantlets leaves showed the lowest Al concentrations (120-220 µg/g DW), whereas the roots displayed higher concentrations (> 900 µg/g DW) which suggests about the existence of a mechanism that immobilizes and sequesters Al preventing its translocation to the above-ground plant parts.

The effect of low pH and Al on the Ca, P, K and Mg contents (mg/g DW) in *P. algarbiensis* and *P. almogravensis* shoots and plantlets of both species were investigated (Table 2.3). These nutrients have been reported as key nutrients involved in Al toxicity and the genotypes with the ability to maintain or increase the uptake of these nutrients had been considered tolerant [41, 42].

Table 2.4 – Effect of low pH and Al on the Ca, P, K and Mg contents (mg.g^{-1} DW) of *P. algarbiensis* and *P. almogravensis* shoots and plantlets [40].

Nutrient	pH	Al (µM)	*P. algarbiensis*			*P. almogravensis*		
			Shoot	Plantlet		Shoot	Plantlet	
				Leaves	Roots		Leaves	Roots
Ca	5.75	0	3.67 ± 0.12 a	3.63 ± 0.03 b	2.80 ± 0.06 a	3.93 ± 0.03 a	3.87 ± 0.03 a	2.53 ± 0.03 a
	4.00	0	3.57 ± 0.03 a	3.87 ± 0.09 a	2.70 ± 0.06 a	3.57 ± 0.03 b	4.10 ± 0.12 a	2.77 ± 0.03 a
	4.00	400	3.33 ± 0.07 a	3.60 ± 0.06 b	2.07 ± 0.09 b	3.53 ± 0.03 b	4.03 ± 0.03 a	2.60 ± 0.10 a
P	5.75	0	5.00 ± 0.06 a	5.97 ± 0.03 a	8.10 ± 0.38 ab	3.00 ± 0.06 a	4.30 ± 0.06 a	6.10 ± 0.06 c
	4.00	0	4.03 ± 0.03 b	5.70 ± 0.12 b	7.53 ± 0.09 b	3.13 ± 0.03 a	3.77 ± 0.03 b	8.33 ± 0.20 a
	4.00	400	3.87 ± 0.07 b	5.50 ± 0.06 b	8.70 ± 0.10 a	3.03 ± 0.03 a	4.20 ± 0.00 a	7.37 ± 0.07 b
K	5.75	0	27.33 ± 0.52 a	24.60 ± 0.10 b	28.93 ± 0.29 b	27.33 ± 0.64 a	29.57 ± 0.41 a	32.30 ± 0.49 b
	4.00	0	27.70 ± 0.55 a	26.10 ± 0.10 a	27.23 ± 0.98 b	28.27 ± 0.43 a	27.83 ± 0.13 b	31.67 ± 0.58 b
	4.00	400	25.83 ± 0.82 a	24.60 ± 0.21 b	34.60 ± 1.21 a	28.73 ± 0.43 a	29.73 ± 0.34 a	37.60 ± 1.77 a
Mg	5.75	0	1.50 ± 0.00 a	1.40 ± 0.00 c	1.07 ± 0.03 b	1.67 ± 0.03 a	1.53 ± 0.03 a	1.17 ± 0.03 a
	4.00	0	1.53 ± 0.03 a	1.60 ± 0.00 a	1.20 ± 0.00 a	1.53 ± 0.03 b	1.47 ± 0.03 a	1.17 ± 0.03 a
	4.00	400	1.43 ± 0.03 a	1.50 ± 0.00 b	1.20 ± 0.00 a	1.40 ± 0.00 c	1.50 ± 0.00 a	1.20 ± 0.00 a

Values are expressed as the mean ± SE (n = 3). For each nutrient and in each column, mean values followed by different letters are significantly different at $P < 0.05$, according to Duncan's test

It was observed that the *P. algarbiensis* plantlets were more affected by both stress treatments than the *P. almogravensis* plantlets, indicating that the inhibition of root elongation found in *P. algarbiensis* may be associated with nutrient homeostasis break. In *P. algarbiensis*, the amount of Mg increased in both leaves and roots, and P decreased only in leaves at low pH and in the presence of Al. The amount of Ca and K increased in low pH treated leaves, whereas K was higher and Ca was lower in Al-treated roots in both species. In *P. almogravensis*, the amount of P increased in roots for both treatments, whereas P and K decreased in response to low pH in leaves and K increased in roots under Al treatment (Table 2.4). The nutrient accumulation in both *Plantago* species were markedly affected by low pH and Al, however, the response was rather variable (Table 2.4). Thus, the maintenance or increase of Ca, Mg, P and K contents observed in the *Plantago* species studied are in agreement with the fact that both species colonize acidic Al-rich soils.

2.5.2.3. Effect of pH and Al on biochemical and physiological parameters

It has been shown that Al causes morphological and/or damage to plant tissues [43]. The severity of Al phytotoxicity depends on the quantity of Al and the amount of free radicals of oxygen so called reactive oxygen species (ROS), including superoxide radical (O_2^-), hydroxyl radical (HO^-), and hydrogen peroxide (H_2O_2) that are produced in plant tissues during exposure to stress. ROS can cause oxidative damage to biomolecules such as lipids, proteins, and nucleic acids, leading to cell membrane peroxidation, loss of ions and carbonylation of proteins [2]. However, plants developed some defense systems to scavenge ROS and to overcome oxidative stress. The cells are able to protect themselves by engaging enzymatic and nonenzymatic mechanisms. Al enhances the peroxidation of lipids and increases the activities of antioxidant enzymes, catalase (CAT), superoxide dismutase (SOD), peroxidase (POD), and glutathione reductase (GPX), in several species. Besides this, Al also alters water relations reduces stomatal opening, affects photosynthesis by lowering chlorophyll and carotenoid content and reducing electron flow [43, 44].

It was also studied the effect of Al on SOD, CAT, APX and GPX activities in shoots and roots of *P. algarbiensis* and *P. almogravensis* (Fig. 2.5).

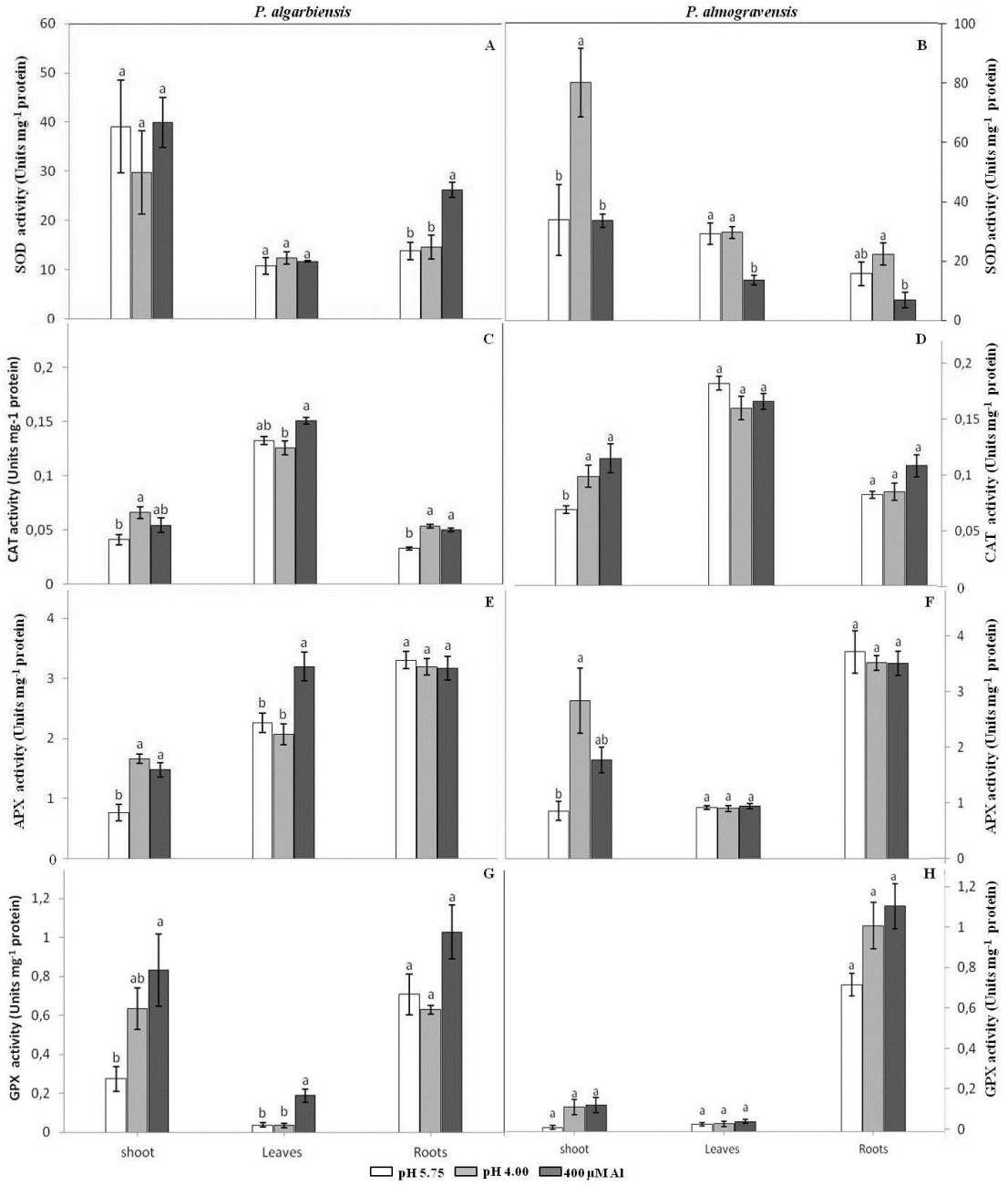

Figure 2.5 – Effect of low pH and Al on SOD (A, B), CAT (C, D), APX (E, F) and GPX (G, H) activities in shoots, leaves and roots of *P. algarbiensis* and *P. almogravensis*. Values are expressed as the mean ± SE (n = 5). For each species, mean values followed by different letters are significantly different at $P<0.05$ and the absence of letters indicates that no significant differences were observed [45, 46].

According to Fig. 2.5, the activity of SOD, CAT and APX activities of *P. almogravensis* increased in media without Al at pH 4.00 (Fig 2.5B, D and F, respectively). The activity of SOD did not present differences in shoots and leaves, whereas the CAT activity increased in shoots and roots at pH 4.00 without and with Al in *P. algarbiensis* (Fig 2.5A, C). Also for *P. algarbiensis* the APX activity increased in

shoots at pH 4.00 without Al and in leaves at pH 4.00 with Al and the GPX activity increased in shoots and leaves in the presence of Al (Fig 2.5E, G).

The low pH and the presence of Al has induced to an increase in the activity of antioxidant enzymes in *P. algarbiensis*, which suggests that this specie is more sensitive and that *P. almogravensis* is the more stress-tolerant of the two species.

This study continued and was posteriorly published by Martins *et al* [45, 46].

2.5.2.4. Photosynthetic pigments analysis

The effect of low pH and Al on the photosynthetic pigment contents of *P. algarbiensis* and *P. almogravensis* shoots and plantlets was studied (Table 2.5).

Table 2.5 – Effect of low pH and Al on the photosynthetic pigment contents of *P. algarbiensis* and *P. almogravensis* shoots and plantlets [40].

pH	Al (µM)	Chl *a* (mg g^{-1} FW)		Chl *b* (mg g^{-1} FW)		Chl *a+b* (mg g^{-1} FW)		Crt (mg g^{-1} FW)	
		Shoot	Plantlet	Shoot	Plantlet	Shoot	Plantlet	Shoot	Plantlet
P. algarbiensis									
5.75	0	0.66 ± 0.06 a	0.60 ± 0.04 a	0.22 ± 0.02 a	0.19 ± 0.02 a	0.89 ± 0.08 a	0.78 ± 0.06 a	0.22 ± 0.02 a	0.19 ± 0.01 a
4.00	0	0.51 ± 0.01 b	0.56 ± 0.05 a	0.16 ± 0.01 b	0.18 ± 0.02 a	0.67 ± 0.01 b	0.73 ± 0.06 a	0.16 ± 0.00 b	0.18 ± 0.02 a
4.00	400	0.43 ± 0.05 b	0.62 ± 0.05 a	0.13 ± 0.01 b	0.19 ± 0.02 a	0.56 ± 0.06 b	0.81 ± 0.06 a	0.13 ± 0.01 b	0.20 ± 0.02 a
P. almogravensis									
5.75	0	0.64 ± 0.04 a	0.58 ± 0.05 a	0.22 ± 0.01 a	0.19 ± 0.02 b	0.86 ± 0.05 a	0.77 ± 0.07 b	0.19 ± 0.01 a	0.17 ± 0.01 a
4.00	0	0.66 ± 0.06 a	0.56 ± 0.04 a	0.22 ± 0.02 a	0.19 ± 0.01 b	0.88 ± 0.08 a	0.75 ± 0.05 b	0.20 ± 0.02 a	0.17 ± 0.01 a
4.00	400	0.58 ± 0.05 a	0.72 ± 0.05 a	0.21 ± 0.01 a	0.25 ± 0.01 a	0.79 ± 0.06 a	0.97 ± 0.06 a	0.18 ± 0.01 a	0.22 ± 0.02 a

Values are expressed as the mean ± SE (n = 5). For each species and in each column, mean values followed by different letters are significantly different at $P < 0.05$, according to Duncan's test.

After Al treatment it was observed a decrease in contents of Chl *a*, Chl *b*, and total carotenoids, in *P. algarbiensis* shoots. This decrease denotes that *P. algarbiensis* need to reduce the efficiency to harvest light to protect leaves from photooxidative damage, which is an indication of high sensitivity to H^+ and Al^{3+} toxicity (Table 2.5). The photosynthetic pigments contents did not differ in shoots and plantlets of *P. almogravensis* and in plantlets of *P. algarbiensis* grown in medium with Al (Table 2.5). Chl contents could be one of the most important physiological basis of plant adaptation to Al stress [47]. Thus, the obtained results suggested that *P. almogravensis* is better adapted to high Al concentration than *P. algarbiensis*.

2.5.3. Insights on Al tolerance mechanism: effects of Al in the activity of the enzymes related to the organic acids metabolism

Plants that grown in acid soils developed metabolic and cellular strategies to deal with Al toxicity that include mechanisms that exclude Al from entry into the plant and/or those detoxifying or sequestering Al symplast. Organic acids have been shown to play a rule both in Al exclusion, via release from the root and in Al detoxification by chelating Al and reduce or prevent toxic effects [9, 48].

Over a dozen Al-tolerant plant species are known to secrete organic acids from their roots in response to Al treatment. Exudation of organic acids, mainly citric and malic acids appears to be one of the main mechanisms for Al tolerance [48]. Thus, the secretion of citrate, oxalate and malate are part of the Al-tolerance mechanism, increasing evidence shows that many Al-tolerant species or cultivars are able to secrete high levels of those compounds from roots when exposed to Al. At sufficient concentrations, these organic acids can form complexes with Al ions, preventing the Al ions from binding to the fixed negative sites of the cell wall and plasma membrane [48].

The activity of fumarase and enzymes linked with the citrate biosynthesis [Citrate synthase (CS), phosphoenolpyruvate carboxylase (PEPC) and malate dehydrogenase (MDH)] or degradation as NADP-dependent isocitrate dehydrogenase (NADP-ICDH) was measured.

The effect of Al concentrations (0 µM and 400 µM $AlCl_3$) on MDH, Fumarase, PEPcase, CS and NADP-ICDH activities in shoots and roots of *P. algarbiensis* and *P. almogravensis* is shown in Figure 2.6.

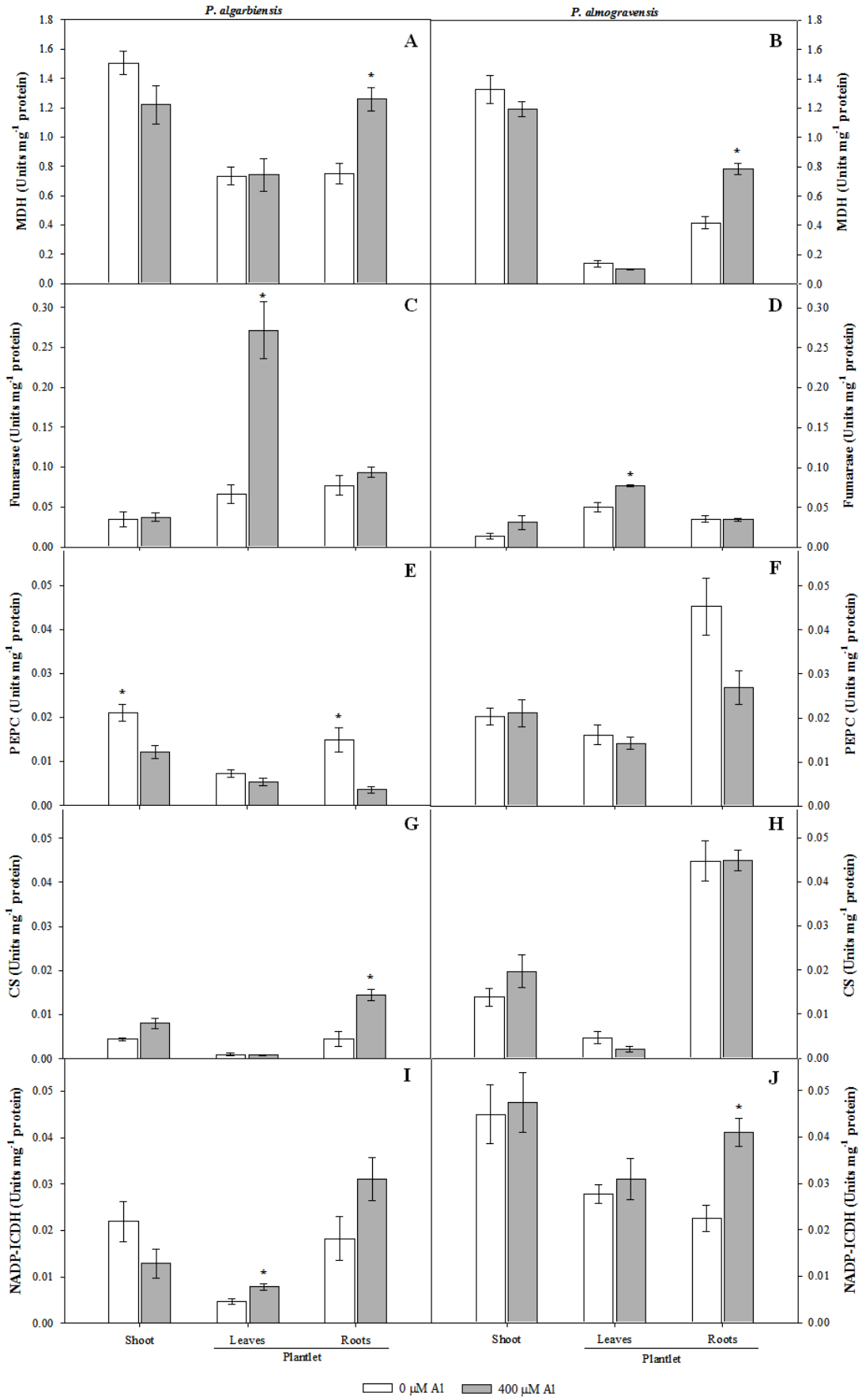

Figure 2.6 – Effect of 0 µM Al and 400 µM on MDH (A, B), Fumarase (C, D), PEPcase (E, F), CS (G, H) and NADP-ICDH (I, J) activities in shoots and roots of *P. algarbiensis* and *P.*

almogravensis. Values are expressed as the mean ± SE (n = 5). For each species, mean values followed by * are significantly different at P<0.05 and the absence of letters indicates that no significant differences were observed.

When *P. algarbiensis* and *P. almogravensis* were subjected to Al treatment, MDH increased in the roots of both species (Fig 2.6A, B). In other hand, fumarase increased in leaves of both species after Al treatment (Fig 2.6C, D). After 400 µM $AlCl_3$ exposure, the PEPcase activity increased in shoots and roots of *P. algarbiensis* whereas the activity of this enzyme did not present differences in *P. almogravensis* (Fig 2.6E, F)). In the presence of Al it was observed an increase of CS activity in the *P. algarbiensis* roots, whereas no differences were observed in treatments with and without Al for *P. almogravensis* (Fig 2.6G, H). NADP-ICDH increase in the presence of Al compared with control in *P. algarbiensis* leaves and in *P. almogravensis* roots (Fig 2.6I, J).

The increased activity of enzymes involved in the pathways of malate and citrate synthesis it is an indicator that these organic acids are involved in the Al tolerance mechanism of these *Plantago* species.

The results obtained by Martins *et al*. [49] suggest that organic acids play an important role in Al detoxification in both *Plantago* species, mainly in *P. almogravensis*. In these species the Al detoxification may be achieved by the combination of organic acids secretion from roots and Al intracellular chelation by OAs.

2.5.4. Seed germination requirements

To evaluate the effect of Al on seed germination of *P. algarbiensis* and *P. almogravensis* it was early necessary to study the germination requirements. The specific requirement for seed germination can be associated to the life form of each species, to the environment where the plant will be established and also the geographic distribution or phylogenetic origin of species and still the seed characteristics as its life history and development and maturation conditions. The temperature is an essential factor to end the dormancy and subsequent seed germination. The optimal germination temperature is one of most important factors in seed germination. Light is also an important environmental regulatory of seed dormancy and trigger for germination.

Seed morphological features, such as size (length and width), weight and water content, were investigated.

It was also studied the effect of light and temperature on germination parameters (germination percentage, Mean Germination Time (MGT) and T_{50}-time to get 50% of

final germination percentage) of *P. almogravensis* and *P. algarbiensis*. Constant temperatures (15 and 25ºC) and alternating temperature regime of 25/15ºC, with 16/8 h light/dark photoperiod and constant darkness conditions were used.

Table 2.6 – Length, width, weight and water content of *Plantago algarbiensis* and *P. almogravensis* seeds [50].

Species	Collection year	Seed length (µm)	Seed width (µm)	Length-to-width ratio	Weight of 100 seeds (mg)	Seed water content (% f.w.b..)
P. algarbiensis	2010	1768.0 ± 13.11*	1067.6 ± 9.26 *, †	1.7 ± 0.01*	79.3 ± 0.22 *, †	8.8 ± 0.75
P. almogravensis	2010	1538.8 ±12.82	963.4 ± 7.46	1.6 ± 0.02	66.8 ± 0.29	9.1 ± 1.08

Values are expressed as the mean ± SE. *: indicates significant differences (P<0.05) between results of seeds of different species collected in the same year (2010). The absence of symbol indicates that no significant differences were observed.

Table 2.7 – Effects of temperature on the final germination percentages and mean germination time (MGT) of *Plantago algarbiensis* and *P. almogravensis.* Results obtained after 40 days of incubation under 16 h light photoperiod (light) or constant darkness [50].

Species	Collection year	Temperature (ºC)	Germination (%)			MGT (days)		
			Light	Dark	S[(1)]	Light	Darks	S
P. algarbiensis	2010	15	100.0 ± 0.00 a	100.0 ± 0.00 a	Ns	3.8 ± 0.23 b	3.1 ± 0.44 b	ns
		25	83.3 ± 6.67 b	90.0 ± 5.77 a	Ns	15.8 ± 0.80 a	16.2 ± 0.85 a	ns
		15/25	66.7 ± 6.67 b	33.3 ± 8.82 b	*	18.2 ± 2.43 a	21.6 ± 3.22 a	ns
P. almogravensis	2010	15	100.0 ± 0.00 a	100.0 ± 0.00 a	ns	3.9 ± 0.07 b	2.7 ± 0.07 b	***
		25	90.0 ± 5.77 a	66.7 ± 17.64 ab	ns	13.0 ± 1.37 a	19.7 ± 1.39 a	*
		15/25	90.0 ± 0.00 a	53.3 ± 3.33b	***	12.4 ± 0.97 a	20.7 ± 1.99 a	*

Values are expressed as the mean ± SE. For each species mean values followed by different letters are significantly different at P<0.05, according to Duncan's test. For each temperature, the significance level (S) between results from light and darkness is showed. S[(1)]: ***Significantly different at P<0.001; *P<0.05; ns, not significant

The *P. almogravensis* and *P. algarbiensis* seed water content was 9.06 and 8.84 (f.w.b), respectively. *P. almogravensis* seeds are very small with mean length and width of 1538.79 and 963.41 µm, respectively. *P. algarbiensis* seeds had a slight higher size with mean length of 1767.97 µm and width of 1067.64 µm. The observed mean weight per 100 seeds was 66.77 mg for *P. almogravensis* and 79.33 mg for *P. algarbiensis* (Table 2.6).

The highest percentage of germination (100%) was obtained at 15 °C, under either light or darkness, for both species, while for 25ºC a decrease occurred in the final percentage of germination (60 - 80%). Moreover, the lower MGT and T_{50} values were also obtained under the lowest temperature. The germination was not affected by light conditions under constant temperatures of 15 and 25ºC, respectively. However, light had a positive effect on germination under alternate temperature of 25/15ºC on both species. It can be concluded that low temperature (15ºC) is advantageous to the seed germination of *P. almogravensis* and *P. algarbiensis* (Table 2.7).

Although significant differences were detected in the seed size between the two species with *P. algarbiensis* seeds showing the higher size and weight. However, no differences were observed between both species in terms of germination capability.

2.6. Conclusion

It was concluded that medium pH did not affect *in vitro* proliferation and rooting of micropropagated shoots of *P. almogravensis* and *P. algarbiensis* species. This fact confirms that *Plantago* species are able to grow *in vitro* in medium at pH values much lower than the normally used in tissue culture (pH 5.70 to 5.80). The decrease of medium pH during the root formation is in accordance with the fact that both species colonize acid soils.

Both *Plantago* species accumulate substantial and similar quantities of Al, nevertheless this metal induced the inhibition of root elongation in *P. algarbiensis*, whereas *P. almogravensis* showed to be more tolerant.

In the present study the activities of enzymes involved in organic acid metabolism were studied in response to Al in order to obtain insights on Al tolerance mechanism. The obtained results demonstrated an increase in the activity of enzymes involved in the pathways of malate and citrate synthesis. According to these results Martins *et al*. [49] suggested that organic acids play an important role in Al detoxification in both *Plantago* species, mainly in *P. almogravensis*.

The best germination results were obtained at 15°C under either light or darkness, along with the shortest mean germination time. The insights about the optimal germination of these *Plantago* species are crucial for further Al tolerance evaluation in germination and also to develop conservation strategies.

2.7. Bibliographic references

[1] Von UexkUll, H. R., Mutert, E. (1995) Global extent, development and economic impact of acid soils. Plant Soil 171, 1-15.
[2] Guo, T. R., Zhang, G. P., Zhang, Y., H. (2007) Physiological changes in barley plants under combined toxicity of aluminum, copper and cadmium. Colloids and Surfaces B: Biointerfaces 57, 182–188.
[3] Simon, L., Kieger, M., Sung, S. S., Smalley, T. J. (1994) Aluminium toxicity in tomato. Part 2. Leaf gas exchange chlorophyll content, and invertase activity. J. Plant Nutr. 17, 303-317.
[4] Meloni, D. A., Oliva, M. A., Martinez, C. A., Cambraia, J. (2003) Photosynthesis and activity of superoxide dismutase, peroxidase and glutathione reductase in cotton under salt stress. Environ. Exp. Bot. 49:69-76.
[5] Walter, K. S., Gillet, H. J.: IUCN Red List of Threatened Plants. – IUCN – The World Conservation Union, Gland – Cambridge 1998.
[6] Branquinho, C., Serrano, H. C., Pinto, M. J., Martins-Loução, M. A. (2007) Revisiting the plant hypperaccumulation criteria to rare plants and earth abundant elements. – Environ. Pollut. 146:437-443.
[7] Gonçalves, S., Martins, N., Romano, A. (2009) Micropropagation and conservation of endangered species *Plantago algarbiensis* and *P. almogravensis*. Biol Plant 53:774-778.
[8] Hue, N. V., Craddock, G. R., and Adams, F. (1986) Effect of organic acids on aluminum toxicity in subsoils. Soil Sci Am J 50:28-34.
[9] Ma, J. F., Ryan, P. R., Delhaize, E. (2001) Aluminium tolerance in plants and the complexing role of organic acids, Trends Plant Sci. 6: 273–278.
[10] Klug, B., Horst, W. (2010) Oxalate exudation into the root-tip water free space confers protection from aluminum toxicity and allows aluminum accumulation in the symplast in buckwheat (*Fagopyrum esculentum*), New Phytol. 187 380–391.
[11] Gonçalves, S., Fernandes, L., Pérez-García, F., González-Benito, M. E. and Romano, A. (2009) Germination requirements and cryopreservation tolerance of seeds of the endangered species *Tuberaria major*. *Seed Science and Technology*, **37**, 480-484.
[12] Kikui, S., Sasaki, T., Maekawa, M., Miyao, A., Hirochika, H., Matsumoto, H., Yamamoto, Y. (2005) Physiological and genetic analyses of aluminium tolerance in rice, focusing on root growth during germination. J. Inorg. Biochem. 99, 1837e1844.
[13] Murashige, T., Shoog, F. (1962) A revised medium for rapid growth and bio-assays with tobacco tissue cultures. Physiol Plant 15: 473–497.
[14] Beauchamp, C. O., Fridovich, I. (1971) Superoxide dismutase: improved assays and assays applicable to acrylamide gels. Anal Biochem 44:276–287.
[15] Aebi, H. E. (1983) Catalase. In: Bergmeyer H. U. (3rd ed) Methods of enzymatic analysis. Verlag Chemie, Weinhern, pp 273–286.
[16] Nakano, Y., Asada, K. (1981) Hydrogen peroxide is scavenged by ascorbate-specific peroxidase in spinach chloroplasts. Plant Cell Physiol 22:867–880.
[17] Egley, G. H., Paul, R. N., Vaughn, K. C., Duke, S. O. (1983) Role of peroxidase in the development of water impermeable seed coats in *Sida spinosa* L. Planta 157:224–232.
[18] Bradford, M. (1976) A rapid and sensitive method for the quantification of microgram quantities of protein utilizing the principle of protein-dye binding. Anal Biochem 72:248–254.
[19] A.O.A.C. (1990) Official Methods of Analysis, Association of Official Agricultural Chemists, Washington, DC.

[20] Hodges, D. M., Delong, J. M., Forney, C. F., Prange R. K. (1999) Improving the thiobarbituric acid-reactive-substances assay for estimating lipid peroxidation in plant tissues containing anthocyanin and other interfering compounds. Planta 207:604–611.
[21] Lichtenthaler, H. K. (1987) Chlorophylls and carotenoids: pigments of photosynthetic biomembranes. Methods Enzymol 148:350–382.
[22] Srere, P. A. (1967) Citrate synthase, Methods Enzymol. 13, 3-11.
[23] Bergmeyer, H. U., Gawehn, K. & Grassl, M. (1974) Enzymes as biochemical reagents. In Methods of Enzymatic Analysis, Bergmeyer, H. U. (ed) p. 425. 2nd ed. Academic Press: New York.
[24] Miller, S. S., Driscoll, B. T., Gregerson, R. G., Gantt, J. S., Vance, C. P. (1998) Alfalfa malate dehydrogenase (MDH): molecular cloning and characterization of five different forms reveals a unique nodule enhanced MDH. Plant J. 15: 173-184.
[25] Blanke, M., Notton, B., and Hucklesby, D. (1986) Physical and kinetic properties of photosynthetic PEP carboxylase in developing apple fruit. Phytochem, 25: 601-606.
[26] Ellis, R. H. and Roberts, E. H. (1981) The quantification of ageing and survival in orthodox seeds. Seed Sci. Technol., 9: 373-409.
[27] Martins, N., Gonçalves, S., Palma, T. and Romano, A. (2011) The influence of low pH on in vitro growth and biochemical parameters of *Plantago almogravensis* and *P. algarbiensis*. Plant Cell, Tissue and Organ Culture 107: 113-121. DOI: 10.1007/s11240-011-9963-1.
[28] Schuch, M. W., Cellini, A., Masia, A., Marino, G. (2010) Aluminium induced effects on growth, morphogenesis and oxidative stress reactions *in vitro* cultures of quince. Sci Hortic 125:151–158.
[29] Leifert, C., Pryce, S., Lumsden, P. J., Waites, W. M. (1992) Effect of medium acidity on growth and rooting of different plant species *in vitro*. Plant Cell Tissue Organ Cult 30:171–179.
[30] Shibli, R. A., Mohammad, M. J., Ajlouni, M. M., Shatnawi, M. A., Obeidat, A. F. (1999) Stability of chemical parameters of tissue culture medium (pH, osmolarity, electrical conductivity) as a function of time of growth. J Plant Nutr 22:501–510.
[31] Marschner, H., Römheld, V., Horst, W. J., Martin, P. (1986) Root-induced changes in the rhizosphere: Importance for the mineral nutrition of plants. Z Pflanzenernaehr Bodenkd 149:441–456.
[32] Marschner, H. (1995) Mineral nutrition of higher plants, 2nd ed. Academic Press, London.
[33] Sivanesan, I., Song, J. Y., Hwang, S. J., Jeong, B. R. (2011) Micropropagation of Cotoneaster wilsonii Nakai—a rare endemic ornamental plant. Plant Cell Tissue Organ Cult 105:55–63.
[34] Xu, F. J., Li, G., Jin, C. W., Liu, W. J., Zhang, S. S., Zhang, Y. S., Lin, X. Y. (2012) Aluminum-induced changes in reactive oxygen species accumulation, lipid peroxidation and antioxidant capacity in wheat root tips. Biol. Plant. **56**: 89-96.
[35] Singh, P. K., Tewari, R. K. (2003) Cadmium toxicity induced changes in plant water relations and oxidative metabolism of *Brassica juncea* L. plants. J Environ Biol 24:107–112.
[36] Ashraf, M., Harris, P. J. C. (2004) Potential biochemical indicators of salinity tolerance in plants. Plant Sci 166:3–16.
[37] Costa, M. A., Pinheiro, H. A., Shimizu, E. S. C., Fonseca, F. T., Filho, B. G. S., Moraes, F. K. C., Figueiredo, D. M. (2010) Lipid peroxidation, chloroplastic pigments and antioxidant strategies in *Carapa guianensis* (Aubl.) subjected to water-deficit and short-term rewetting. Trees 24:275–283.

[38] Kidd, P. S., Proctor, J. (2001) Why plants grow poorly on very acid soils: are ecologists missing the obvious? J Exp Bot 52:791–799.
[39] Bose, J., Babourina, O., Shabala, S., Rengel, Z. (2010) Aluminum dependent dynamics of ion transport in Arabidopsis: specificity of low pH and aluminum responses. Physiol Plant 139:401–412.
[40] Martins, N., Osório, M. L., Gonçalves, S., Osório, J., Palma, T., Romano, A. (2012). Physiological responses of *Plantago algarbiensis* and *P. almogravensis* shoots and plantlets to low pH and aluminium stress. Acta Physiol Plant 35:615-625 (2). DOI 10.1007/s11738-012-1102z.
[41] Chen, Y. M., Tsao, T. M., Liu, C. C., Lin, K. C., Wang, M. K. (2011) Aluminium and nutrients induce changes in the profiles of phenolic substances in tea plants (*Camellia sinensis* CV TTES, No.12 (TTE)). J Sci Food Agric 91:1111–1117.
[42] Choudhary, A. K., Singh, D. (2011) Screening of pigeon pea genotypes for nutrient uptake efficiency under aluminium toxicity. Physiol Mol Biol Plants 17:145–152.
[43] Wang, J. P., Raman, H., Zhang, G. P., Mendham, N., Zhou, M. X. (2006) Aluminium tolerance in barley (*Hordeum vulgare* L.): physiological mechanisms, genetics and screening methods. J. Zhejiang Univ. SCIENCE B, 7(10):769-787.
[44] Sharma, P., Jha, A. B., Dubey, R. S. and Pessarakli, M. (2012) Reactive Oxygen Species, Oxidative Damage, and Antioxidative Defense Mechanism in Plants under Stressful Conditions. Journal of Botany: Doi:10.1155/2012/217037.
[45] Martins, N., Osório, M. L., Gonçalves, S., Osório, J., Romano, A. (2013) Differences in Al tolerance between *Plantago algarbiensis* and *P. almogravensis* reflect their ability to respond to oxidative stress Biometals DOI 10.1007/s10534-013-9625-3.
[46] Martins, N., Gonçalves, S., Romano, A. (2013) Metabolism and aluminum accumulation in *Plantago almogravensis* and *P. algarbiensis* in response to low pH and aluminum stress. Biol Plant 57:325–331.
[47] Liu, P., Yang, Y. S., Xu, G., Guo, S., Zheng, X., Wang, M. (2006) Physiological responses of four herbaceous plants to aluminum stress in South China. Front Biol China 3:295–302.
[48] Yang, L. T., Qi, Y. P., Jiang, H. X. and Cheng, L. S. (2013) Role of organic acid anion secretion in Aluminium tolerance of Higher Plants. Biom Rearch Inter Doi: 10.1155/2013/173682.
[49] Martins, N., Gonçalves, S., Andrade, P., Valentão, P. and Romano, A. (2013) Changes on organic acid secretion and accumulation in *Plantago almogravensis* Franco and *Plantago algarbiensis* Samp. Under aluminum stress. Plant Science 198: 1-6.
[50] Martins, N., Gonçalves, S., Palma, T. and Romano, A. (2012) Seed germination of two critically endangered plantain species, *Plantago algarbiensis* and *P. almogravensis* (Plantaginaceae). *Seed Sci. & Technol.*, Vol.40, Nº1, 144-149 (6).

Chapter 3. Bio-recovery of palladium (II) and biosynthesis of metal sulphide nanoparticles by anaerobic bacteria communities.

3.1. Resume

Presently, I am working in the Environmental Technologies laboratory, of Centre of Marine Sciences (CCMAR) in the area of environmental biotechnology, performing biosynthesis and bioremediation studies. The work includes enrichment of anaerobic bacteria communities from environmental samples and screening of their resistance and ability to recover palladium (Pd (II)). Among the several samples tested a metal resistant bacteria consortium with ability to recover Pd (II) was obtained from a sludge sample of the Wastewater Treatment Plant of Lagos (Southern Portugal). This bacterial community was maintained in anaerobic conditions in medium with and without sulphate. The consortium was able to recover 50 mg/L of Pd (II) from an aqueous solution. Also, it was able to remove 98% of palladium (II) from an aqueous solution containing 70 mg/L of Pd (II) in the presence of sulphate and 82.7% of 70 mg/L of Pd (II) in the absence of sulphate. Thus, this consortium has shown an excellent palladium (II) resistance and consequently can be a potential candidate for Pd (II) removal from aqueous media. In addition, the Pd (II) removal mechanism for both cultures (growth in the presence and absence of sulphate) was also investigated.

Once it has been difficult to maintain the optimal performance of the culture a protocol was developed, in order to investigate the best storage conditions and stability of that bacterial community.

Simultaneously, other study is in course, which consists on the synthesis of metal sulphide nanoparticles using sulphide generated by sulphate-reducing bacteria (SRB).

ZnS and PbS precipitates and also their derived nanocomposites of TiO_2 were obtained and were analyzed by X-Ray diffraction and by diffuse reflectance.

The obtained nanoparticles are being applied in the degradation of emerging pollutants .

Keywords: Bio-recovery; Metal resistant bacteria; Palladium (II); Sulphate-reducing bacteria (SRB); Synthesis of metal sulphide nanoparticles

3.2. Palladium (II) recovery by an anaerobic bacteria community

3.2.1. Introduction

Platinum group metals (PGMs), *e.g.* Pd, Pt and Rh, are of interest due to their high value and catalytic properties. PGM demand is increasing due to their widespread and often obligatory utilization in automotive catalytic converters [1]. In the last decades, there has been a considerable expansion in the use of precious metals in medicine, optical devices, electronics and catalysis [2]. Especially Pd has become a very widespread catalyst. In addition, due to the limitation of the primary resources recovery of palladium from waste is required [3]. There is a trend to switch from the use of bulk material towards nanoparticles (NPs) (sized between 1 and 100 nanometers) of palladium, since NPs are more active and thus less catalyst is needed. Conventional production methods of these NPs require the use of a series of toxic and expensive chemical agents [4].

Thus, bio-recovery of metals from dilute industrial waste using bacteria can be a promising alternative to primary raw material resources. Therefore, search and identification of palladium resistant bacteria with ability to remove that metal from solutions is very important. The main goal of this study was to find palladium (II) resistant bacterial communities able to bio-recover this metal from solutions.

Physico-chemical mechanisms such as ionic interactions, complexation, and chelation between metal ions and ligands, depending on the specific properties of the biomass (alive, or dead, or as a derived product) can be involved in metals removal. Biosorption is a very complex metabolism independent process, in which there is physical or chemical sorption onto the cell wall, or alternatively biosorption can be related to cell metabolism [5, 6]. Other metal-removal mechanisms dependent on metabolism include metal precipitation as sulfides or phosphates, sequestration by metal binding proteins, peptides or siderophores, transport and internal compartmentalization [6]. Several SRB-based technologies have been successfully developed to treat heavy metal contaminated effluents [3]. Thus, in the present work mixed bacterial cultures were studied, therefore the communities were enriched in media with sulphate to favor the growth of SRB and without sulphate to growth the other potential anaerobic bacteria important for bioremediation processes. Thereafter, the consortium grown in media with and without sulphate, were used to evaluate the bacterial palladium (II) removal ability.

3.2.2. Material and methods

3.2.2.1. Microorganisms and growth conditions

The bacterial communities used in this experiment were obtained from sludge from a municipal wastewater treatment plant located in Lagos in southern Portugal (denominated Lag 1). These consortia were enriched in Postgate B medium supplemented with resazurin as redox indicator (3.2 mL/L of a stock solution 0.1 g/L), at room temperature, in anaerobic conditions. Subsequently, the bacterial consortium was grown in palladium test medium (PdTM) which contains, 1.0 g/L NH_4Cl, 0.5 g/L KH_2PO_4, 4.5 g/L Na_2SO_4, 0.06 g/L $CaCl_2.6H_2O$, 0.06 g/L $MgSO_4.7H_2O$, 6 g/L sodium lactate, 1 g/L yeast extract, 0.3 g/L Tri-sodium citrate, 0.1 g/L NaCl, 0.0072 g/L $FeSO_4.7H_2O$ and supplemented with different Pd concentrations: 50 mg/L, 70 mg/L and 100 mg/L as palladium(II) chloride. The media without sulphate was the same but $MgSO_4$ salt was replaced by $MgCl_2.6H_2O$ (0.048 g/L) and Na_2SO_4 was removed from the medium. The medium were sterilized and after the addition of palladium (II) chloride at 50, 70 and 100 mg/L the pH was corrected to pH ~7.

As negative control it was used medium supplemented only with palladium (II) without bacteria and as positive control it was used medium supplemented with inoculum without that Pd (II). The culture was sub-cultured every 4 weeks using 10% (v/v) inoculum and the bacterial growth was monitored by weekly determination of pH, Eh (mV), sulphate concentration, ($O.D._{600nm}$) optical density at 600 nm to monitor bacterial growth and concentration of Pd (II).

3.2.2.2. Batch experiments

After the enrichment of the bacterial consortium the assays were performed in batch under anaerobic conditions, using the palladium test medium (PdTM) previously described (pH~7.5). All experiments were performed in triplicates using glass bottles (120 mL) containing 100 mL of PdTM and 10% (v/v) of inoculum. The bacterial cells obtained previously were harvested by centrifugation at 4000 rpm for 10 min, washed with growth medium and transferred to the bottles containing the medium to be tested. The medium was purged with nitrogen gas to achieve an anaerobic environment prior to the inoculation and then about 10 mL of paraffin was added. Finally, the bottles were

sealed with butyl rubber stoppers and aluminum crimp seals and incubated at room temperature.

The ability of palladium (II) removal from the medium by the bacterial consortium was investigated in the presence and absence of sulphate. The mechanism of Pd (II) removal by ***live cells*** and **by *heat-killed cells*** was investigated.

- **Pd (II) removal by *live cells***

The studies of Pd (II) bio-removal were performed in 120 mL glass bottles containing PdTM, previously described, supplemented with palladium (II) at range concentrations from 50 to 100 mg/L. For each experiment an abiotic control was performed in parallel. The abiotic controls were prepared in the same way as the biotic tests, but without the addition of inoculum.

The ability of Pd (II) removal from the medium by the bacterial culture was also investigated in the absence of sulphate.

- **Pd (II) removal by *heat-killed cells***

Palladium (II) bio-removal by heat-killed cells was also explored using 35 mL glass bottles. Bacterial cells (30 mL) were harvested by centrifugation at 4000 rpm for 10 min and washed with growth medium. The cells were killed by autoclaving (121ºC, 30 min) and added to bottles containing PdTM with 70.0 ± 0.5 mg/L of Pd (II)**.**

3.2.2.3. Analytical Methods

Periodically, samples from cultures were collected using a syringe and optical density at 600 nm (OD_{600}nm) was measured in each sample. The samples were analysed after centrifugation at 4000 rpm for 5 min. Redox potential and pH were determined using a pH/E Meter (GLP 21, Crison). Sulphate concentration was quantified by UV/visible spectrophotometry (Hach-Lange DR2800 spectrometer) using the method of SulfaVerR4. Pd (II) removal was monitored by flame atomic absorption spectroscopy (AAS, Varian Spectrometer model AA-20). In palladium analysis, for each sample five readings were considered and the results were critically treated and only accepted with a reasonable standard deviation (< 2%).

The precipitates generated during the bio-removal process were characterized by X-ray powder diffraction (XRD) using a PANalytical X'Pert Pro powder difractommeter operating at 45 kV and 40 mA, with CuKα radiation filtered by Ni. XRD patterns were recorded using a X'Celerator detector, with a step size of 0.016 and a time per step of

50 seconds. The HighScore Plus software, with the ICDD PDF-2 database, was used for peak analysis and crystalline phase identification.

3.2.2.4. Long term storage of anaerobic bacteria consortium

The assays were performed in batch under anaerobic conditions, with and without palladium in the growth medium previously described (pH range 6.0 – 7.5). The conditions of storage were: room temperature, 4-6ºC and -80ºC with 5%, 25% and 10% of a 50% and 86% glycerol stock solution, respectively. All experiments were performed in triplicate using glass bottles (35 mL) with 15 mL of growth medium with and without Pd and 10% (v/v) of inoculum. For the storage at -80ºC the samples were aliquoted and stored in cryovials. The viability of bacterial populations will be studied for 3, 6, 9 and 12 months.

3.2.3. Results and discussion

Although the use of mixed bacterial cultures presents advantages over pure cultures, few studies have been focused in PGM recovery using mixed cultures and their use for Pd (II) recovery was only reported for the first time very recently [7]. Thus, in the present study mixed enriched consortia was used to evaluate its palladium (II) removal ability. This study hopes to contribute for the development of low cost and environmentally acceptable metals bio-recovery procedures.

A palladium (II) resistant bacteria community able to remove that metal from the growth medium was obtained from a sludge sample from a municipal waste water treatment plant.

Bacterial growth and Pd (II) removal in the presence and absence of sulphate for different concentrations of Pd (II): 50 mg/L, 70 mg/L and 100 mg/L was studied. The results obtained for 50 mg/L Pd (II) are shown in Fig. 3.1.

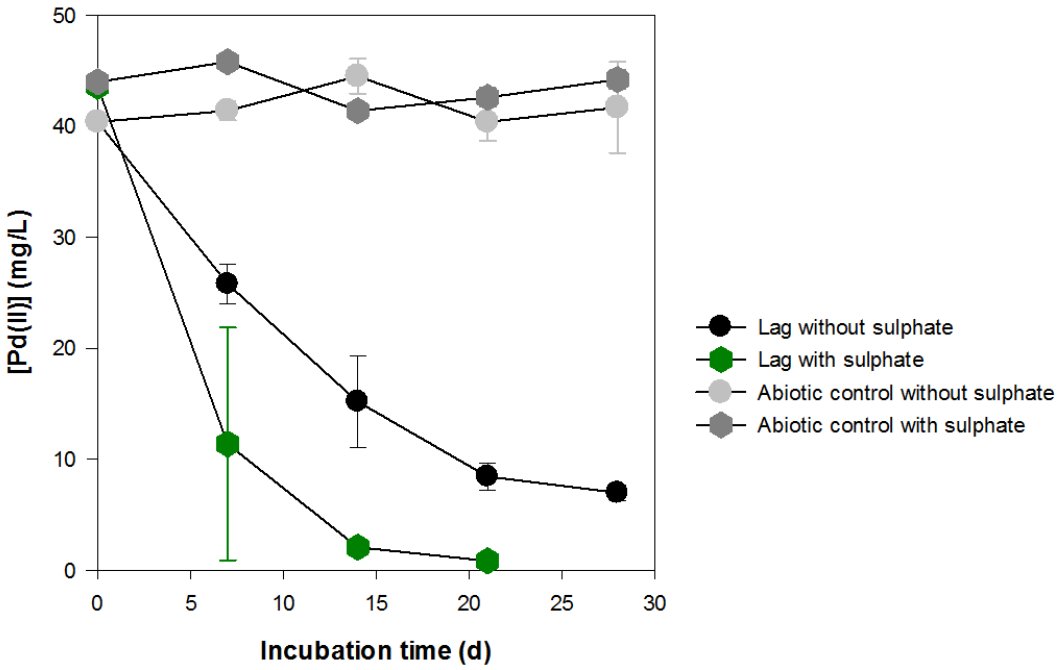

Figure 3.1 – Palladium (II) removal ability of bacterial consortium Lag 1 for 50 mg/L Pd (II) from the medium in the presence and absence of sulphate and abiotic control with and without sulphate. Values are expressed as the mean ± Standard Deviation (n = 3).

The bacterial growth of the biotic control without Pd (II) was of 1.214 ($O.D._{600nm}$) after 21 days. The results of $O.D._{600\ nm}$ were of 1.352 and 0.575 for 50 mg/L Pd (II), in the presence and absence of sulphate, respectively after 28 days. The bacterial growth decreased in the absence of sulphate at 50 mg/L Pd (II).

Lag 1 was efficient in the removal of 50 mg/L de Pd (II). However, the removal was faster in the presence of sulphate reaching 98.0% of removal of Pd (II) in 21 days of incubation, whereas for Lag 1 without sulphate the removal in 28 days achieved 82.7% of Pd (II) removal (Fig.3.1).

Once an almost complete removal of 50 mg/L was obtained, a higher concentration of Pd (II), 70 mg/L, was tested. For comparison, an inoculation at 50 mg/L Pd (II) was also performed simultaneously and the results are presented in Figure 3.2.

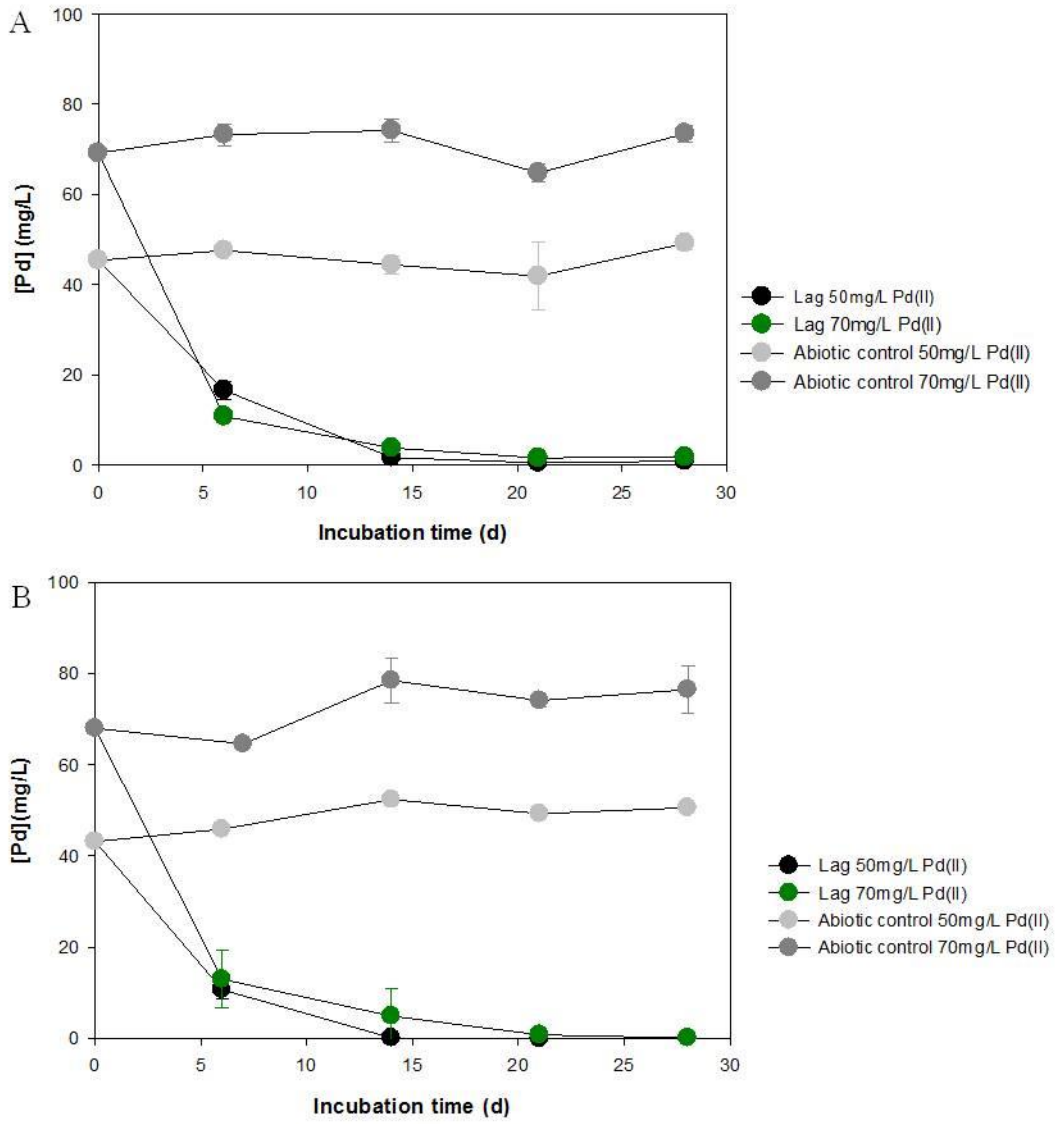

Figure 3.2 – Palladium (II) removal from the medium in the absence (A) and presence (B) of sulphate at 50 mg/L and 70 mg/L of Pd (II). Values are expressed as the mean ± Standard Deviation (n = 3).

The bacterial growth of the biotic control without Pd (II) was of 1.214 ($O.D._{600nm}$) after 21 days. The results of $O.D._{600\ nm}$ were of 1.686 and 1.067 for 50 mg/L Pd (II), in the presence and absence of sulphate, respectively and of 1.783 and 1.511 for 70 mg/L Pd(II) in the presence and absence of sulphate, respectively, after 28 days. Thus for 70 mg/L Pd (II) the bacterial growth presented slightly higher values than for 50 mg/L.

According to Fig. 3.2 (A), the performance of Pd (II) bio-removal at 50 mg/L in the absence of sulphate was approximately 97.4% of Pd (II), whereas in the presence of sulphate (Fig. 3.2 (B)) 98.9% of Pd (II) removal was obtained after 14 days.
According to Fig. 3.2 (A), in the absence of sulphate approximately 97.4% of Pd (II) was removed from the solution after 28 days of incubation at 70 mg/L, whereas in the presence of sulphate (Fig. 3.2 (B)) complete removal of 70 mg/L was obtained after 28 days of incubation.

The increase of metal concentration from 50 to 70 mg/L revealed that although complete removal of Pd (II) was attained for both concentrations, the removal was faster at 50 mg/L (21 days) than at 70 mg/L (28 days).

Once an almost complete removal of 70 mg/L was obtained, a higher concentration of Pd (II) was tested (100 mg/L). Again, a simultaneous inoculation at 50 mg/L of Pd (II) was performed and the results are presented in Fig. 3.3.

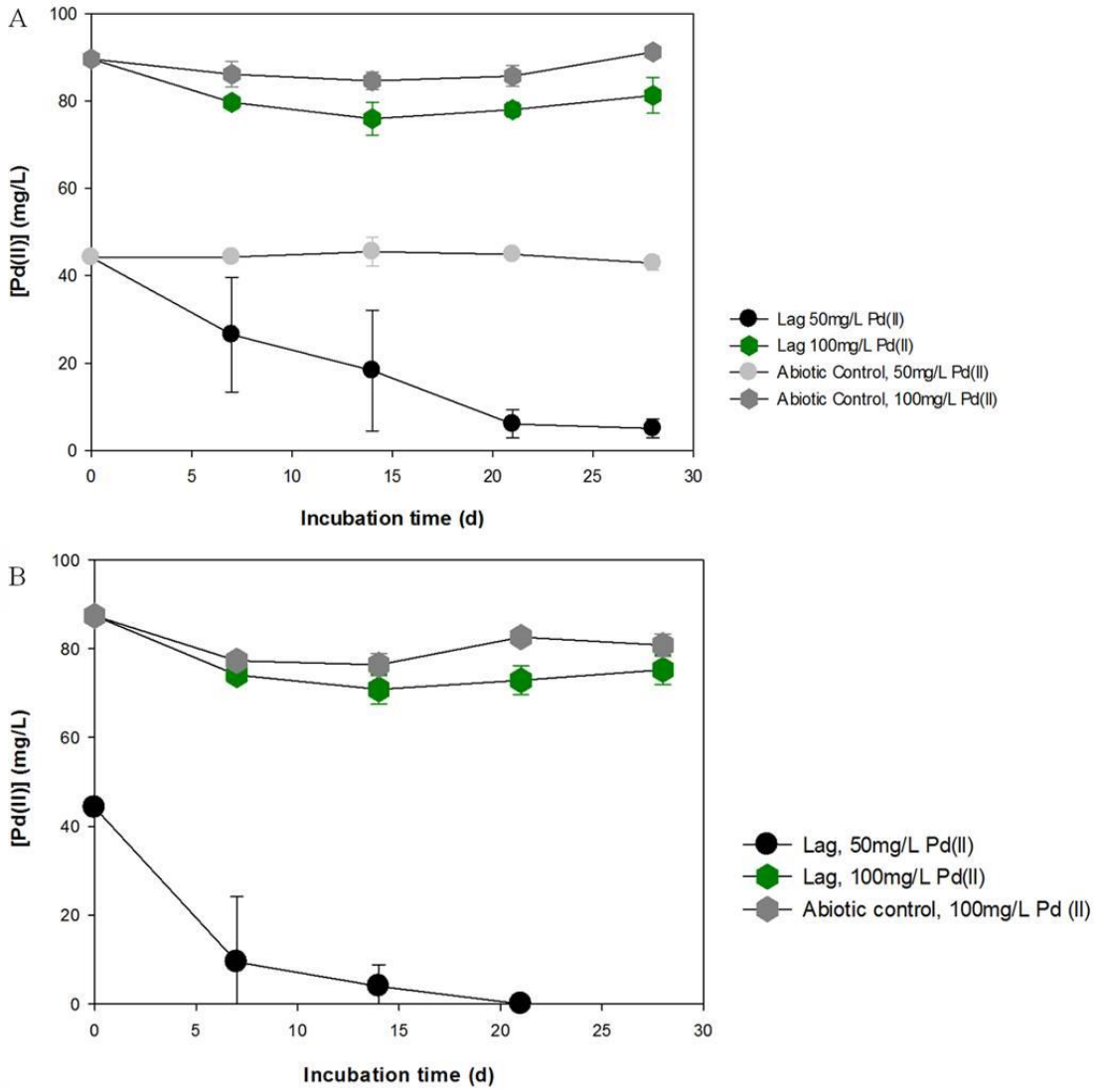

Figure 3.3 – Palladium (II) removal from the medium in the absence (A) and presence (B) of sulphate at 50 mg/L and 100 mg/L of Pd (II). Values are expressed as the mean ± Standard Deviation (n = 3).

As a results of bacterial growth the optical density ($O.D._{600\ nm}$) was of 1.000 and 0.752 for 50 mg/L Pd (II), in the presence and absence of sulphate, respectively.
Comparatively with the results obtained in the previous re-inoculations at 50 mg/L Pd (II) the optical density slightly decreased in the presence of sulphate, after 28 days.

According to the Fig. 3.3 (A) in this re-inoculation the removal of 50 mg/L Pd (II) from the medium in the absence of sulphate remained in 88.5%. It was observed that Lag 1 in the medium in the presence of sulphate (Fig. 3.3 (B)) was effective in the removal of 50mg/L Pd (II) reaching up to 100 % removal after 21 days of incubation.

When the concentration of metal was increased up to 100 mg/L the bacterial community did not resist, in both conditions (Fig 3.3 (A, B)), probably due to the high concentration and consequent toxicity of the metal. The results were also confirmed by the low optical density ($O.D._{600nm}$) values observed, 0.157 and 0.183, in presence and absence of sulphate, respectively.

It is very important that the consortium has high stability. Comparing the three inoculations at 50 mg/L Pd (II) it was evident that the consortium was losing the performance in the absence of sulphate, whereas in the presence of sulphate remained more or less stable. These may reveal that both consortia are different and that the consortium grown in the absence of sulphate is not stable.

To assess the removal mechanism of 70 mg/L of Pd (II) (the best removal concentration obtained) by the bacterial consortium in the absence or presence of sulphate Pd (II) removal by *live cell* and *heat-killed cells* was investigated.
Fig. 3.4 shows the removal ability by bacterial consortium Lag 1 for 70 mg/L Pd (II) from the medium in the absence of sulphate by cells (live and heat-killed) and by metabolic products.

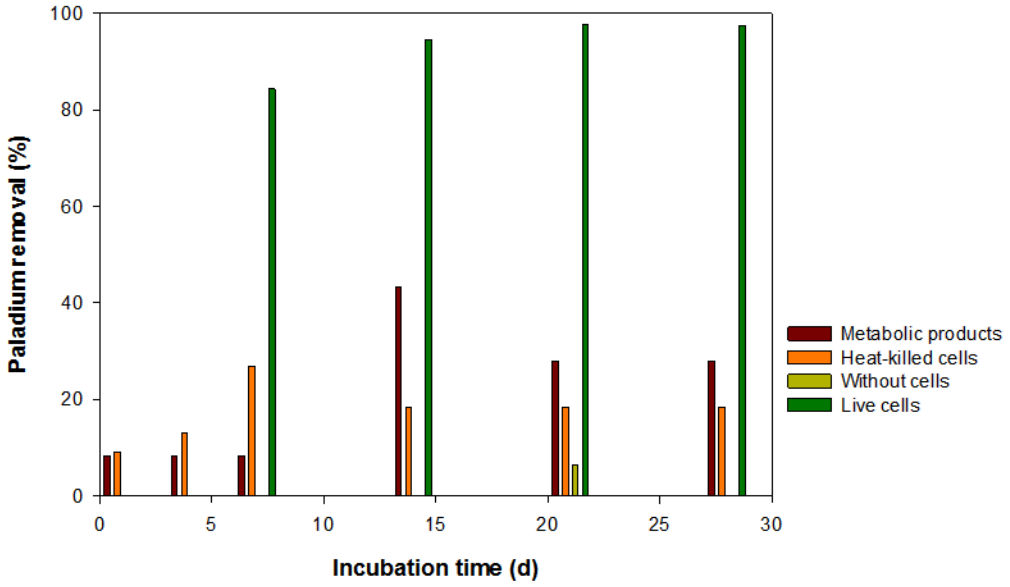

Figure 3.4 – Palladium (II) removal from the medium in the absence of sulphate at 70 mg/L of Pd (II) by Lag 1 bacterial consortium (live and heat-killed cells) and by metabolic products.

It was verified that the highest removal of Pd (II), in the absence of sulphate, occurs mainly by *live cells* (Fig 3.4).

The removal ability of the bacterial consortium in the presence of sulphate by cells (live and heat-killed) and through the action of metabolic products is represented in Fig. 3.5.

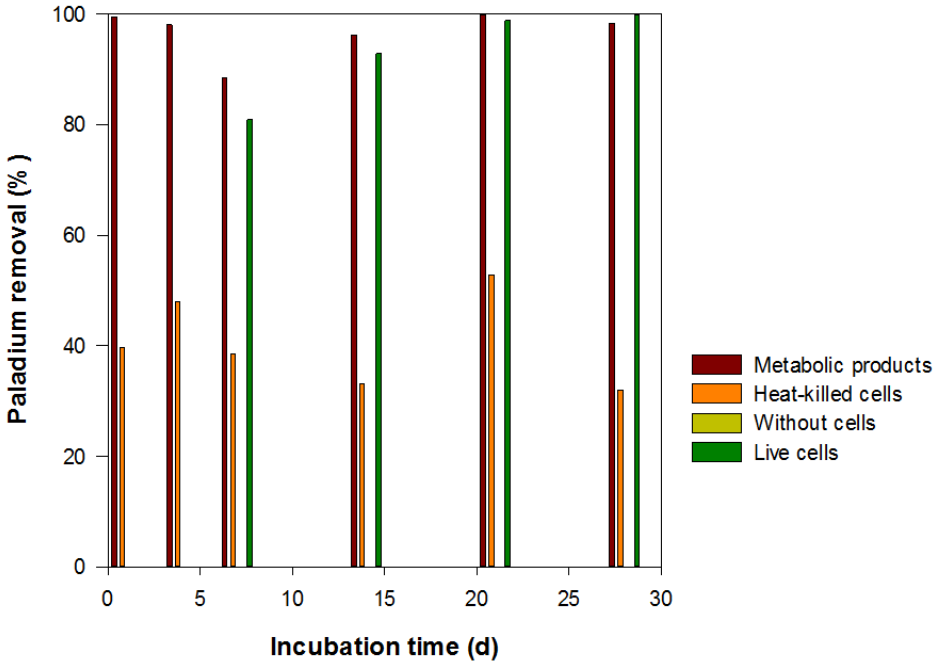

Figure 3.5 – Palladium (II) removal from the medium in the presence of sulphate at 70 mg/L of Pd (II) by cells (live and heat-killed) and by metabolic products.

It was verified that the highest removal of Pd (II) occurs when the metabolic products entered in contact with the metal (>90%). The percentage of Pd (II) removal by heated-killed cells did not exceed 53%. Living cells removed 81% Pd (II) after 7 days of incubation. This community was able to remove 98% of palladium (II) from an aqueous solution containing 70 mg/L of Pd (II) in the presence of sulphate, in this case the removal mechanism was mainly by metabolic products whereas in the absence of sulphate the consortium was capable to remove 82.7% of 70 mg/L of Pd (II) mainly by *live cells* (Fig. 3.4 and 3.5). Thus, this consortium has shown an excellent metal resistance and consequently can be a potential candidate for Pd (II) removal from aqueous media. Thus, the mechanism of Pd (II) removal, in the absence of sulphate, revealed to be different than the one presented by the community grown in the presence of sulphate. The obtained results could also indicate that the community is not the same.

The XRD analysis of these biological generated precipitates showed that they are mainly composed of amorphous material (data not shown). This result can be explained by the high ratio between cells, medium compounds and metal amount.

Very recently Martins and colleagues [7] demonstrated for the first time the ability of a Pd (II)-resistant mixed bacterial culture (enriched from a sludge sample from a municipal waste water treatment plant) to recover 60 % palladium from an aqueous medium, leading to the formation of Pd (0) nanoparticles [7]. They investigated palladium (II) removal by live cells and heat-killed cells in the presence and in the absence of sulphate and the results indicated that the mechanism associated to viable cells could be the main responsible for palladium (II) removal from solution in the absence of sulphate [7]. These results, although performed with bacteria enriched from different samples and in the presence of lower Pd (II) concentrations (~18 mg/L), the removal mechanism are consistent with the present study. Martins and colleagues [7] verified that the occurrence of Pd (II) bioreduction to form Pd nanoparticles was consistent with the composition of the bacterial community, which was mainly composed of *Clostridium* species. In fact, it has been demonstrated that the H_2 produced by bacteria belonging to the *Clostridium* genus can subsequently reduce Pd (II) to Pd (0). Moreover, the reduction of Pd (II) to Pd (0) by H_2 produced by species of *Citrobacter* and *Bacteroides*, that were also present in the community of that study, has also been reported. However, according to the literature [7], a mechanism of direct enzymatic reduction of Pd (II) to Pd (0) by these bacteria species cannot be excluded.
In the present study a community with a higher Pd (II) resistance than the community reported by Martins and colleagues [7] (which was only resistant to Pd (II) concentrations $\leq$18 mg/L) was obtained. This new community has also ability to remove higher concentrations of this metal, namely 70 mg/L Pd (II), which is a relevant improvement considering its biorecovery.

3.2.4. Conclusion

In the present study a mixed bacterial culture highly resistant to Pd (II) was enriched from a sludge sample from a municipal wastewater treatment plant. In addition, it presents a remarkable ability to remove 70 mg/L of this metal, in the presence or absence of sulphate.

The Pd (II) removal mechanism depends on the presence or absence of sulphate in the growth medium, which may indicate a different composition of both communities.

3.2.5. Studies in course

Transmission electron microscopy coupled with an energy dispersive spectrometer TEM-EDX will be used to establish the distribution and localization of the palladium precipitates in the cells, the elemental characterization of the metal deposits and their sizes. The results obtained can also be an important contribution for the investigation of the mechanism of Pd (II) removal.

However, the high performance of the consortium appears to be difficult to maintain, thus a protocol of storage is under investigation.

It is of great importance the search and identification of palladium (II) resistant and stable bacterial communities with ability to remove that metal from aqueous solutions to be used in processes of bioremediation or bio-recovery.
The investigation of the stability of the consortia after three months in which the inocula are maintained in the following different conditions:
room temperature, 4-6ºC and -80ºC with 5%, 25% and 10% of a 50% and 86% glycerol stock solution is in course. After three months the samples will be re-inoculated and the viability of community will be studied by measuring several growth parameters, such as the optical density, the redox potential and the consumption of sulphate.
The structure of the bacterial communities with ability for palladium (II) removal from medium in the presence and in the absence of sulphate will be determined by phylogenetic (molecular characterization) analysis, in order to identify the bacteria responsible for Pd (II) removal. Also, PCR-DGGE (Denaturing gradient gel electrophoresis) will be used as a fingerprinting method for the analysis of bacterial biodiversity and identification. Those studies are already in course.

3.3. Synthesis of metal sulphide nanoparticles using sulphide generated by sulphate-reducing bacteria (SRB)

3.3.1. Introduction

Bacterial reduction of sulphate is a potential mechanism to process mine drainage and other waste streams polluted with toxic metals. Many metals can be precipitated with sulphide, and their formation imobilise metals, thus helps to decrease their toxicity. The role of sulphate reducing bacteria (SRB) in producing sulphide as a precipitation agent of many metal ions Fe, Ni, Cu, and Zn is well known [8]. These precipitates can be filtered out and by this way the aqueous media contaminated with metal ions can be bio-remediated [9].

Sulphate-reducing bacteria (SRB) use sulphate as the terminal electron acceptor during the metabolism of organic matter (CH_2O), resulting in the production of H_2S according toreaction 1 [10]:

$SO_4^{2-} + 2CH_2O \rightarrow H_2S\ (g) + 2HCO_3^-$ (reaction 1)

The generation of sulphide provide the precipitation of metals as sulphides [11]:

$M^{2+} + H_2S \rightarrow MS(\downarrow) + 2H^+$ (reaction 2), where M^{2+} represents the dissolved metal.

Thus, SRB have been used in bioremediation processes, namely, in the reduction of high-content of sulphate and metals in effluents [11]. However, this process generates an excess of sulphide and this excess and disposal of the metal sulphides are also problems that need to be carefully addressed.

Therefore, the production of functional nanomaterials using bacterial growth media solutions containing biologically produced sulphide, at room temperature and atmospheric pressure, thus avoiding the use of toxic and expensive chemicals is a welcome approach. This process is an interesting alternative once its application presents evident economic advantages and safety, as the sulphide is biologically produced in the growth media by SRB simply enriched from environmental samples. Thus, the use of the sulphide in excess to produce nanocrystalline materials is an important contribution to solve the problem caused by that excess, having as an extra value the production of metal sulphide nanoparticles and nanocomposites. such as ZnS (zinc sulphide) [12] and CuS (copper sulphide) [13], with potential environmental applications mainly related to their semi-conductor properties.

For 20 years, many articles have reported the presence of new compounds, called "emerging pollutants", in wastewater and aquatic environments [14]. Emerging pollutants are new products or chemicals without regulatory status and whose effects on environment and human health are unknown [14]. The EU water framework directive 2000/06/CE announced in Annex X a list of 33 priority substances or groups of substances which include metals, pesticides, phthalates, polycyclic aromatic hydrocarbons, and endocrine disruptors. These substances must be removed within an objective of quality and preservation of good ecological status of water by 2015 [14]. Authorities should pay particular attention to their industrial discharge into the water but they also have to ensure safety for the population. The presence of metals, bacteria, hydrocarbons or other ions like nitrates (NO_3^-) and ammonia (NH_4^+) in water have been described for several decades and their impact on human health and the environment are known; these contaminants are subject to regulation and control. But the occurrence and effects of phthalates, pharmaceuticals compounds, PAHs (Polyhydroxyalkanoates), PCBs (Polychlorinated Biphenyls), Bisphenol A ($(CH_3)_2C(C_6H_4OH)_2$) is often not available [14]. Actually, there is an interest to process wastewaters which contain emerging contaminants from effluents discharged of food, pharmaceutical, additive, steroids, hormones and personal care products industries. Those substances negatively change the properties of water, which is a vital space, nutritive medium for plants and terrestrial animals and especially a natural resource [15]. The accumulation of antibiotics in organisms may cause arthropathy, nephropathy, damage in the central nervous system and spermatogenesis, mutagenic effects, and light sensitivity [16]

The antibiotics in the biosphere are contaminants that produce the phenomenon of bacterial resistance. When those products come in contact with a microorganism it can become resistant which could not be controlled with the same antibiotic formula [15].

The photocatalytic degradation is considered a favored, promising, cleaner and greener technology for the removal of toxic organic and inorganic pollutants from water and wastewater [17]. Using semiconductors is an effective and fast technique that results in fast oxidation of the pollutants [17]. The photocatalytic materials will facilitate chemical reactions without being consumed or transformed. In the photocatalytic degradation procedure, a semiconductor heterogeneous catalyst is used and, when light irradiated at the adequate wavelength, this semiconductor becomes a powerful oxidant, which can result in the conversion of the organic pollutant into water and carbon dioxide [18].

TiO_2 has the most efficient photoactivity, the highest stability and the lowest cost [19].

In this work, nanocrystalline structures of metallic sulphides and the respective nanocomposites supported on TiO_2 particles have been synthesized under ambient conditions and using biogenic sulphide in order to evaluate their efficiency in the photodegradation of emergent pollutants. For that purpose chloramphenicol, a broad-spectrum antibiotic largely utilised and exhibiting activity against both Gram-positive and Gram-negative bacteria, as well as other groups of microorganisms was chosen.

The IUPAC name of CAP is 2-dichloro-N-[(1R,2R)-2-hydroxy-1-(hydroxymethyl)-2-(4-nitrophenyl)ethyl]acetamide. Its molecular weight is 323,13 g/mol and presents the following chemical structure [20]:

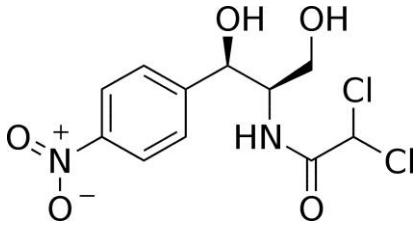

Figure 3.6 – Chloramphenicol ($C_{11}H_{12}N_2O_5Cl_2$) chemical structure.

3.3.2 Materials and methods

3.3.2.1. Microorganisms and growth conditions

A SRB consortium isolated from the wetland of the Urgeiriça mine (North of Portugal) and selected from previous studies [21], containing mainly species affiliated to *Desulfovibrio desulfuricans*, was used as inoculum. These cultures were grown and maintained in modified Postgate B medium (Postgate, 1966) (MPM: 0.5 $g.L^{-1}$ $K_3PO_4.H_2O$; 1 $g.L^{-1}$ NH_4Cl; 1 $g.L^{-1}$ $CaSO_4.2H_2O$; 1 $g.L^{-1}$ yeast extract; 2 $g.L^{-1}$ $MgSO_4.7H_2O$; 0.01 $g.L^{-1}$ resazurin; 0.5 $g.L^{-1}$ Na_2SO_3; 7.75 $g.L^{-1}$ $C_3H_5NaO_3$) in anaerobic conditions, at room temperature in 100 mL batches.

Growth parameters, such as sulphate and soluble sulphide, pH and redox potential were measured over time. The cultures were subcultured every three weeks, using 5% (v/v) of SRB inoculum. In the described experiments, only stable cultures (subcultured a minimum of three times) were used.

3.3.2.2. Zinc sulphide and Lead sulphide precipitation

Zinc (II) solution (~100 mgL^{-1}) was prepared with milliQ water using zinc sulphate hepta-hydrate ($ZnSO_4.7H_2O$ >99.5%, Panreac).

Pb(II) solution (~100 mgL^{-1}) was prepared with milliQ water using Lead (II) nitrate ($Pb(NO_3)_2$ >99.8%, Prolabo).

The chemical synthesis was performed using an aqueous solution of $Na_2S.9H_2O$ (Fluka, 32-38%) as precipitating agent.

TiO_2 powder commercial P-25 TiO_2, (Degussa) (*ca.* 80% anatase, 20% rutile) with a average primary particle size of ~21 nm was used as support for the precipitation of PbS and ZnS nanocomposites and in the photoreactor experiments.

After evaluation of the SRB growth parameters, as previously described, depending of the measured concentration of sulphide, an aliquot of the sulphide containing growth media was added to the zinc ion or lead ion solution described above. The addition was performed when over 90% of the sulphate had been converted to sulphide. The growth culture volume added was calculated based on twice the sulphide content necessary to ensure the complete precipitation of the zinc or lead ions present in the solution. This addition, to 500 mL of the metal solution, was carried out without filtration; in the absence or presence of TiO_2 (0.04 g, 0.06 g and 0.08 g per 50 mL).

This operation was done drop-by-drop, using a gas tight syringe with a hypodermic needle, and the metal solution under magnetic stirring at room temperature. After ZnS or PbS precipitation, the pH of the resulting suspension was measured, as well as the zinc ion or lead ion concentration.

The suspensions were centrifuged two times (Rotofix 32A, Hettich) for 10 minutes at 4000 rpm, washed twice with ethanol 70% and dried under vacuum at room temperature (APT.Line VD, Binder).

Each precipitation was repeated three times.

3.3.2.3. Analytical methods

Periodically, SRB growth media samples were collected from each batch with a syringe *via* the top of the glass flasks. Sulphide concentration was measured immediately after sampling using a UV-Visible spectrophotometer (DR 2800, Hach-Lange) by the Methylene Blue Method (665 nm, Hach-Lange). Sulphate concentration was also measured by UV/Visible spectroscopy at 450 nm (Hach-Lange) using the sulfaVer4 method (Hach-Lange).

Redox potential and pH of the growth media were measured using a pH/Eh Meter (GLP 21, Crison). Zn (II) and Pb (II) concentrations, before and after precipitation, were measured by flame atomic absorption spectroscopy using a Shimadzu AA-680 model spectrometer.

The precipitated materials were analyzed by XRD, using a PANalytical X'Pert Pro powder diffractometer operating at 45 kV and 35 mA, with CuKα radiation filtered by Ni. XRD patterns were recorded using a X'Celerator detector, with a step size (2θ) of 0.016 and a time per step of 1500 seconds.

The diffuse reflection was measured in a UV-2600-Shimadzu using BaSO4 (barium sulphide ReagentPlus, 99%-Sigma-Aldrich) as standard white board. The powder samples were placed in a sphere with a barium sulphate-coated inside and the reflectance percentage was measured from 200 to 1400 nm.

3.3.2.4. Photoreactor experiments

The photodegradation experiments were conducted in the Faculty of Science of Lisbon University, under the supervision of Dr. Olinda Coelho Monteiro, using an Ace Glass photoreactor cooled by water circulation with a radiation source of 450 W medium-pressure mercury-vapor lamp (Hanovia).

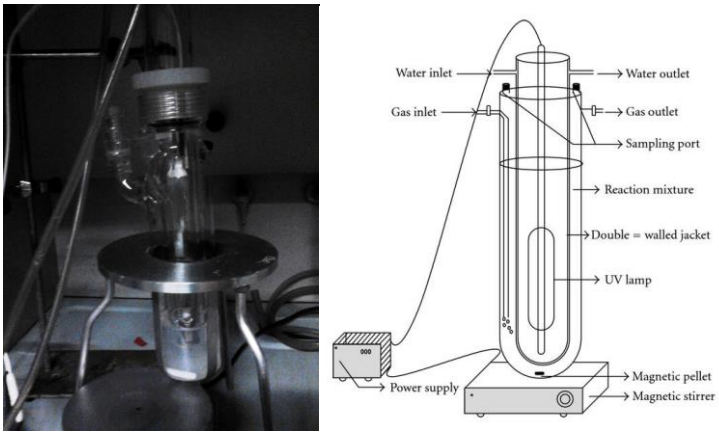

Figure 3.7 – Schematic representation of the photoreactor.

The suspensions were prepared by adding 30 mg of the photocatalyst into 150 mL of a 10 ppm (10 mg/L) chloramphenicol solution. Prior to irradiation, suspensions were adsorved during 60 minutes under stirring in the dark. The sample collected imediatelly after the adsorption and before irradiation is denominated A0. During light exposure the samples were collected at 5, 10, 20, 30, 45 and 60 minutes denominated as A1, A2, A3, A4, A5 and A6, respectivelly. All the samples were centrifuged (Rotofix 32A, Hettich) for 3.0 minutes at 3500 rpm. When TiO_2 was used alone as photocatalyst it was also necessary to proceed to 2 times the centrifugation (minispin, eppendorf) step at 10000 rpm during 10 min, whereas for the nanocomposites it was necessary to centrifuge at 10000 rpm during 10 min only once. The samples were analyzed by UV-Vis (UV-2600 Shimadzu) spectrophotometry in a spectrum range of 200 to 500 nm.

3.3.3. Results and discussion

The synthesis of nanocrystalline ZnS and the respective nanocomposite was already performed by Costa and colleagues [12]. In this study the synthesis of nanocrystalline ZnS and of the nanocomposite ($ZnS\text{-}TiO_2$) was repeated in order to carry out chloramphenicol photodegradation.

Several amounts of TiO_2 (0.02 g, 0.06 g and 0.08 g per 50 mL) were tested in previous photocatalysis studies performed by Costa and colleagues [22] which corresponded to a ratio of 9.3%, 12.4% and 37.3% of $ZnS\text{-}TiO_2$ (w/w), respectively.

ZnS and PbS powders were obtained using the non-filtered MPM growth medium as the sulphide source. In fact, the use of filtered (with 0.2 μm filter) and non-filtered media were previously tested by Costa and colleagues [12] and the results revealed no differences in terms of the synthesized NPs for both conditions. The average ZnS and PbS crystallite size was estimated based on the XRD data using the Scherrer equation (Scherrer, 1922) (Equation 1):

$$Dp = K.\lambda/\beta.\cos(\theta) \quad \text{(Equation 1)}$$

The diameter of the particles (*Dp*) was calculated based on the form factor (K, 0.94), the wavelength of the radiation source (λ), full width at half maximum in radians (β) and the Bragg angle (θ). The most intense peak observed was considered in the determination of the diameter using Equation 1.

The chemical synthesis was performed in order to compare it with the biological synthesis and once this synthesis was already performed by Costa and colleagues [12] it was not necessary to repeat it. Since that the synthesis of ZnS and of their derived nanocomposites of $ZnS\text{-}TiO_2$ was already performed, the repetition of these syntheses was made in order to obtain material for further studies of antibiotic photodegradation.

The ZnS powders newly synthesised were analyzed by XRD. The XRD results showed that the crystalline phase of the analyzed was predominantly rhombohedral ZnS (Fig. 3.8).

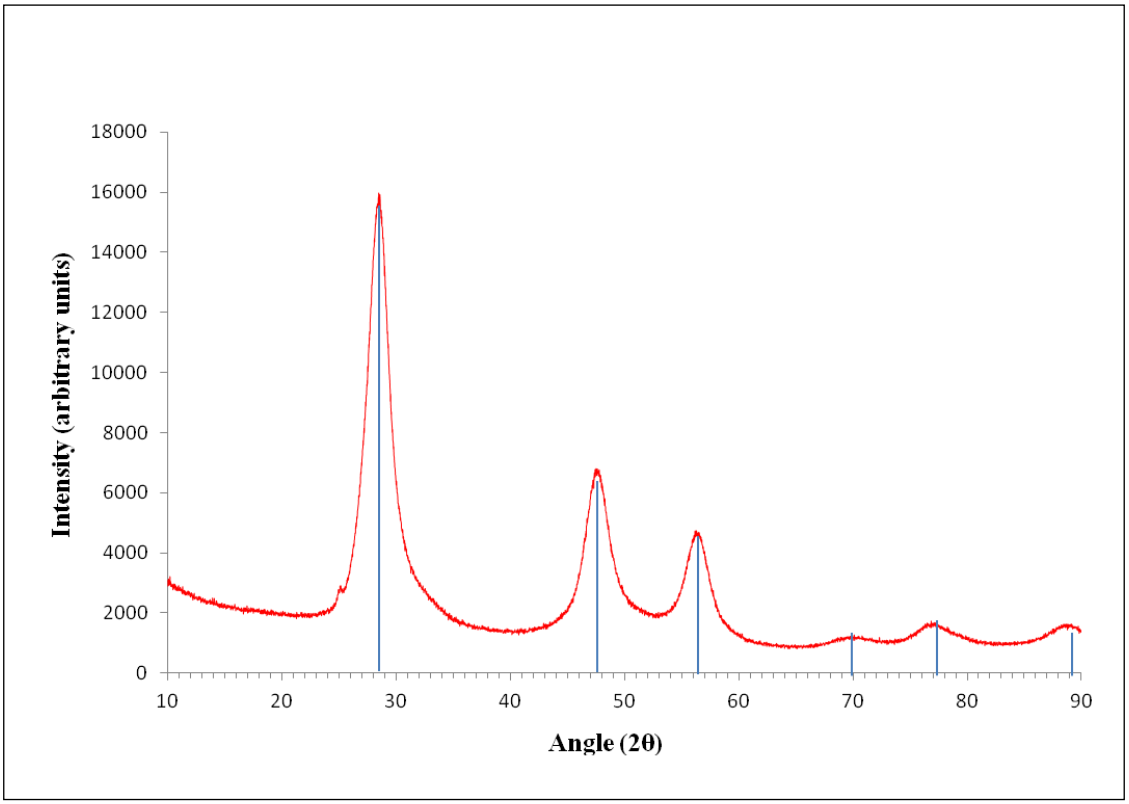

Figure 3.8 – X-Ray pattern of the precipitate obtained using biologically produced sulphide for the precipitation of dissolved Zn (II). The peaks shown correspond to ZnS (JCPD#01-083-1700).

According to the Figure 3.8, the broadening of XRD peaks observed indicate that the samples prepared in the present study are nano structured and using the Scherrer equation (Equation 1), the average ZnS crystallite size was estimated as 21 nm. In Fig. 3.8 it is represented the three main peaks with 2θ values of 28.91º, 48.11º, 57.10º consistent with that of ZnS standard and the peaks 70º, 77,3º and 89º compatible to the rhombohedral structure of ZnS (reference code: JCPD#01-083-1700).

ZnS-TiO_2 (0.06 g per 50 mL) powders were obtained when non-filtered MPM growth medium was added as the sulphide source. The ZnS-TiO_2 (0.06 g per 50 mL) powders were analyzed by XRD (Fig. 3.9).

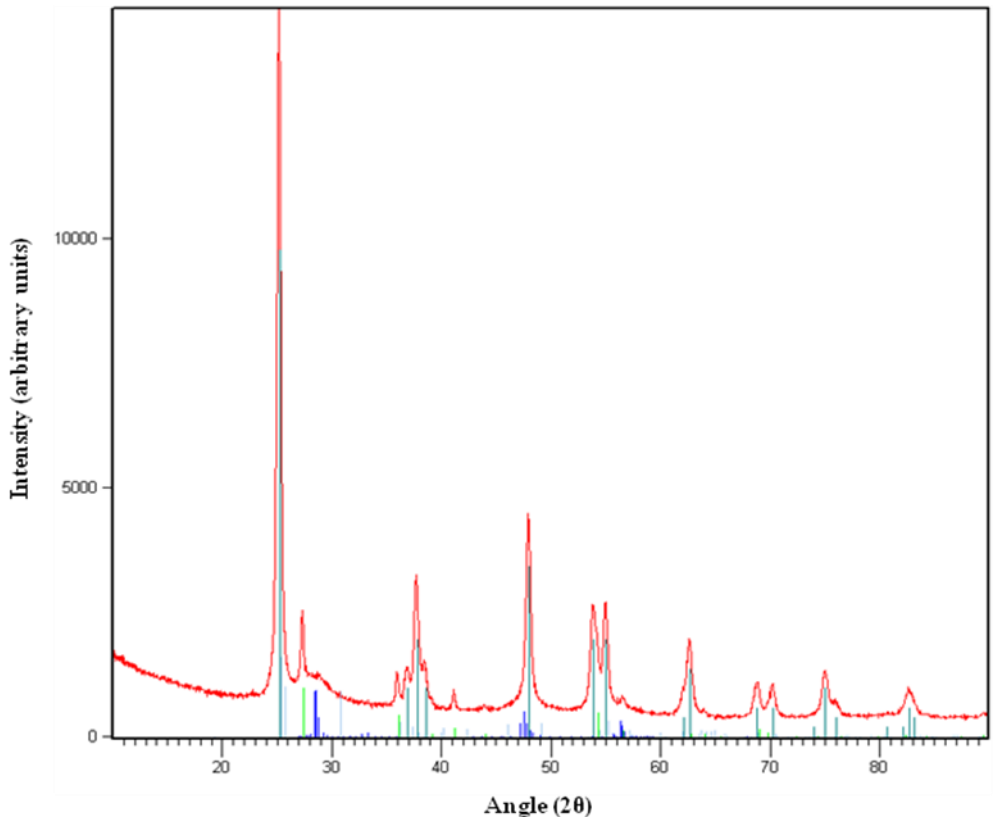

Figure 3.9 – X-Ray diffraction pattern of ZnS in association with TiO_2 (0.06 g per 50 mL) precipitates obtained using biological generated sulphide as source. The colour lines indicate the characteristic X-ray diffraction of the respective phases. The diffraction peaks shown correspond to: - Anatase, - Rutilo, - ZnS.

X-Ray powder diffraction revealed rutile and anatase, two of the crystal phases of TiO_2 (Fig. 3.9) and ZnS compatible with that of cubic crystalline structure. The XRD patterns exhibited strong diffraction peaks at 25.2°, 38º, 48.2º, 55º and 62.5° indicating TiO_2 in the anatase phase and strong diffraction peaks at 27.5°, 36° and 54°and 69º indicating TiO_2 in the rutile phase. All peaks are in good agreement with the standard spectrum (reference codes: JCPD#00-004-0477 corresponding to anatase and JCPD#00-004-0551 to rutile).

The most intense peak observed (25º) was considered for the determination of the average diameter of the particles using the Scherrer equation (Equation 1). Thus, the values were obtained from the graphic represented by Fig. 3.9 and the average ZnS-TiO_2 (0.06 g per 50 mL) nanocomposite crystallite size was estimated as 21 nm.

The results are consistent with those obtained by Costa and colleagues [12] for the biological synthesis. The biological synthesis was performed with a starting solution containing 108.32 mg/L of Zn^{2+}. When a solution containing the biological generated

sulphide was added to the zinc (II) solution in the presence and absence of TiO_2, the pH after precipitation was 6.37 and the percentage of Zn removal was high (≥90%) since only vestigial concentrations of zinc species remained in solution (concentrations lower than 2.8 mg/L). In the work performed by Costa and colleagues [12] for the chemical synthesis of ZnS using Na_2S as precipitating agent, the zinc removal percentage was approximately 80%. According to Costa and colleagues [12] the lower percentage of zinc removal, obtained in the chemical synthesis of ZnS, may be due to the low pH of the solution after precipitation. At lower pH values, the equilibrium of the dissolved sulphide species changes leading to a lower availability of sulphide for interacting with the metal ions in the solution.

The size of ZnS nanocrystallites was estimated as 21 nm. This result is consistent with that obtained by SEM analysis by Costa and colleagues [12] and an average diameter between 20 – 30 nm, was estimated by XRD using the Scherrer equation.

PbS particles were also obtained either using chemical and biological sulphide for comparison. For the chemical synthesis of lead sulphide a solution of ~100 mg/L of $Na_2S.9H_2O$ was used as the sulphide source. The obtained precipitates were analyzed by XRD and the result is represented in the Fig. 3.10.

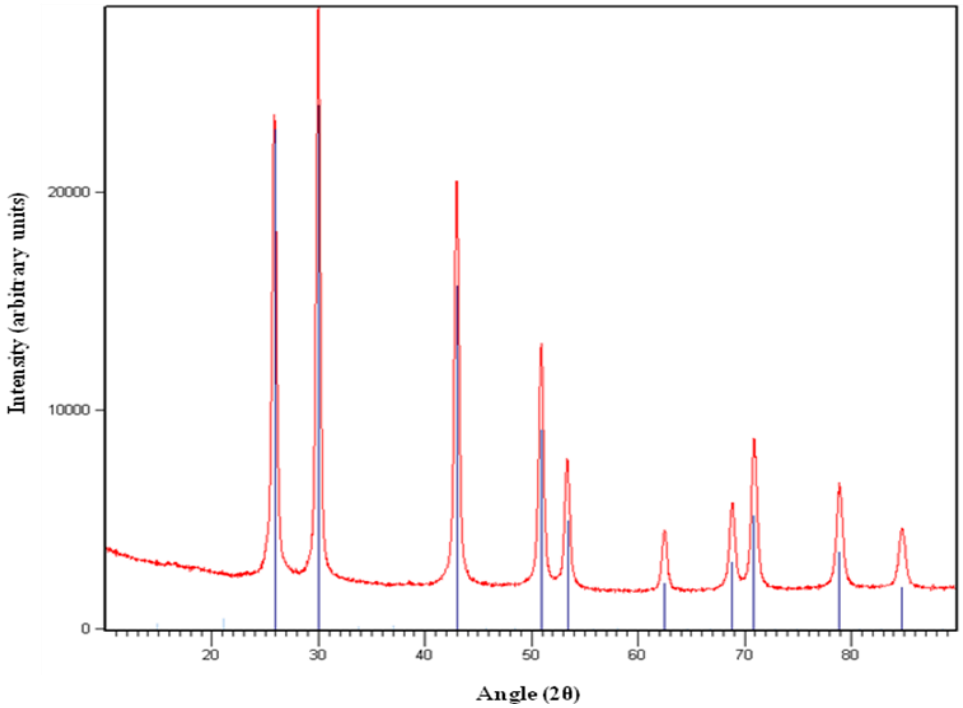

Figure 3.10 – X-Ray pattern of PbS precipitates obtained when $Na_2S.9H_2O$ was used as the sulphide source for the precipitation of dissolved Pb (II) (chemical synthesis). The peaks shown correspond to *galena* (JCPD#01-077-0244).

The XRD results showed that the crystalline phase of the analyzed sample was consistent with that of cubic (PbS) *galena*. According to the most intense peak observed at 30.24º (Fig. 3.10) and using the Scherrer equation (Equation 1), the average PbS crystallite size was estimated as 25 nm. The spectrum showed various diffraction peaks of PbS at 2θ values of 25.94º, 30.24º, 43.08º, 51.05º, 53.47º, 62.56º, 68.85º, 70.96º, 78.93º and 84.9º. All peaks are in good agreement with the standard spectrum (reference code: JCPD#01-077-0244).

PbS powders were obtained using non-filtered MPM growth medium as the sulphide source. The PbS powders were measured by XRD and according to the most intense peak observed the average PbS crystallite size was estimated using the Scherrer equation (Equation 1). The XRD result of PbS powders obtained by biological synthesis is represented in the Fig. 3.11.

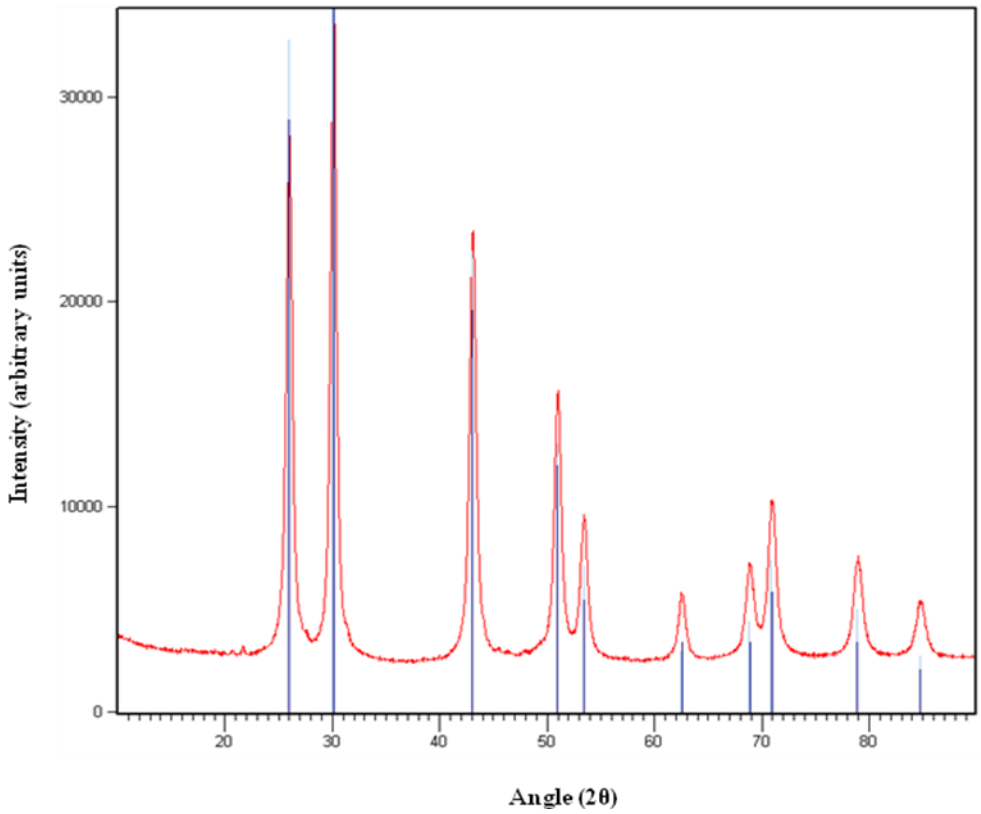

Figure 3.11 – X-Ray pattern of the precipitate obtained using biologically produced sulphide for the precipitation of dissolved Pb (II) (biological synthesis). The peaks shown correspond to *galena* (JCPD#01-077-0244).

The XRD results showed that the crystalline phase of the analyzed sample was predominantly consistent with that of cubic PbS (*galena*). The spectrum showed various

diffraction peaks of PbS at 2θ values of 25.94º, 30.24º, 43.08º, 51.05º, 53.47º, 62.56º, 68.85º, 70.96º, 78.93º and 84.9º (reference code: JCPD#01-077-0244).
According to the most intense peak observed in Figure 3.11 and using the Scherrer equation (Equation 1), the average PbS crystallite size was estimated as 17 nm.

There are different methods described in the literature to prepare successfully PbS nanoparticles. Some examples include microwave irradiation, in which XRD pattern showed PbS nano crystals with a mean particle diameter of 12 nm calculated from the Scherrer equation [23], chemical bath deposition (CBD) [24] and by sol gel spin coating technique synthesis [25]. The nanoparticles of PbS formed by CBD are spherical in nature and the X-ray diffraction showed that the film is crystalline with average grain size of 40 nm, which was also confirmed by SEM [24]. The XRD of the particles obtained by sol gel spin coating showed various diffraction peaks at 2θ values of 25.94º, 30.24º, 43.08º, 51.05º, 53.47º, 62.56º, 68.85º, 70.96º and 78.93º, the same peaks verified for PbS precipitate obtained using biogenic generated sulphide [25]. The SEM image showed an abundance of cube crystallites which have a mean particle size of ~7 nm [25].

PbS-TiO_2 (0.04, 0.06 and 0.08 g per 50 mL) powders were obtained when the non-filtered MPM growth medium was used as the sulphide source. The PbS-TiO_2 (0.04 g, 0.06 g and 0.08 g per 50 mL) powders were analyzed by XRD (Fig. 3.12).

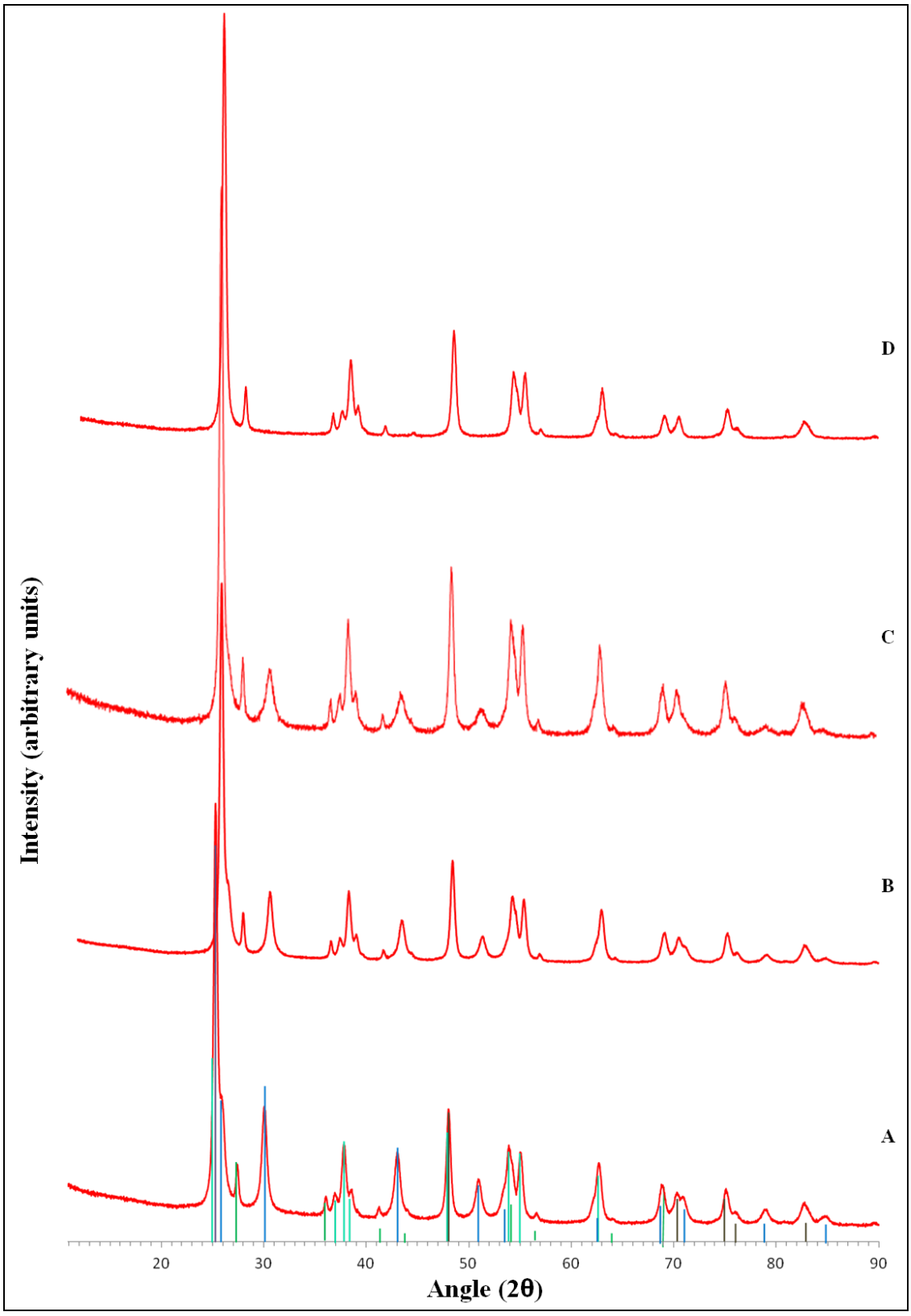

Figure 3.12 – X-Ray powder diffraction patterns of PbS in association with TiO_2 (0.04 g, 0.06 g and 0.08 g per 50 mL and only TiO_2 represented by A, B, C and D, respectively) precipitates obtained using biological generated sulphide as source. The colour lines indicate the characteristic X-ray diffraction of the respective phases. Legend of the diffraction peaks: – TiO_2, – Rutilo, – Anatase, – PbS

X-Ray powder diffraction revealed rutile and anatase phases, two of the crystal forms of TiO_2 (Fig. 3.12). The diffraction peaks consistent with TiO_2 in the anatase phase appear at 2θ values 25.2°, 38º, 48.2º, 55º and 62.5°, while the diffraction peaks at 2θ values 27.5°, 36° and 54° and 69º are compatible with the TiO_2 in the rutile phase (reference codes: JCPD#00-004-0477 corresponding to anatase and JCPD#00-004-0551 to rutile). The spectrum also showed various diffraction peaks of PbS at 2θ values of 25.94º, 30.24º, 43.08º, 51.05º, 53.47º, 62.56º, 68.85º, 70.96º, 78.93º and 84.9º that are consistent with that of cubic *galena* (reference code: JCPD#01-077-0244) for 0.04, 0.06 g and 0.08 g quantities of TiO_2. All peaks are in good agreement with the standard spectrum. According to the most intense peak observed in the Fig 3.12 and using the Scherrer equation (Equation 1), the average PbS-TiO_2 (0.04, 0.06 and 0.08 g TiO_2 per 50 mL) nanocomposite crystallite size was estimated as 19, 20 and 21 nm, respectively and the crystallite size of TiO_2 alone was estimated as 20 nm, which are in agreement with the manufacturer's informations (TiO_2 particle size of ~21 nm).

The biological and chemical synthesis was performed with a starting solution containing 101.4 mg/L of Pb^{2+}. When a solution containing the biological generated sulphide was added to the lead (II) solution in absence and presence of 0.04 g, 0.06 g and 0.08 g TiO_2 per 50 mL, the pH after precipitation was 6.79, 6.81, 6,84 and 6.86, respectively and the percentage of removal was very high (100%). In the chemical synthesis obtained using aqueous Na_2S as precipitating agent, the removal percentage of lead from the metal solution was (<90%). The lower percentage of lead removal, obtained by chemical synthesis of PbS, can be due to the high pH of the solution after precipitation (pH=10.7), since for pH values above 10 the formation of metal hydroxy complexes is promoted and that can increase the metal solubility and reduce the precipitation effectiveness [26].

An important aspect that it is necessary to take into account is that an ideal photocatalyst is characterised by the following attributes: photo-stability, chemically and biologically inert nature, availability and low cost and capability to adsorb the reactant under efficient photonic activation [27].

The diffuse reflectance was measured using the powders obtained by biological generated sulphide. The diffuse reflectance results tells much about the physical and

chemical characteristics that are not available by other analytical means and allow the quantitation of colour measurement [28]. By this method it is possible to have an ideia about the semicondutor powder that presents the best photocatalystic properties.

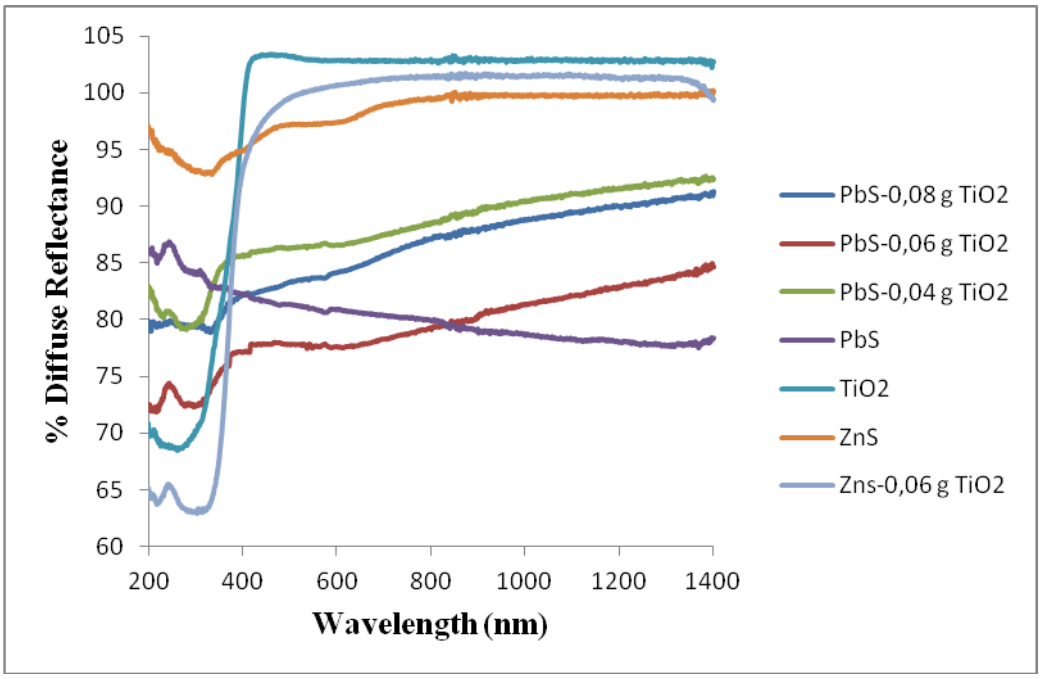

Figure 3.13 – Representation of difuse reflectance (%) versus wavelength (nm) for the different precipitates.

In the diffuse reflectance spectra, low percentage of diffuse reflectance means high absorption in the corresponding wavelength, and vice versa.

The ZnS-0.06 g TiO_2, TiO_2 and PbS-0.06 g TiO_2 powders exhibited the highest absorptions at lower wavelengths, therefore presented the lowest percentages of diffuse reflectance from all the precipitates in study (Fig. 3.13)

The reflectance spectra were analyzed using the Kubelka-Munk (KM) function to convert the reflectance into the equivalent absorption coefficient [29].

Thus, $KM=(1-R)^2/2.R$ (Equation 2), where R (%) is the Reflectance/100.

The graphic representing KM versus wavelenght (nm) for the different powders is presented in the Fig. 3.14.

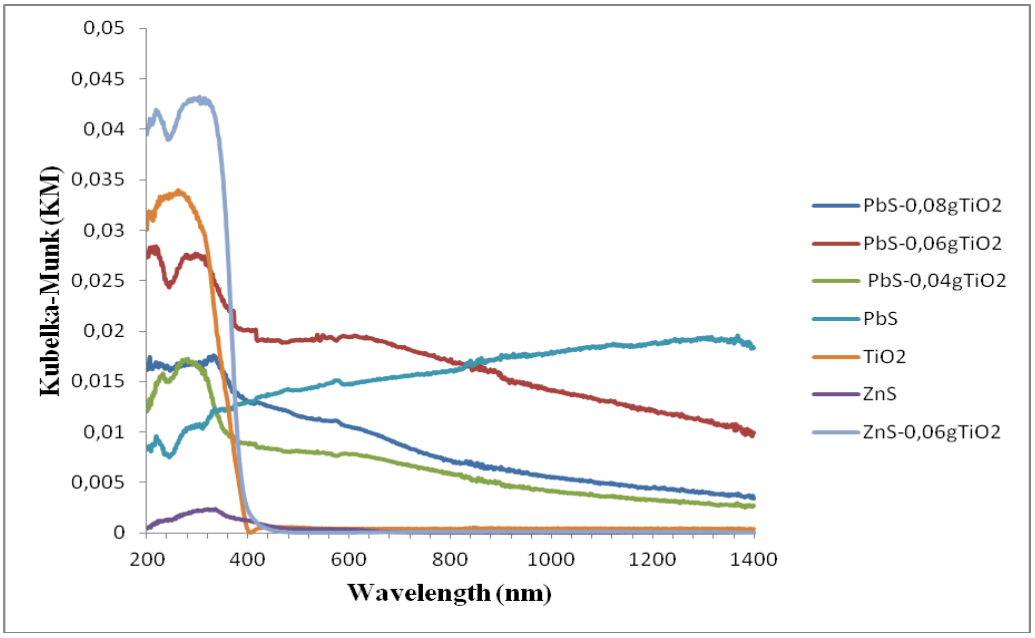

Figure 3.14 – Representation of KM (Kubelka-Munk) vs. wavelength for the different precipitates in study.

The studied powders revealed a strong absorption at the wavelength range from 240 to 390 nm (lower wavelengths (blue shift)) with exception of PbS. The blue shift is the shift of the optical absorption edge to the high-frequency (decrease of wavelength) range observed in semiconductors with the decrease of particle size [30].

The PbS powder without TiO_2 exhibited a high absorption in the visible region (>400 nm), whereas the absorption wavelength of the PbS-TiO_2 nanocomposites was extended to a visible region (higher wavelength (red shift)), due to absorption of visible light by PbS (black powder). The TiO_2, ZnS nanocomposite and ZnS presented practically an uniform absorption spectra in the visible range (790-390 nm) (Fig. 3.14).

The results demonstrated that the compounds were in the expected KM vs wavelength range with exception of ZnS that seems to be contaminated. In theory, because the absorption wavelength range is extended towards the visible light, the formation rate of electron–hole pairs on the photocatalyst surface also increases greatly, which can result in higher photocatalytic activities.

The term “band gap” refers to the energy difference between the top of the valence band to the bottom of the conduction band. Band electrons are able to jump from one band to another. The band gap energy is a specific minimum amount of energy required for the electron transition from the valence band to the conduction band (Fig. 3.15) [31].

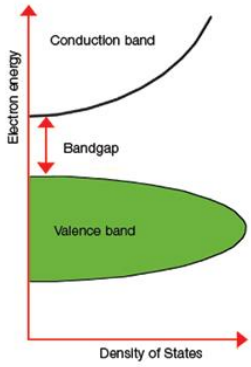

Figure 3.15 – Diagram illustrating the "band gap".

In semiconductor (0.2 to 4 eV) photocatalys excitation of an electron from the valence band to the conduction band ocurrs when the absorption of a photon of energy is identical to or higher than the band gap energy of the semiconductor. Wide-band gap semiconductors, such as TiO_2, demonstrated to be better photocatalysts than low-band gap materials, mainly due to the higher free energy of photogenerated charge carriers. [32]. However, low band gap semiconductors are better adapted to the solar spectrum. When TiO_2 particles are doped with transition metals, midgap states are generated where direct recombination occurs, producing composites with high visible light photocatalytic activity. Therefore, the semiconductor with lower bandgap absorbs the photons from visible light and the resulting photogenerated electrons are subsequently transferred to the semiconductor with larger bandgap [22].

This light induced generation of an electron-hole pair is a precondition step in all semiconductor-mediated photocatalytic processes. Photogenerated species tend to recombine and dissipate energy as heat of photons, because the kinetic barrier for the electron-hole recombination process is low. Thus, the lifetimes of photogenerated carriers increase giving the opportunity to these species to exchange charge with substrates adsorbed on the photocatalyst surface and initiate chemical reactions [32], such as photodegradation processes.

The most direct way of obtaining the optical band gap is to simply determine the photon energy at which there is a sudden increase in the absorption. For nanocrystalline samples the band gap is determined from the maximum absorption. The optical band gap of the nanocrystalline samples are calculated from the absorption peak using the formula $E_g = h.c/\lambda$ (Equation 3), where h is the Planks constant = 6.626E-34 Joules.sec, C is the speed of light in vaccum = 3.0E8 meter/sec and λ is the wavelength at which

the absorption peak corresponds to a sudden increase in the absorption of each material, in meters [31, 33].

The band gaps (E_g) of TiO_2 and of the nanocomposites were calculated and are presented in Table 3.1:

Table 3.1 – Band gap values of metal sulphide nanoparticles and their nanocomposites obtained by biologically generated sulphide.

Sample	Wavelength (nm)	$E_{g\ (eV)}$
TiO_2	400	3.11
ZnS	390	3.19
ZnS-0.06g TiO_2	398	3.12
PbS	1364	0.91
PbS-0.04g TiO_2	410	3.03
PbS-0.06g TiO_2	520	2.39
PbS-0.08g TiO_2	450	2.76

Extrapolation of the KM (Fig. 3.14) versus wavelength curves shown results that allowed to estimate the band gap energy using the equation 3: 3.11 eV for TiO_2, 0,91 eV for PbS, 3.53 for ZnS and 3.03, 2.39 and 2.76 eV for PbS nanocomposites with 0.04, 0.06 and 0.08 g of TiO_2, respectively (Table 3.1).

Some preliminary results of photodegradation were obtained. The photolysis (without photocatalyst) was performed in the photoreactor with an initial solution of 10 ppm (10 mg/L) of CAP during 60 minutes of irradiation time (Fig. 3.16). Each photodegradation assay was performed using an initial solution of 10 mg/L of chloramphenicol in the presence of 30 mg of TiO_2 (Fig. 3.17) and of 30 mg of each nanocomposites (ZnS supported with 0.06 g TiO_2 and PbS supported with 0.06 g TiO_2, Fig. 3.18 and Fig. 3.19, respectivelly) used as photocatalysts. The variations in the concentration of CAP along the reaction time were measured using the absorption peak intensity at the wavelength of 276 nm.

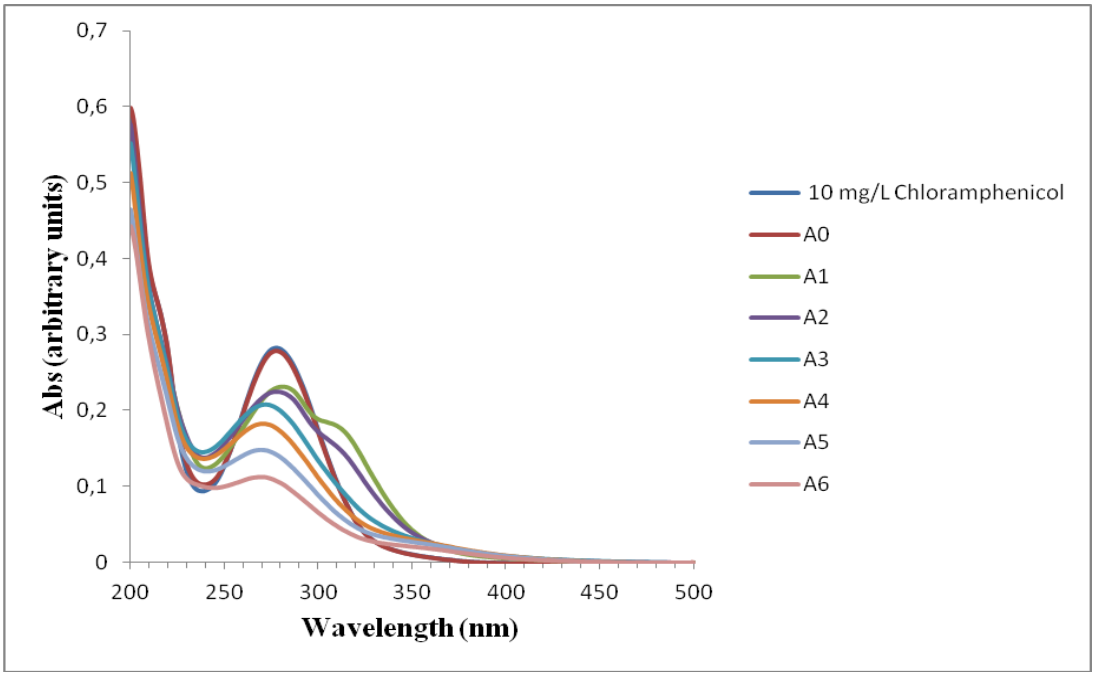

Figure 3.16 – Representation of UV absorption spectra of 10 mg/L chloramphenicol photolysis, in the photoreactor with irradiation time of 60 minutes. The sample collected imediatelly after the adsorption and before irradiation is denominated A0. During light exposure the samples were collected at 5, 10, 20, 30, 45 and 60 minutes denominated as A1, A2, A3, A4, A5 and A6, respectivelly.

The UV absorption spectra demonstrated that chloramphenicol suffered degradation in the absence of catalyst (photolysis), at the described conditions along the 60 minutes of irradiation (Fig. 3.16), thus the assay conditions were maintained for the subsequent studies.

In the presence of a semiconductor used as photocatalyst (nanocomposites) is expected that the photodegradation of the antibiotic will be faster and complete.

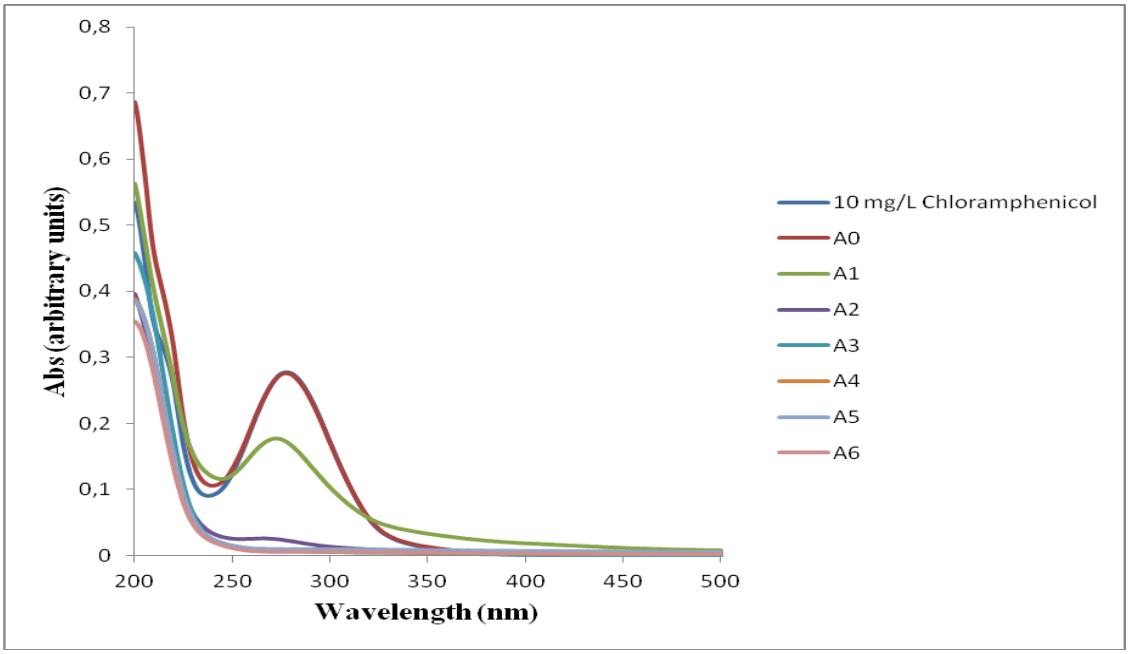

Figure 3.17 – Representation of UV absorption spectra of 10 mg/L CAP photodegradation using TiO_2 as photocatalyst, in the photoreactor with irradiation time of 60 minutes. The sample collected imediatelly after the adsorption and before irradiation is denominated A0. During light exposure the samples were collected at 5, 10, 20, 30, 45 and 60 minutes denominated as A1, A2, A3, A4, A5 and A6, respectivelly.

The UV absorption spectra of 10 mg/L CAP photodegradation revealed that when TiO_2 (positive reference) was used as photocatalyst a faster and almost complete photodegradation of the antibiotic was achieved after 60 minutes of irradiation (Fig. 3.17). Therefore, the produced nanocomposites need to present a better performance than TiO_2 in order to be considered good photocatatysts.

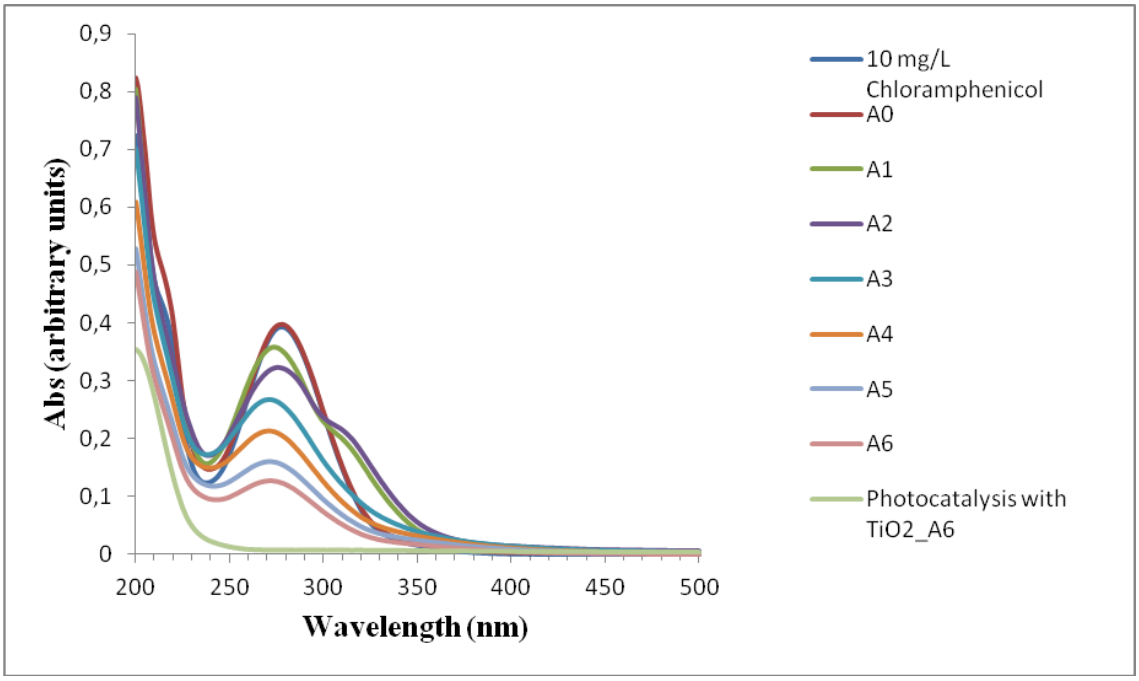

Figure 3.18 – Representation of UV absorption spectra of 10 mg/L CAP photodegradation using the nanocomposite ZnS with 0.06 g of TiO_2 as photocatalyst, in the photoreactor with irradiation time of 60 minutes. The sample collected imediatelly after the adsorption and before irradiation is denominated A0. During light exposure the samples were collected at 5, 10, 20, 30, 45 and 60 minutes denominated as A1, A2, A3, A4, A5 and A6, respectivelly.

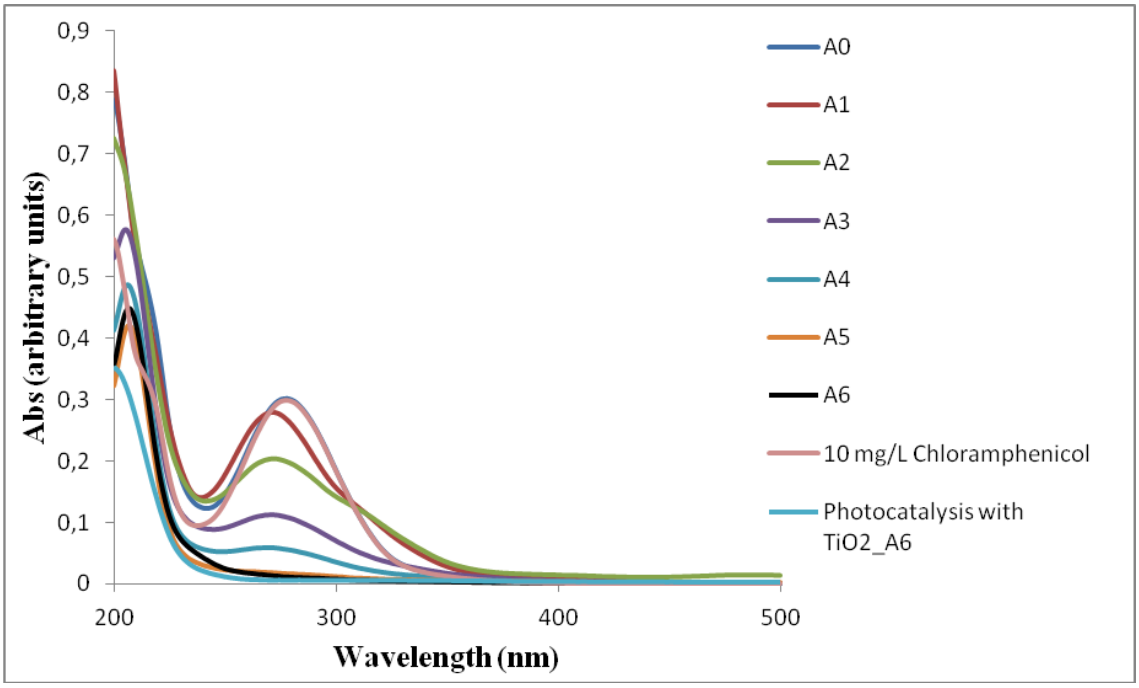

Figure 3.19 – Representation of UV absorption spectra of 10 mg/L CAP photodegradation using PbS with 0.06 g of TiO_2 as photocatalyst, in the photoreactor with irradiation time of 60 minutes. The sample collected imediatelly after the adsorption and before irradiation is denominated A0. During light exposure the samples

were collected at 5, 10, 20, 30, 45 and 60 minutes denominated as A1, A2, A3, A4, A5 and A6, respectivelly.

According to the obtained results the best photocatalyst were TiO_2 alone, used as reference (Fig. 3.17), whereas ZnS-0.06 g TiO_2 revealed to have a far away behaviour from the photocatalytic behaviour of TiO_2 (Fig. 3.18). The nanocomposite PbS-0.06 g TiO_2 presented a very similar activity to TiO_2 (Fig. 3.19).

The photocatalytic activity of TiO_2 and nanocomposites was presented by degradation efficiency percentage: $[1-(A/A_0)].100\%$ (Equation 4) of CAP versus time of illumination (Fig. 3.20), where A represents the chloramphenicol absorvance of collected samples along the 60 minutes at 276 nm and A_0 was the absorvance of the initial solution of CAP.

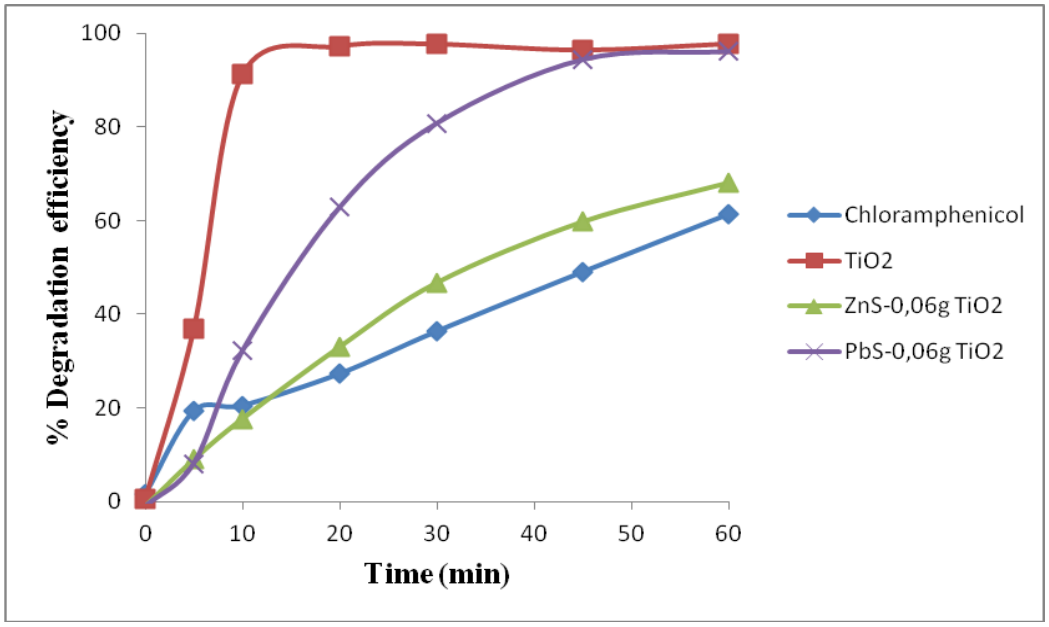

Figure 3.20 – Degradation efficiency (%) of 10 mg/L solution of CAP using different nanocomposites as photocatalysts versus irradiation time at 450 W.

The degradation efficiency corroborate the results described above. The best photocatalyst was TiO_2 (the compound used as reference) with 97.8% of efficiency in the photodegradation of CAP, as expected, whereas the nanocomposite PbS-0.06 g TiO_2 removed 96.1% of the antibiotic. The worse nanocomposite in the photodegradation of CAP was ZnS-0.06 g TiO_2, that removed only 68.0%, about the same value obtained by photolysis of CAP that was 61.3% (Fig.3.20).

Assuming that the disappearance of an organic molecule follows approximately a pseudo-first-order kinetics according to the Langmuir–Hinshelwood (L-H) model [34] a plot of $\ln(A/A_0)$ versus time shows a linear adjustment, following $\ln(A_0/A)=K_{app}.t$ (Equation 5), where the slope of the linear regression is the apparent pseudo-first-order rate constant K_{app} and t is the irradiation time (Fig. 3.21).

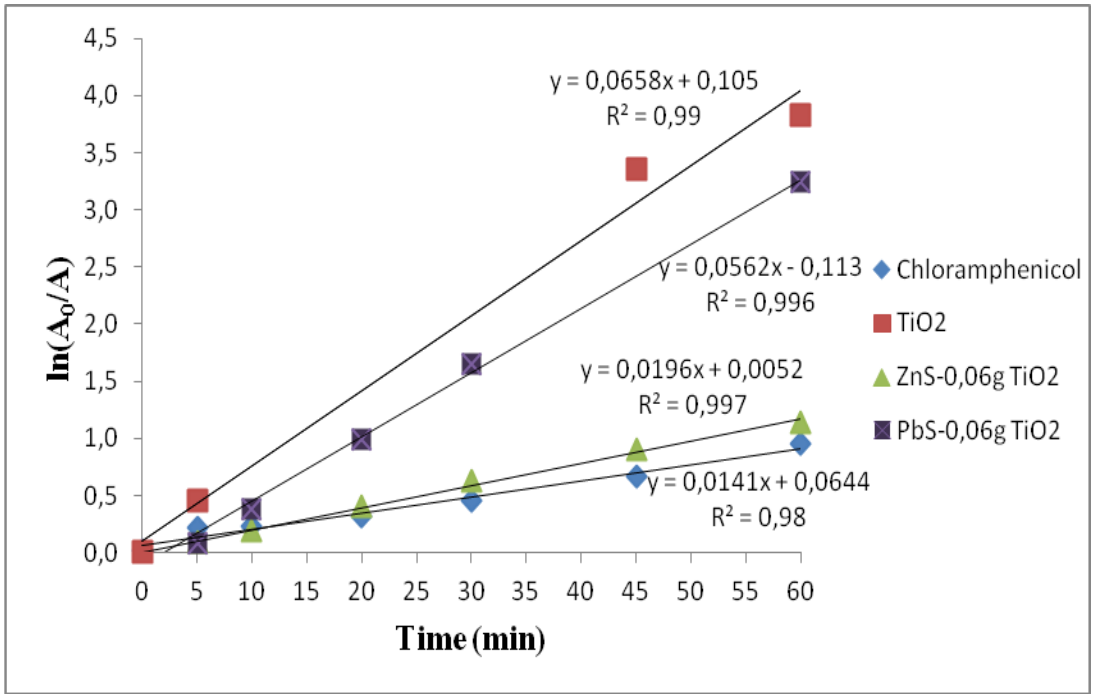

Figure 3.21 – Representation of the linear regression of the function $\ln(A/A_0)$ versus time of irradiation, where A is the absorvance over time and A_0 is the absorvance of the initial solution (λ = 276 nm).

Experimental data are in agreement with the L–H model due to the linear behaviour of each curve which indicates that a pseudo first order reaction was ocurring during CAP degradation. According to the kinetics parameters, the photolysis presented the lowest K_{app} value of 0.0141 min^{-1}, whereas the best photocatalytic activity was observed for TiO_2, the composite used as reference, that exhibited the highest K_{app} of 0.0658 min^{-1} (Fig. 3.21). From the tested nanocomposites the one that displayed the best photocatalyst activity was PbS-0.06 g TiO2 with a K_{app} of 0.0562 min^{-1}, whereas the worse was the ZnS-0.06 g TiO_2 that showed a K_{app} of only 0.0196 min^{-1} (Fig. 3.21).

The nanocomposites of ZnS-0.06 g TiO_2 presented very low photocatalytic activity almost the same than photolysis probably due to the fact that CAP was not adsorbed on the surface of the composite (Fig. 3. 18). This can be due to repulsion of the electric charges on the surface of both antibiotic and nanocomposite or owing to the existence

of segregation of the metal sulphide nanoparticles on the surface of TiO_2 support, which may lead to an unstable nanocomposite structure.

Due to the presented behaviour it does not make make sense to test a ZnS nanocomposite with a high TiO_2 amount. Other negative point is that the excess of catalyst limits the amount of light reaching the CAP, thus blocking the photodegradation of it.

The degradation efficiency of the photocatalyst exhibits an increase by increasing the catalyst dosage up to 0.06 g and above this dosage the removal efficiency decreases. The removal of CAP increases due to the increase in active sites available for photocatalytic reaction to ocurr and with the increase in the amount of catalyst up to a level corresponding to the optimum light absorption. Above this value the suspended particles of the catalyst block the UV light passage and increase the light scattering having an inverse effect on photocatalytic reaction [20].

Despite the good photocatalytic activity of the nanocomposite PbS-0.06 g TiO_2 is suspected that PbS suffered photocorrosion because of the appearance of a white colour precipitate in the final of the photoreaction, while initialy the powder was dark grey. Then it is not possible to know if the good photocatalytic activity is of the nanocomposite or only due to the TiO_2 action. An atomic absortion will be performed in order to analyze the existence of Pb (II) in solution. This study is in course.

To overcome this problem other support can be used or a non toxic compound that binds the particle surface and can be used to act as a stabilizer of the PbS composite.

3.3.4. Conclusion

Nanoparticles of ZnS (rhomboedric) e PbS (galena) and the respective nanocomposites of ZnS-TiO_2 (cubic) and PbS-TiO_2, with different ratios of TiO_2, were successfully produced using biogenic sulphide.

According to XRD the estimated size of their crystalites ranged from 15 to 21 nm.

The synthesized ZnS demonstrated to have a crystalline structure compatible to rhombohedral crystal system, different from the cubic crystalline structure obtained by Costa and colleagues [12].

Since the particles size was only estimated based on the Scherrer equation, to determine and confirm their size and elementary composition (morphology) is mandatory to carry out TEM-EDX or SEM-EDX analysis.

3.3.5. Studies in course

Once the Scherrer equation only gives an estimative of the nanocrystalline size the morphological characterization of precipitates will be performed by Scanning Electron Microscopy (SEM) or Transmission electron microscopy (TEM) coupled to EDX.

This research will evaluated the potential of ZnS or PbS and ZnS-TiO_2 or PbS-TiO_2 nanocomposites as catalysts in the photodegradation of chloramphenicol, an antibiotic of widespread use in the recent past, classified as emerging pollutant, selected for these studies. The photodegradation was already performed in photoreactor. Soon the photocatalytic biodegradation under direct sunlight will be carried out to know more about the degradation mechanisms that are occuring during the photocatalysis of CAP and about the stability of the nanocomposites. To carry out this assays is necessary to have favorable meteorological conditions, namely high levels of UV radiation. The efficiency of the precipitates as catalysts in sunlight mediated photodegradation will be investigated, using different volumes of antibiotic-contaminated water (150 mL and 10 L).

Comparative studies using powder XRD and TEM/EDX (Energy-Dispersive X-ray Spectroscopy), before and after photodegradation, will be carried out in order to monitor possible structural and morphological changes on the particles. The influence of the catalyst amount, initial pH and antibiotic concentration will be evaluated. The final solutions will be possibly characterized by UV-Vis, by Liquid chromatography–mass spectrometry (LC/MS**)** and by AAS, in order to determine the chloramphenicol concentration, the compounds that resulted from the photodegradation and the possibility of degradation of the fotocatalyst, respectively. This work will reveal if all tested nanocrystalline particles and derived composites obtained by using biologically produced sulphide will have potential to be used as photocatalysts for the degradation of antibiotic.

The experiments that will be carried out under sunlight shall prove to be more advantageous, not only for its simplicity and consequent lower cost, but because in these conditions the Sun UV radiation is less intense and probably will not cause degradation of the catalysts as verified in photoreactor experiments.

3.4. Bibliographic references

[1] Hoffman, J. E. (1988) Recovering platinum-group metals from autocatalysts. J. Met. 40:40-44.
[2] Das, N. (2010) Recovery of precious metals through biosorption – a review. Hidrometallurgy 103: 180-189.
[3] Rashamuse, K. J. and Whiteley, C. G. (2007) Bioreduction of Pt (IV) from aqueous solution using sulphate-reducing bacteria. Appl Microbiol Biotechnol 75:1429–1435.
[4] Hennebel, T., De Gusseme, B., Boon, N., and Verstraete, W. (2009) Biogenic metals in advanced water treatment. Trends Biotechnol 27: 90-98.
[5] Gadd, G.M. (2000) Bioremedial potential of microbial mechanisms of metal mobilization and immobilization. Curr Opin Biotechnol 11:271-279.
[6] White, C., Wilkinson, S.C. and Gadd, G.M. (1995) The role of microorganisms in biosorption of toxic metals and radionuclides. Int Biodeterior Biodegrad 35:17-40.
[7] Martins, M., Assunção, A., Martins, H., Matos, A. P., Costa, M.C. (2013) Palladium recovery as nanoparticles by an anaerobic bacterial community. Journal of Chemical Technology and Biotechnology DOI: 10.1002/jctb.4064.
[8] Mandal, D., Bolander M. E., Mukhopadhyay, D., Sarkar, G., Mukherjee, P. (2006) The use of microorganisms for the formation of metal nanoparticles and their application. Appl Microbiol Biotechnol 69:485–492.
[9] Labrenz, M., and Banfield J. F. (2004) Sulfate-reducing bacteria-dominated biofilms that precipitate ZnS in a subsurface circumneutral-pH mine drainage system. *Microb Ecol* 47: 205-217.
[10] Barnes, L. J., Janssen, F. J., Scheeren, P. J. H., Versteegh, J. H. and Koch, R. O. (1992) Simultaneous Microbial Removal of Sulfate and Heavy-Metals from Waste-Water. T I Min Metall C, 101: C183-C189.
[11] Costa, M. C. and Duarte, J. C., (2005) Bioremediation of acid mine drainage using acidic soil and organic wastes for promoting sulphate-reducing bacteria activity on a column reactor. Water Air Soil Poll, 165(1-4): 325-345.
[12] Costa, J. P., Girão, A. V., Lourenço J. P., Monteiro, O. C., Trindade, T., Costa, M. C. (2012) Synthesis of nanocrystalline ZnS using biologically generated sulfide. Hydrometallurgy. Vol. 117–118, pp. 57–63; doi: 10.1012/j.hydromet.2012.02.005.
[13] Costa, J. P., Girão, A. V., Lourenço J. P., Monteiro, O. C., Trindade, T., Costa, M. C., (2013) Green synthesis of *covellit*e nanocrystals using biologically generated sulfide: Potential for bioremediation systems, in press.
[14] Deblonde, T., Cossu-Leguille, C, Hartemann, P., (2011) Emerging pollutants in wastewater: A review of the literature. International Journal of Hygiene and Environmental Health, 214:442-448.
[15] Hernández, F., Rivera, A., Ojeda, A., Zayas, T., and Cedillo, L., (2012) Photochemical Degradation of the Ciprofloxacin Antibiotic and Its Microbiological Validation. Journal of Environmental Science and Engineering A 1, 448-453.
[16] Kümmerer, K., Al-Ahmad, A. and Mersch-Sundermann, V. (2000) Biodegradability of some antibiotics, elimination of their genotoxicity and affection of wastewater bacteria in a simple test. Chemosphere 40, pp. 701–710.
[17] Parsons, S., (2004) Advanced Oxidative Processes for Water and Wastewater Treatment, IWA Publishing, UK.
[18] Gupta, V. K., Jain, R., Mittal, A., Mathur, M. and Sikarwar, S. (2007) Photochemical degradation of the hazardous dye Safranin-T using TiO_2 catalyst. J. Colloid. Interf. Sci, 309(2): 464-469.

[19] Hashimoto, K., Irie, H., and Fujishima, A. (2005) TiO_2 Photocatalysis: A historical overview and future prospects. Japanese Journal of Applied Physics Vol. 44, No. 12, 2005, pp. 8269–8285.
[20] Shokri, M., Jodat, A., Modirshahla, N. and Behnajady, M. A. (2013) Photocatalytic degradation of chloramphenicol in an aqueous suspension of silver-doped TiO2 nanoparticles. Environmental Technology, 34:9, 1161-1166.
[21] Martins, M., Faleiro, M. L., Chaves, S., Tenreiro, R. and Costa, M.C. (2010) Effect of uranium (IV) on two sulfate-reducing bacteria cultures from a uranium mine site. Sci Total Environ, 408 (12): 2621-2628.
[22] Costa, J. P., Girão, A. V., Monteiro, O. C., Trindade, T., Costa M. C., Degradation of Safranin-T Using Biologically Produced ZnS-TiO2 photocatalysts: UV-Visible and Solar Studies: Submitted.
[23] Mispa, J. K., Subramaniam, P. and Murugesan, R. (2010) Microwave-assisted route for synthesis of nanosized metal sulphides. Chalcogenide Letters, 7(5):335-340.
[24] Kumar, D., Agarwal, G., Tripathi, B., Vyas, D., Kulshrestha, V. (2009) Characterization of PbS nanoparticles synthesized by chemical bath deposition Journal of Alloys and Compounds. 484:463–466.
[25] Mulik, R. N., Pawar, S. G., More, P. D., Pawar, S. A. and Patil, V. B. (2010) Nanocrystalline PbS thin films: Synthesis, microtructural and optoelectronic properties. Archives of Applied Science Research, 2(4):1-6.
[26] Armenante, P. M. (1997) Precipitation of Heavy Metals from Wastewaters, New Jersey Institute Technology: [cited 2013; Available from: http://cpe.njit.edu/dlnotes/CHE685/Cls06-2.pdf].
[27] García, C. G., Llorach, R. G., Vicent, M. L., Gómez, M. A. T., Tomás, G. M., March, J. A. B. (2009) Photocatalytic degradation of Orange II by titania addition to sol–gel glasses. J Sol-Gel Sci Technol 50:314–320.
[28] Workman, Jr. J., Springsteen, A. (1998) Applied Spectroscopy: A Compact Reference for Practitioners. Academic Press, 1ª edition, pp. 539.
[29] Reyes-Coronado, D., Rodríguez-Gattorno, G., Espinosa-Pesqueira, M. E., Cab, C., Coss, R., Oskam, G. (2008) Phase-pure TiO2 nanoparticles: anatase, brookite and rutile Nanotechnology. 19, 145605, pp. 10.
[30] Weller, H. (1993) Colloidal semiconductor Q-particles: chemistry in the transition region between solid state // Angew. Chem. Int. Ed. Engl.. Vol. 32, pp. 41-53.
[31] Dharma, J., Pisal, A., Simple Method of Measuring the Band Gap Energy Value of TiO_2 in the Powder Form using a UV/Vis/NIR Spectrometer. Aplication note, Copyright ©2009-2102, PerkinElmer, Inc. Shelton, CT USA.
[32] Kondarides, D. I. (2012) Encyclopedia of Life Support Systems (EOLSS) [cited 2013; Available from: http://www.eolss.net/Eolss-sampleAllChapter.aspx.
[33] Gupta, P., Ramrakhian, M. (2009) Influence of the Particle Size on the Optical Properties of CdSe Nanoparticles. The Open Nanoscience Journal 3, 15-19.
[34] Chatzitakis, A. Berberidou, C, Paspaltsis, I, Kyriakou, G., Sklaviadis, T., Poulios, I, (2008) Photocatalytic degradation and drug activity reduction of Chloramphenicol. Water research 42, 386–394.

VIII. Detailed *Curriculum Vitae*

i) Academic degree

2007 Degree in Biotechnology Engineering (5 years, pré-Bologna), by University of Algarve - Faculty of Engineering of Natural Resources (final average of 15 values).

ii) Professional experience

- I was selected to be research fellow in the project FCT: PTDC/AAG-TEC/2721/2012, "BIONANOMINE - Bio-síntese de nanomateriais semicondutores usando resíduos de minas e aplicações amigas do ambiente", to begin at 01/08/2013 - under the direction of Prof. Dr. Maria Clara Costa.

- **7/01/2013 – until presente:** I am working in the Environmental Technologies laboratory, of Centre of Marine Sciences (CCMAR) in the area of environmental biotechnology, performing biosynthesis and bioremediation studies for metal removal and/or recuperation using chemical and biological approaches - under the direction of Prof. Dr. Maria Clara Costa.

- **1/04/2010 – 15/06/2012:** As research fellow in the project FCT: PTDC/AGR-AAM/102664/2008, "Is *Plantago almogravensis* an aluminium hyperaccumulator? Elucidation of the tolerance mechanism using micropropagated plants" my work was based in the use of micropropagation techniques as well as subsequent assays to assess aluminium (Al) tolerance of two critically endangered plantain species *Plantago almogravensis* and *P. algarbiensis* - under the direction of Prof. Dr. Anabela Romano.

- **6/11/2008 – 8/05/2009:** The professional training in Progenus S.A. (Gembloux – Belgium) was under the direction of Dr. Robert Renaville. This work consisted at genotyping and in the identification SNPs (Single Nucleotide Polymorphisms) of interest and of major genes affecting the regulation, composition and percentage of fatty acids (FA) and of mono-unsaturated fatty acids (MUFAs) in the milk cows – 17 values, Grant under Leonardo da Vinci Programme Funding (6 months).

- **7/02/2007 – 30/07/2007:** Workpractice to obtain the degree of Biotechnology engineering, under the direction of Dr. Alain Jacquet - Service de Génétique Appliquée, Institut de Biologie et de Médecine Moléculaire (Université Libre de Bruxelles - Belgium) - *"Potential interactions between the cationic liposome X and some LPS binding proteins"* – 18 values, under a Erasmus Grant (6 meses).

In this workpractice I performed the expression and production of recombinant proteins in *E. coli*; Proteins Purification by affinity chromatography, ultrafiltration, precipitation and concentration; in Protein Biochemistry - SDS-PAGE, Western blot, enzymatic digestion, quantification methods of proteins as MicroBCA, Lowry and Bradford, among other study protocols for recombinant proteins; immunoassays - ELISA, immunohistochemistry, immunoprecipitation, cell activation and transfection of bone marrow derived dendritic cells (BMDC), among many other techniques which I have had the opportunity to learn during my traineeship.

iii) Articles

- Martins, N., Osório, M. L., Gonçalves, S., Osório, J., Palma, P., Romano, A. (2013) Physiological responses of *Plantago algarbiensis* and *P. almogravensis* shoots and plantlets to low pH and aluminium stress. Acta Physiol Plant 35:615-625 (2). DOI 10.1007/s11738-012-1102-z.

- Martins, N., Gonçalves, S., Palma, T. and Romano, A. (2012) Seed germination of two critically endangered plantain species, *Plantago algarbiensis* and *P. almogravensis* (Plantaginaceae). *Seed Sci. & Technol.*, Vol.40, Nº1, 144-149 (6).

- Martins, N., Gonçalves, S., Palma, T. and Romano, A. (2011) The influence of low pH on in vitro growth and biochemical parameters of *Plantago almogravensis* and *P. algarbiensis*. Plant Cell, Tissue and Organ Culture 107: 113-121. DOI: 10.1007/s11240-011-9963-1.

iv) Poster and communications in international congresses

- Palma, T., Costa, J., Lourenço, J., Costa, M. C. (2013) Production of PbS (*galena*) nanoparticles and nanocomposites using biologically generated sulphide. 2nd international conference on WASTES: Solutions, Treatments and Opportunities. September 12-13, Braga, Portugal, oral presentation.

- Aazza, S., Palma, T., Lyossi, B., Miguel, M. G. (2012) Actividade antioxidante do mel de Marrocos. II Iberian Apiculture Congress. October 18-20, Guadalajara, Espanha, oral presentation.

- Martins, N., Gonçalves, S., Palma, T., Romano, A. (2011) Oxidative stress status in *P. algarbiensis* and *P. almogravensis* after exposure to aluminum. 10th International Conference on Reactive Oxygen and Nitrogen Species in Plants. July 5-8, Budapest, Hungary, pp. 175.

v) Personal skills and competences

- ✓ **Portuguese** : Mother tongue;
- ✓ **French** : Good;
- ✓ **English** : Very Good;
- ✓ **Spanish** : Good.

Computers skills:

Very good knowledge in Excel, Word, Power Point, Outlook – Operative Systems Windows 7, Windows Vista and Windows 8.

IX. Annex

Progenus s.a.
Avenue Maréchal Juin 13
5030 Gembloux
Belgique

Téléphonie : +32-(0)81-616901
Télécopie : +32-(0)81-601723
Courriel : info@progenus.be

TRAINING COURSE REPORT OF TANIA CRISTINA DA LUZ PALMA

The period of the training course of Mrs Tânia Cristina Da Luz Palma has been realized during the period between the 6 November 2008 and the height May 2009.

The objectives of the training course included the development of various methods of PCR, sequencing and electrophoresis to study genetic variations on dairy cows. Miss Tânia Cristina Da Luz Palma had also used her time to learn other techniques developped at the laboratory like the quantitative PCR (qPCR).

Miss Tânia Cristina Da Luz Palma perfectly carried out work requested. During her training course, she has integrated perfectly in the team by respecting the instructions while knowing to make proof of constructive initiatives. Additionnally to improve its French knowledges, she has shown a fast comprehension of the techniques used.

She has shown the qualities necessary for this work and I will not hesitate to recommend her to its future employer.

With regard to her human qualities, I underline her capacity to integrate a team and to learn new methods and her team spirit

Based on these arguments, I estimate to be able to grant her a note of 17/20

PROGENUS s.a. Gembloux - Belgium

Renaville Robert
General Manager